Department of Energy
Carlsbad Area Office
P. O. Box 3090
Carlsbad, New Mexico 88221

WIPP File

DEC 2 0 1993

ENTERED

Ms. Judith Espinosa
Secretary
New Mexico Environment Department
Camino de Los Marquez #4
P.O. Box 26110
Santa Fe, NM 87502

Dear Ms. Espinosa:

Enclosed is a position paper regarding the Non-Salado Fluid Flow, which will be discussed during the System Prioritization Method (SPM) Workshop. This workshop will be held Monday, January 9, 1994, at the Holiday Inn of Carlsbad, New Mexico.

The SPM is designed to:

- Address regulator and stakeholder concerns early and throughout the process of regulatory compliance.
- Lead to scientifically sound Performance Assessment used in demonstrating regulatory compliance.
- Use taxpayer dollars efficiently.

The Department of Energy (DOE), Carlsbad Area Office (CAO), is commited to keeping project stakeholders informed of pertinent information. If you have any questions regarding the SPM, please contact Bob Bills of the DOE/CAO, at (505) 234-7481.

Sincerely

George E. Dials

George E. Dials
Manager

Enclosure

Printed on recycled paper

941213

CONF-9401111--1-Rev.1

NON-SALADO FLOW AND TRANSPORT POSITION PAPER

Revision 1
December 15, 1994

Contributors: C. Axness, R. Beauheim, Y. Behl, K. Brinster, T. Corbet, K. Economy, G. Freeze, L. Meigs, H. Papenguth, D. Powers, P. Swift, M. Wallace, S. Webb

DISCLAIMER

This report was prepared as an account of work sponsored by an agency of the United States Government. Neither the United States Government nor any agency thereof, nor any of their employees, makes any warranty, express or implied, or assumes any legal liability or responsibility for the accuracy, completeness, or usefulness of any information, apparatus, product, or process disclosed, or represents that its use would not infringe privately owned rights. Reference herein to any specific commercial product, process, or service by trade name, trademark, manufacturer, or otherwise does not necessarily constitute or imply its endorsement, recommendation, or favoring by the United States Government or any agency thereof. The views and opinions of authors expressed herein do not necessarily state or reflect those of the United States Government or any agency thereof.

DISTRIBUTION OF THIS DOCUMENT IS UNLIMITED

MASTER

DISCLAIMER

Portions of this document may be illegible in electronic image products. Images are produced from the best available original document.

CONTENTS

1.0 INTRODUCTION 1-1

2.0 FEATURES, EVENTS, AND PROCESSES INVOLVING NON-SALADO HYDROLOGY 2-1

3.0 CONCEPTUAL AND MECHANISTIC MODELS INVOLVING NON-SALADO HYDROLOGY 3-1

3.1 Hydrostratigraphy and Regional Groundwater Flow 3-1
- 3.1.1 Stratigraphy and Lithology in the Vicinity of the WIPP Site 3-1
- 3.1.2 Conceptual Models of Groundwater Flow above the Salado Formation 3-17
- 3.1.3 Groundwater Geochemistry and Regional Groundwater Flow 3-29
- 3.1.4 Castile Brine Reservoirs 3-31
- 3.1.5 Multi-Phase Flow 3-33

3.2 Culebra Flow and Advective Transport 3-34
- 3.2.1 Transmissivity 3-35
- 3.2.2 Storativity 3-35
- 3.2.3 Variable-Density Flow 3-36
- 3.2.4 Fluid from an Intrusion Hole 3-37
- 3.2.5 Double Porosity 3-37
- 3.2.6 Channeling 3-40
- 3.2.7 Plume Dispersion 3-41

3.3 Culebra Chemical Retardation 3-47
- 3.3.1 Rock-Water Interaction in the Culebra 3-47
- 3.3.2 Adsorption 3-52
- 3.3.3 Colloid-Facilitated Radionuclide Transport 3-54
- 3.3.4 Actinide Coprecipitation from Brine Mixing 3-59

3.4 Long Term Processes 3-60
- 3.4.1 Climate Change 3-60
- 3.4.2 Drill Holes That May Affect Regional Flow 3-63
- 3.4.4 Subsidence Over Potash Mines 3-64

4.0 CURRENTLY AVAILABLE DATA FOR ASSESSING LONG-TERM PERFORMANCE . 4-1

4.1 Supra-Rustler Units 4-1

4.2 Rustler Formation 4-1
- 4.2.1 Unnamed Lower Member and Contact Zone with Upper Salado Formation .. 4-1
- 4.2.2 Culebra Dolomite Member 4-6
- 4.2.3 Tamarisk Member 4-15
- 4.2.4 Magenta Dolomite Member 4-15
- 4.2.5 Forty-niner Member 4-19
- 4.2.6 Discussion of Rustler Hydraulic Heads 4-26

4.3 Castile Formation 4-29

4.4 Bell Canyon Formation 4-33

4.5 Formations Below the Bell Canyon Formation 4-33

4.6 Documentation of Experimental Data and Interpretive Techniques 4-17

5.0 REFERENCES 5-0

APPENDIX A: Evolution of Patterns of Regional Groundwater Flow in Southeastern New Mexico; Response to Post-Pleistocene Changes in Climate A-0

1.0 INTRODUCTION

The U.S. Department of Energy (DOE) is preparing to request the U.S. Environmental Protection Agency (EPA) to certify compliance of the Waste Isolation Pilot Plant (WIPP) with long-term requirements of *the environmental Radiation Protection Standards for Management and Disposal of Spent Nuclear Fuel, High-Level and Transuranic Waste* (40 CFR Part 191). The DOE must also demonstrate compliance with the long-term requirements of the *Land Disposal Restrictions* of the *Resource Conservation and Recovery Act* (RCRA) (40 CFR Part 268.6). Sandia National Laboratories (SNL) has been conducting iterative performance assessments (PAs) for the WIPP to provide guidance to the project on the technical activities required to determine long-term performance of the WIPP disposal system. The most recent PA was conducted in 1992.

An effort is under way within the project to prioritize the activities needed to demonstrate with a reasonable expectation that the WIPP will satisfy the relevant quantitative long-term performance requirements. This principal tool used in this effort is referred to as Systems Prioritization Method (SPM).

SPM is a decision-analysis methodology developed for the DOE Carlsbad Area Office (DOE-CAO) by SNL that will identify relationships among schedule constraints, resource constraints, current and proposed technical programs, and the likelihood of demonstrating compliance within these constraints. In particular, the probability that specific combinations of activities will lead to a demonstration of compliance with respect to applicable long-term regulations will be estimated. These activities include experimental programs designed to reduce uncertainty in data and models used to characterize the disposal system for long-term performance assessment, and also include potential modifications to the waste acceptance criteria, waste form, and repository design. The DOE-CAO will use results of future iterations of the SPM in combination with information about time and cost of the various activities to set priorities for WIPP activities and to select a combination of activities that will form the basis for a compliance determination.

In parallel with the SPM, a Project Technical Baseline (PTB) document is being prepared that will contain the technical basis for a compliance application. Technical programs conducted in the period leading up to a final compliance determination may lead to changed or improved understanding in areas critical to defending this determination. The PTB can be updated periodically as required.

In support of both the SPM and the PTB, a series of position papers is being prepared that will document the current understanding of the main components of the disposal system and the long-term performance assessment. This paper addresses hydrology of units other than the Salado Formation, which contains the repository. Specifically, units considered here are the Castile, Bell Canyon, and other formations below the Salado Formation, and the Rustler, Dewey Lake, and other formations above the Salado. Hydrology of these units is relevant to compliance with the long-term requirements of 40 CFR 191. Because the upper and lower boundaries of the disposal unit for 40 CFR 268.6 are defined to be the top and bottom of the Salado Formation, this paper has less relevance to RCRA compliance. Hydrology of the Salado Formation is important for both regulations, and is addressed in a separate position paper.

The objectives of this paper are to:

1) Identify and describe the relationship between non-Salado hydrology and the array of scenarios that might be relevant to the long-term performance of the repository.

2) Identify and describe the array of conceptual and mechanistic models that are required to evaluate the scenarios for the purpose of compliance.

3) Identify and describe the data/information that are required to support the conceptual and mechanistic models.

4) Identify conceptual and computational models and appropriate parameter values for use in the second iteration of the SPM.

The scenarios that involve non-Salado hydrology are summarized in Section 2. The conceptual and mechanistic models are described in Section 3. Section 4 contains a summary of data and information that is presently available for use in a compliance application. Objective 4 will be addressed after the positions regarding conceptual and mechanistic models are finalized.

2.0 FEATURES, EVENTS, AND PROCESSES INVOLVING NON-SALADO HYDROLOGY

This section summarizes the features, events, and processes (FEPs) that form the basis of scenarios involving groundwater flow and radionuclide transport in the non-Salado units. Authors of this paper reviewed the Draft Position Paper for Scenario Development for Postclosure Performance dated September 9, 1994 and did not identify any additional FEPs to be included. FEPs considered in this paper are therefore those described in the Scenario Development Position Paper that involve the non-Salado units and have been retained by the Scenario Development Team for further evaluation.

All FEPs relevant to non-Salado flow and transport result directly from, or require as prerequisites, either disruptive events due to future human actions or a failure of the sealing system that will be emplaced in the shafts that access the waste disposal region. As discussed in the Scenario Development Position Paper, no FEPs have been identified that will result in the migration of radionuclides to the non-Salado units in the absence of disruptive events or seal failure. Potentially disruptive events include drilling for natural resources, mining, and other human activities. Disruptive events must occur before the effects on flow and transport in the non-Salado units of natural processes such as climate change become relevant to disposal-system performance.

Disruptive events shown in previous analyses (e.g., WIPP PA Department, 1992, Volume 1, Section 5) to have the greatest potential to affect disposal-system performance involve drill holes that penetrate a disposal room and thereby provide a pathway for brines to carry radionuclides to the surface or to hydraulically conductive strata located above or below the repository. Once introduced into the conductive strata, the radionuclides potentially could migrate laterally to the accessible environment or to another drill hole. Vertical movement of fluids in drill holes, regardless of whether the drill holes intersect the repository, could potentially modify the flow field and/or the retardation properties of the strata. These modifications could occur because of physical processes, i.e., change the pressure, density, or phase of fluids in the penetrated strata, or because of rock-water interactions that change the porosity, permeability, or retardation properties of the rock. Drill holes that are used to withdraw or inject fluid could potentially have a greater impact than those that do not because injection or withdrawal could increase flow rates and/or inadvertently introduces fluids with compositions different from natural waters. Inadvertent high pressure injections could also fracture brittle units and enhance or create migration pathways. In any case, the largest impact of injection or withdrawal wells would occur during the time the well was in active use and in the time following during which the system returns to pre-disruption conditions.

Fluids could potentially move into or out of a number of stratigraphic units above the repository (conductive zones in the Dockum Group and the Dewey Lake Formation, if these units become saturated, and the Rustler Formation) or conductive units below the repository (Castile and Bell Canyon Formations and deeper rocks). The rate at which fluids move vertically in drill holes depends mainly on the permeability, porosity, compressibility, and hydraulic head of the conductive zones connected by the drill hole, as well as the permeability of the drill hole, if plugged or closed. The permeability and hydraulic head of the conductive units are considerably different, and many flow paths are possible depending on the position, depth, and time of the drill holes. Heads at some locations in the Castile Formation and deeper rocks are high enough to drive fluid to the land surface.

Consequently, fluids could move up boreholes from these units to the repository, if it were not highly pressurized, or to conductive units above the repository.

As discussed in the Scenario Development Position Paper, climate change is the principal natural process currently considered relevant to non-Salado flow and transport. A change in climate could impact the amount of moisture that infiltrates into the soil and is thereby available to recharge the groundwater system. Patterns and rates of groundwater flow are determined partly by the amount and distribution of recharge. Vegetational changes could also impact infiltration rates, but this FEP has been screened out on the basis of low consequence.

3.0 CONCEPTUAL AND MECHANISTIC MODELS INVOLVING NON-SALADO HYDROLOGY

This section describes or refers to the conceptual and mechanistic models used to evaluate features, events, and processes (FEPs) involving flow and transport in stratigraphic units other than the Salado Formation. This paper adopts a modular approach in which we describe conceptual and mechanistic models for the individual aspects of the flow and transport system. These modules can be combined, as required, to evaluate particular FEPs.

One example, to illustrate the modular approach, is the treatment of an intrusion borehole penetrates the repository and provides a pathway for radionuclides to move upward to the Culebra dolomite and then migrate laterally in the Culebra toward the accessible environment. Evaluation of scenarios including this event require a conceptual model of flow above the Salado, a model for fluid flowing from an intrusion hole, models for determining distributions for transmissivity, storage, and representative head gradients for the Culebra, and a suite of conceptual and mechanistic models to describe physical and chemical retardation along the flow path. These models are discussed separately in this paper, rather than in a linked sequence as they appear in performance assessment system-level modeling.

Each model description in this chapter contains a summary statement that presents the position supported and a discussion section that details the supporting reasoning and data. Conceptual and mechanistic models are divided into four Sections. Section 3.1 contains a basic description of the hydrostratigraphy and models that describe processes or considerations that apply to multiple stratigraphic units. Section 3.2 includes models that address flow and advective transport in the Culebra. Section 3.3 includes models that deal with chemical retardation. The final section, 3.4, addresses long-term processes that could impact performance of the repository during 10,000 years.

3.1 Hydrostratigraphy and Regional Groundwater Flow

3.1.1 Stratigraphy and Lithology in the Vicinity of the WIPP Site

This section presents the stratigraphy and lithology of the Paleozoic and younger rocks underlying the WIPP site and vicinity (Figures 3.1.1-1 and 3.1.1-2), emphasizing the units nearer the surface and excluding the Salado Formation which is discussed in a separate document. Details begin with the Permian (Guadalupian) Bell Canyon Formation, the upper unit of the Delaware Mountain Group, because this is the uppermost water-bearing formation below the evaporites that host the WIPP repository. The principal stratigraphic data are the chronologic sequence, age, and extent of rock units, including some of the nearby, relevant facies changes. Characteristics such as

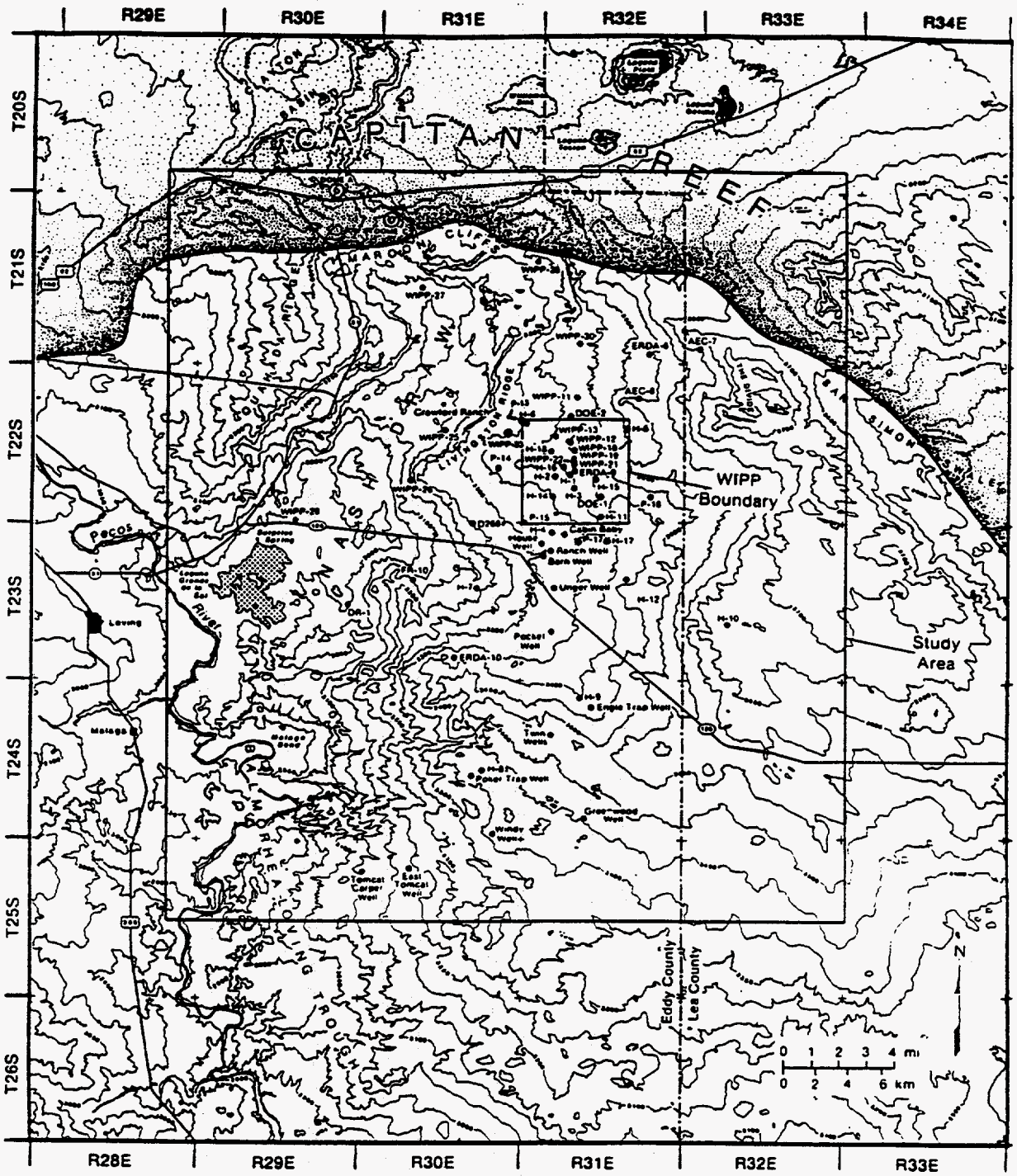

Figure 3.1.1-1. Surface topography and drillholes near the WIPP site.

System	Series	Group	Formation	Member
Recent	Recent		Surficial Deposits	
Quater-nary	Pleisto-cene		Mescalero Caliche	
			Gatuña	
Triassic		Dockum	Undivided	
Permian	Ochoan		Dewey Lake Red Beds	
			Rustler	Forty-niner
				Magenta Dolomite
				Tamarisk
				Culebra Dolomite
				unnamed
			Salado	
			Castile	
	Guadalupian	Delaware Mountain	Bell Canyon	
			Cherry Canyon	
			Brushy Canyon	

TRI-6330-89-1

Figure 3.1.1-2. Stratigraphic column for the WIPP vicinity.

thickness and depth are summarized here from published sources for deeper rocks and are mainly based on WIPP data for shallower rocks (above Bell Canyon). The main lithologies for upper formations and members of some formations are described. Some of the systems (e.g., Jurassic) are not described because they do not occur at or near the WIPP Site.

3.1.1.1 GENERAL STRATIGRAPHY AND LITHOLOGY BELOW THE BELL CANYON FORMATION

The most thorough summaries of the formations and lithologies below the Bell Canyon for the site area have been prepared by Foster (1974) and Powers et al. (1978). This section is modified from those sources; the details of these units are scattered and often exist as raw data in geophysical logs or files of government agencies. Some stratigraphic detail is given as support for later discussions of hydrocarbon resources from units below the Bell Canyon.

The known Precambrian basement near the site is projected to be about 18,191 feet (5,545 meters) below the surface (Sipes, Williamson & Aycock, 1976, Vol. II, Exhibit No. 2), consistent with information presented by Foster (1974). Ages of similar metamorphic suites in the area range from about 1.14 to 1.35 billion years.

The basal units overlying Precambrian rocks are clastic rocks commonly attributed either to the Bliss Sandstone or the Ellenberger Group (Foster, 1974, p. 10ff), considered most likely to be Ordovician in age in this area. The Ordovician System comprises the Ellenberger, Simpson, and Montoya Groups in the northern Delaware Basin. Carbonates are predominant in these groups, with sandstones and shales common in the Simpson Group. Foster (1974, p. 12) reported 975 feet (297 meters of Ordovician north of the site area and extrapolated a thicker section of about 1,300 feet (396 meters) at the present site (p. 17). Sipes, Williamson & Aycock, Inc. (1976, Vol. II, Exhibit No. 2) projected a thickness of 1,200 feet (366 meters) within the site boundaries.

Silurian-Devonian rocks in the Delaware Basin are not stratigraphically well-defined, and there are various notions for extending nomenclature into the basin. Common drilling practice is not to differentiate, though the Upper Devonian Woodford Shale at the top of the sequence is frequently distinguished from the underlying dolomite and limestone (Foster, 1974, p. 18). Foster (p. 21) showed a reference thickness of 1,260 and 160 feet for the carbonates and the Woodford shale, respectively; he estimated thickness contours for the present WIPP site of about 1,150 (351 meters) and 170 feet (52 meters), respectively. Sipes, Williamson & Aycock, Inc. (1976) projected 1,250 feet (381 meters) of carbonate and showed 82 feet (25 meters) of Woodford.

The Mississippian System in the northern Delaware Basin is commonly attributed to "Mississippian limestone" and the overlying Barnett Shale (Foster, 1974, p. 24), but the nomenclature is not well-settled. At the reference well used by Foster (p. 25), the limestone is 540 feet (165 meters) thick and the shale is 80 feet (24 meters); isopachs at the WIPP are 480 feet (146

meters) and less than 200 feet (61 meters). Sipes, Williamson & Aycock (1976) indicate 511 feet (156 meters) and 164 feet (50 meters), respectively, within the site boundaries.

The nomenclature of the Pennsylvanian System applied within the Delaware Basin is both varied and commonly not technically consistent with accepted stratigraphic rules. Chronostratigraphic or time-stratigraphic names are applied to these lithologic units: the Morrow, Atoka, and Strawn, from base to top (Foster, 1974, p. 31). Foster (1974, p. 34) extrapolated thicknesses of about 2,200 feet (671 meters) for the Pennsylvanian at the WIPP site. Sipes, Williamson & Aycock , Inc. (1976, Vol. II, Exhibit No. 2) report 2,088 feet (636 meters) for these units. The Pennsylvanian rocks in this area are mixed clastics and carbonates, with carbonates more abundant in the upper half of the sequence.

The Permian System is the thickest system in the northern Delaware Basin, and is divided into four series from the base to top: Wolfcampian, Leonardian, Guadalupian, and Ochoan. The three lower series total 8,684 feet (2,647 meters) near the site (Sipes, Williamson & Aycock, Inc., 1976). Foster (1974) indicates a total thickness for the lower three series of about 7,665 feet (2,336 meters) for a reference will north of WIPP. Foster's isopach maps of these series indicate about 8,500 feet (2,591 meters) for the WIPP site area. The Ochoan Series at the top of the Permian is considered in more detail later because the formations host and surround the WIPP repository horizon. Its thickness at DOE-2, about 2 miles north of the site center, is 3,938 feet (1,200 meters) (Mercer et al., 1987, p. 23-24).

The Wolfcampian Series is also referred to as the Wolfcamp Formation in the Delaware Basin. In the site area, the lower part of the Wolfcamp is dominantly shale with carbonate and some sandstone (Foster, 1974, p. 38); carbonate increases to the north. Clastics increase to the east toward the margin of the Central Basin Platform. The Wolfcamp is 1,493 feet (455 meters) thick at a well near the WIPP site (Sipes, Williamson & Aycock, Inc., 1976).

The Leonardian Series is represented by the Bone Spring Limestone or Formation (erroneously called Bone Springs Limestone in many publications). The lower part of the formation is commonly interbedded carbonate, sandstone, and some shale, while the upper part is dominantly carbonate (Foster, 1974, p. 39). Near the site, the Bone Spring is 3,247 feet (990 meters) thick (Sipes, Williamson & Aycock, In., 1976).

The Guadalupian Series is represented in the general area of the site by a number of formations exhibiting complex facies relationships. The Guadalupian Series is known in considerable detail west of the site from outcrops in the Guadalupe Mountains, where numerous outcrops and subsurface studies have been undertaken, including King (1948), Newell et al. (1953), Dunham (1972), and many others. From the site to the north, similar facies relationships are expected, though mainly in the subsurface (Garber et al., 1989, p. 36).

Within the Delaware Basin, the Guadalupian Series comprises three formations: Brushy

Canyon, Cherry Canyon, and Bell, Canyon, from base to top. These formations are dominated by submarine channel sandstones with interbedded limestone and some shale. A limestone (Lamar) generally tops the series, immediately underneath the evaporative Castile Formation. Around the margin of the Delaware Basin, reefs developed during the same time the Cherry Canyon and Bell Canyon Formations were being deposited. These massive reef limestones, the Goat Seep and Capitan Limestones, are equivalent in time to these basin sandstone formations, but were developed much higher topographically around the basin margin. A complex set of limestone to sandstone and evaporate beds was deposited further away from the basin behind the reef limestones. The Capitan reef limestones are well known because the Carlsbad Caverns are partially developed in these rocks.

3.1.1.2 BELL CANYON FORMATION

The Bell Canyon is known from outcrops on the west side of the Delaware Basin (Newell et al., 1953) and from subsurface intercepts for oil and gas drilling. Mercer et al. (1987, p. 28) stated that DOE-2 penetrated the Lamar Limestone, the Ramsey sand, the Ford shale, the Olds sand, and the Hays sand. This informal nomenclature is used for the Bell Canyon in some other WIPP reports.

The Clayton Williams Badger Federal drillhole near the WIPP (Section 15, T22S, R31E) intercepted 961 feet (293 meters) of Bell Canyon, including the Lamar (Sipes, Williamson & Aycock, Inc., 1976). Reservoir sandstones of the Bell Canyon were deposited in channels that are straight to slightly sinuous. Density or acoustic logs are also distinctive because of the massive and uniform lithology of the anhydrite compared to the underlying beds. In cores, the transition is sharp, as described for DOE-2 (Mercer et al., 1987, p. 312).

3.1.1.3 CASTILE FORMATION

The Castile Formation is the lowermost lithostratigraphic unit of the Late Permian Ochoan Series. It was originally named by Richardson (1904) for outcrops in Culberson County, Texas. The Castile crops out along a lengthy area along the western side of the Delaware Basin. The two distinctive lithologic sequences now known as the Castile and Salado Formations were separated into the upper and lower Castile Formation by Cartwright (1930). Lang (1935) clarified the nomenclature by restricting the Castile Formation to the lower unit and naming the upper unit the Salado Formation. By defining an anhydrite resting on the marginal Capitan Limestone as part of the Salado Formation, Lang 91939, 1942) effectively restricted the Castile to the Delaware Basin inside the ancient reef rocks.

Through detailed studies of the Castile, Anderson et al. (1972) introduced an informal system of names that are widely used and included in many WIPP reports. They named the units from the base as anhydrite 1 (A1), halite 1 (H1), anhydrite 2 (A2), etc. The informal nomenclature varies through the basin from A3 up because of complexity of the depositional system. The Castile consists

almost entirely if thick beds of two lithologies: interlaminated carbonate and anhydrite and high-purity halite. The interlaminated carbonate and anhydrite are well known as possible examples of annual layering or varves (Anderson et al., 1972).

In the eastern part of the Delaware Basin, the Castile is commonly 1,400 to 1,500 feet thick (derived from Borns and Shaffer, 1985, Figures 9, 11, 16). At DOE-2, the Castile is 989 feet (301 meters) thick. The Castile is thinner in the western part of he Delaware Basin, and it lacks halite units. Anderson et al. (1978) correlated geophysical logs, interpreting thin zones equivalent to halite units as dissolution residues. Anderson (1981, 1982) further interpreted the lack of halite in the Castile and overlying units as indicating that about 50 percent of the halite in the basin has been removed by dissolution. Robinson and Powers (1987) analyzed one such unit as partly due to synsedimentary, gravity-driven, clastic deposition and suggested that the extent of dissolution may be overestimated. There is not known to be Castile dissolution in the immediate vicinity of the WIPP site.

In Culberson County, Texas, the Castile hosts major native sulfur deposits (Klemmick, 1993; Guilinger, 1993; Crawford and Wallace 1993). The outcrops of Castile on the Gypsum Plain south of Whites City, New Mexico, have been explored for native sulfur without success (Robinson and Powers, 1987), and there is no reported indicator of native sulfur anywhere in the vicinity of the WIPP (Siemers et al., 1978).

In part of the area around the WIPP, the Castile Formation has been significantly deformed, and pressurized brines are associated with the deformed areas (Powers et al., 1978): drillhole ERDA-6 encountered both. WIPP-12, one mile north of the site center, revealed lesser Castile structure, but it also encountered a zone of pressurized brine within the Castile.

The Castile continues to be an object of research interest unrelated to the WIPP program as an example of evaporites supposedly deposited in "deep water" (King, 1947; Anderson et al., 1972). Leslie et al. (1993) discuss alternatives and contradictory evidence. Although these discussions and a resolution might eventually affect some concepts of Castile deposition and dissolution, there is no apparent effect upon evaluation of the isolation of waste by the WIPP disposal system.

3.1.1.4 RUSTLER FORMATION

The Rustler is the youngest evaporite-bearing formation in the Delaware Basin. It was originally named by Richardson (1904) for outcrops in the Rustler Hills of Culberson County, Texas. Adams (1944, p. 1614) first used the names "Culebra member: and Magenta member" to describe the two carbonates in the formation, indicating that Lang favored the names, though Lang (in Robinson and Lang, 1938) did not use these names in the most recent publication. Vine (1963) later described extensively the Rustler in Nash Draw and proposed the four formal names and one informal tern for the stratigraphic subdivisions still used for the Rustler (from the base): unnamed

lower member, Culebra Dolomite Member, Tamarisk Member, Magenta Dolomite Member, and Forty-niner Member. Though it has been noted (Holt and Powers, 1988; Powers and LeMone, 1990, p. 29) that the unnamed lower member might be named the Los Medaños Member, this nomenclature has not been formalized.

An additional system of informal subdivisions was contributed by Holt and Powers (1988), based on more detailed lithologic units of the non-carbonate members. These subdivisions have partially been related to hydrostratigraphic units for the Rustler (Beauheim and Holt, 1990, p. 145).

Two studies of the Rustler since Vine (1963) contribute important information about the stratigraphy, sedimentology, and regional relationships while examining more local details as well. Eager (1983) reported on relationships of the Rustler observed in the southern Delaware Basin as part of sulfur exploration in the area. Holt and Powers (1988) and Powers and Holt (1990) reported the details of sedimentologic and stratigraphic studies of WIPP shafts and cores as well as of geophysical logs from about 600 drillholes in southeastern New Mexico. Various details of the Rustler have also been reported as either a by-product of other investigations or for more limited purposes (Snyder, 1985; Lowenstein, 1988; Sewards et al.. 1991).

Halite in the unnamed lower member broadly persists to the west of the WIPP site, and halite is found east of the center of the WIPP in the Tamarisk and Forty-niner. Two differing depositional models have been generally used, either implicitly or explicitly, to account for the halite distribution. A long-standing and implicit model in many earlier documents (Jones, 1978) is that halite was originally deposited relatively uniformly in the non-carbonate members across southeastern New Mexico, including the WIPP site area. The modern distribution is caused by dissolution of Rustler halite to the west and progressing toward the east (Snyder, 1985). Holt and Powers (1988) and Powers and Holt (1990) described sedimentary features and textures within WIPP shafts and cores that led them to propose an explicit model of depositional facies for the mudstone-halite units; halite was dissolved syndepositionally from mudflat facies especially to the west, and was redeposited in a halite pan to the east.

In the region around WIPP, the Rustler reaches a maximum thickness of more than 500 feet, while it is about 300 to 350 feet thick within most of the WIPP site. Most of the difference between the site area and the thickest areas is the thickness of the halite within Rustler members. The Tamarisk accounts for a larger part of thickness changes than do either the unnamed lower member or Forty-niner.

For the main Rustler study around WIPP (Holt and Powers, 1988), the shafts were a crucial element, exposing features not previously reported. Cores were available from several WIPP boreholes, and their lithologies were matched to geophysical log signatures to extend the interpretation throughout a larger area in southeastern New Mexico. The procedures and results are described in some detail in Holt and Powers (1988).

3.1.1.4.1 Unnamed Lower Member

The unnamed lower member rests on the Salado with apparent conformity at the WIPP site. It consists of significant proportions of bedded and burrowed siliciclastic rocks with cross-bedding and fossil remains (Holt and Powers, 1988; Powers and Holt, 1990, p. 82-83). These beds record the transition form strongly evaporative environments of the Salado to saline lagoonal environments. The upper part of the unnamed lower member includes halitic and sulfatic beds within clastics. Holt and Powers (1988) interpret these as facies changes within a saline playa environment. The implied model from earlier descriptions (Jones, 1978) is that the non-halitic of the upper unnamed lower member are dissolution residues from post-depositional dissolution.

The unnamed lower member ranges from about 96 to 126 feet thick within the site boundaries (Holt and Powers, 1988, Figure 4.7). The maximum thickness recorded during that study was 208 feet southeast of the WIPP site. Halite extends west of most of the site area in this unit (Snyder, 1985; Powers, in Beauheim, 1987). Cross sections based on geophysical log interpretations (Holt and Powers, 1988, Figure 4.4) show some apparent relationship between the thickness of the unit and the presence of halite.

Some samples from the unnamed lower member have been analyzed to determine clay mineralogy (Sewards et al., 1991, Table 2) and Rb-Sr systematics of clays (Brookins et al., 1990). Brookins et al. (1990, p. 4) concluded that Rb-Sr ages of clay fractions are consistent with a Late Permian age, and they also contrasted Rustler clays with Salado data. Salado clays show Rb-Sr ages and characteristics indicating more limited interaction with water and less alteration of detrital clays during Permian than do Rustler clays.

3.1.1.4.2 Culebra Dolomite Member

The Culebra rests with apparent conformity on the unnamed lower member, though the underlying unit ranges from claystone to its lateral halitic equivalent in the site area. West of the WIPP site, in Nash Draw, the Culebra is disrupted in response to dissolution of underlying halite. Holt and Powers (1988) attribute this principally to dissolution of Salado halite, while Snyder (1985) indicates that salt was dissolved postdepositionally from the unnamed lower member. These alternative models provide the basis for differing explanations of how the existing explanations of how the existing Rustler hydrologic system developed and might continue to develop. The regulatory period of concern is short enough and boundaries close enough that these differences may not affect performance assessment.

The Culebra was described by Lang (Robinson and Lang, 1938) as a dolomite 35 feet in thickness; Adams (1944, p. 78) noted that oolites are present in some outcrops as well. The Culebra is generally "brown, finely crystalline, locally argillaceous and arenaceous dolomite with rare to abundant vugs with variable gypsum and anhydrite filling" (Holt and Powers, 1988,

p. 3-8). Holt and Powers (1988, p. 5-11) described Culebra features in detail, noting that most of the Culebra is microlaminated to thinly laminated while some zones display no depositional fabric. Holt and Powers (1984) described an upper interval of the Culebra consisting of waxy, golden-brown carbonate, dark organic claystone, and some coarser siltstone of probable algal origin. Because of the unique organic composition of this thin layer, Holt and Powers (1988) did not include it in the Culebra for thickness computations, and this will be factored into discussions of Culebra thickness. Based on core descriptions from the WIPP project, Holt and Powers (1988, p. 5-11 concluded that "there is very little variation of depositional sedimentary features throughout the Culebra."

Vugs are an important part of Culebra porosity. They are commonly zoned parallel to bedding (Holt and Powers, 1990). In outcrop, bugs are commonly empty. In the subsurface, bugs may be filled with anhydrite, gypsum, or may have some clay lining (Holt and Powers, 1988, p. 5-11). Lowenstein 1988, (p. 20-21) noted similar features. Holt and Powers (1988, p. 8-4) attributed vugs partly to syndepositional growth as nodules and partly as later replacement textures. Lowenstein (1988) also described textures related to later replacement and alteration of sulfates. Vug or pore fillings vary across the WIPP site and contribute to the porosity structure of the Culebra (Beauheim and Holt, 1990, p. 157). Natural fractures filled with gypsum are common east of the WIPP site center and in a smaller area west of the site center.

Clay is reported as the second most abundant mineral (averaging about 3 to 5 weight percent and ranging from < 1 percent to about 60 percent of bulk samples) of the Culebra, after dolomite, by Sewards et al. (1991; p. IX-1). Clay minerals include corrensite, illite, serpentine, and chlorite. Sewards et al. (1991) examined clay from bulk rock and mainly horizontal fractures in 18 Culebra samples. Clay proportions in bulk rock ranged from 0.67 to 83.77 weight percent (normalized calculations) while in fracture surfaces clay ranged from 0.90 to 54.99 weight percent. Sewards et al. (1991, p. VIII-1) concludes that high cation exchange capacity for clay and the significant proportion of clays within the Culebra are important factors affecting the transport of radionuclides through the Culebra.

In a study of probable authigenic clays from the Rustler, including the Culebra, Brookins et al. (1990), found the Rb-Sr isochron of 259 ± 22 Ma consistent with the Late Permian age of the Rustler. These results indicate that there was not a significant interaction of high-Sr water with these clays since the Late Permian (Brookins et al., 1990, p. 4).

In the WIPP site area, the Culebra varies in thickness. The choice of Culebra thickness and saturated interval are important hydrological parameters for performance assessment. Different data sources provide varying estimates as well (Table 2-2). Holt and Powers (1988) considered the organic-rich layer at the Culebra-Tamarisk contact separately from the Culebra in interpreting geophysical logs. Comparing data sets, Holt and Powers typically interpret the Culebra as about 1 meter thinner than have other sources, including Jones (1978), Richey (1989), and LaVenue et al. (1988). In general, this reflects the difference between including or excluding the unit at the Culebra-Tamarisk contact. Each data set shows areal differences in thickness of the Culebra when

examined township by township.

LaVenue et al. (1988, Appendix B) calculated a mean thickness of 7.7 meters for the Culebra based on 78 drillholes. This thickness has been used uniformly for the Culebra in performance assessment calculations.

3.1.1.4.3 Tamarisk Member

Vine (1963, p. B15) named the Tamarisk Member for outcrops near Tamarisk Flat in Nash Draw. Outcrops of the Tamarisk are distorted, and subsurface information was used to establish member characteristics. Vine reported two sulfate units separated by a siltstone, about 5 feet thick, interpreted by Jones et al. (1960) as a dissolution residue.

The Tamarisk is generally conformable with the underlying Culebra. The transition is marked by an organic-rich unit interpreted as present over most of southeastern New Mexico (Holt and Powers, 1988). The Tamarisk around the site area consists of lower and upper sulfate units separated by a unit that varies from mudstone (generally to the west) to mainly halite (to the east) (Holt and Powers, 1988, p. 5-12). Near the center of the WIPP site, the lower anhydrite was partially eroded during deposition of the middle mudstone unit, as shown in the WIPP Waste Handling and Exhaust Shafts (Holt and Powers, 1984, 1986a). The lower anhydrite was completely eroded at WIPP-19 (Holt and Powers, 1988, p. 5-17). Before shaft exposures were available, the lack of the lower Tamarisk anhydrite at WIPP-19 was interpreted as the result of solution and the mudstone was considered a cave filling (Ferrall and Gibbons, 1980).

Halite is interpreted to be present east of the center of the WIPP site based on geophysical logs and drilling cuttings (Jones, 1978). Based mainly on cores and cuttings records from the WIPP potash drilling program, Snyder (1985) prepared a map showing the halitic areas of each of the noncarbonate Rustler members. A very similar map was prepared independently by Powers (Beauheim, 1987) based on geophysical log characteristics.

Holt and Powers (1988, p. 5-14) described the mudstones and halitic facies in the middle of the Tamarisk, and they interpreted the unit as formed in a salt pan to mudflat system. They cited sedimentary features and the lateral relationships as evidence of syndepositional dissolution of halite in the marginal mudflat areas. In contrast, earlier authors (Jones et al., 1960; Jones, 1978; Snyder, 1985) interpreted the lateral decrease in thickness and absence of halite to the west as evidence of post-depositional dissolution. The differing concepts for halite distribution in the Rustler, and particularly the Tamarisk, have been used in explaining the large changes in hydrologic properties of the Culebra, as explained in later sections.

The Tamarisk thickness varies greatly in southeastern New Mexico, principally as a function of the thickness of halite in the middle unit (Holt and Powers, 1988, Figures 4.9 and 4.11).

Within T22S, R31E, Holt and Powers (1988, Figure 4-9) show a range from 84 to 184 feet (26-56 meters) for the entire Tamarisk and a range from 6 to 110 feet (2-34 meters) (Holt and Powers, 1988, Figure 4.11) for the interval of mudstone-halite between lower and upper anhydrites. Areas on these maps with thickness greater than about 100 feet and 20 feet, respectively, correspond to halitic regions of the Tamarisk.

3.1.1.4.4 Magenta Dolomite Member

Adams (1944, p. 1614) attributes the name "Magenta member" to Lang, based on a feature north of Laguna Grande de la Sal named Magenta Point. The Magenta is a gypsiferous dolomite with abundant primary sedimentary structures and well-developed algal features (Holt and Power, 1988, p. 5-22ff). It does not vary greatly in sedimentary features across the site area (Holt and Powers, 1988, p. 5-22).

Around the WIPP site, Holt and Powers (1988, p. 5-22) reported that the Magenta varies from about 23 to 28 feet (7 to 8.5 meters); they did not contour the thickness because of the limited changes.

3.1.1.4.5 Forty-niner Member

Vine named the Forty-niner Member for outcrops at Forty-niner Ridge in eastern Nash Draw, but the outcrops of the Forty-niner are poorly exposed. In the subsurface around the WIPP, the member consists of basal and upper sulfates separated by a mudstone (Holt and Powers, 1984). It is conformable with the underlying Magenta. As with other members of the Rustler, geophysical log characteristics can be correlated with core and shaft descriptions to extend the geological inferences across a large area (Holt and Powers, 1988).

The Forty-niner ranges from 43 to 77 feet (13 to 23 meters) thick within T22S, R31E (Holt and Powers, 1988, Figure 4.13). East and southeast of the WIPP, the Forty-niner exceeds 80 feet (24 meters) in thickness, and some of the geophysical logs from this area indicate halite is present in the beds between the sulfates (Holt and Powers, 1988, Figure 4.3).

Within the Waste Handling Shaft, the Forty-niner mudstone displayed sedimentary features and bedding relationships indicating sedimentary transport (Holt and Powers, 1984). The mudstone has been commonly interpreted as a residue from the dissolution of halitic beds (Jones, 1978) because it is thinner where there is no halite. These beds are not known to have been described in detail prior to mapping in the Waste Handling Shaft at WIPP, and the features found there led Holt and Powers (1984, 1988) to re-examine the available evidence for, and interpretation of, dissolution of halite in Rustler units.

3.1.1.5 DEWEY LAKE (RED BEDS)

The nomenclature for rocks included in the Dewey Lake Formation (or alternatively, Dewey Lake Red Beds) was introduced during the 1960s to clarify relationships between these rocks assigned to the Upper Permian and the Cenozoic Gatuña Formation (see discussions by Schiel, 1994; Powers and LeMone, 1987). More recently, Lucas and Anderson (1993a) have suggested using the name Quartermaster Formation in place of Dewey Lake based on similar lithology and earlier usage. The Dewey Lake is retained here for WIPP project usage until the utility of using Quartermaster is clearer.

There are three main sources of data about the Dewey Lake in the area around the WIPP. Miller (1955, 1966) studied the petrology of the unit. Schiel (1988, 1994) described outcrops in the Nash Draw areas and interpreted geophysical logs of the unit in southeastern New Mexico and west Texas to infer the depositional environments and stratigraphic relationships. Holt and Powers (1990) were able to describe the Dewey Lake in detail at the Air-Intake Shaft for WIPP, confirming much of Schiel's information and adding data regarding the lower Dewey Lake.

The Dewey Lake overlies the Rustler conformably (Bachman, 1984), though local examples of the contact (e.g., Air-Intake Shaft, Holt and Powers, 1990) show minor disruption by dissolution of some of the upper Rustler sulfate. The formation is predominately reddish-brown fine sandstone to siltstone or silty claystone with greenish-gray reduction spots. Thin bedding, ripple cross-bedding, and larger channeling are common features in outcrops (Schiel, 1988), and additional soft sediment deformation features and early fracturing are described from the lower part of the formation (Holt and Powers, 1990). Schiel (1988, 1994, p. 10) attributed the Dewey Lake to deposition on "a large, arid fluvial plain subject to ephemeral flood events."

There is little direct faunal or radiometric evidence of the age of the Dewey Lake. It is assigned to the Ochoan Series of Late Permian age (Hills and Kottlowski, 1983), and it is regionally correlated with units of similar lithology and stratigraphic position. Schiel (1988, 1994) reviewed the limited radiometric data from lithologically similar rocks (Quartermaster Formation) and concluded that much of the unit could be Early Triassic in age.

Near the center of the WIPP site, Holt and Powers (1990, Figure 5) mapped 498 feet (152 meters) of Dewey Lake. The formation is thicker to the east (Schiel, 1988, 1994, p.6) of the WIPP site, in part because western areas were eroded before the overlying Triassic rocks were deposited.

The Dewey Lake is extensively fractured, and both cements and fracture fillings have been further examined to ascertain the possible contributions of surface infiltration to underlying units. Holt and Powers (1990, p. 3-8ff) described the Dewey Lake as cemented by carbonate above 164.5 feet in the Air-Intake Shaft: some fractures in the lower part of this interval were also filled with carbonate, and the entire interval surface was commonly moist. Below this point, the cement is harder (probably anhydrite), the shaft is dry, and fractures are filled with gypsum. Holt and Powers

suggested the cement change might be related to infiltration of meteoric water. They also determined that some of the gypsum-filled fractures are syndepositional (1990 p. 3-11, Figure 16). Dewey Lake fractures include horizontal to subvertical trends some of which were mapped in detail (Holt and Powers, 1986, Figures 6-8).

Lambert (1991, p. 5-65) analyzed the deuterium/hydrogen (D/H) ratios of gypsum in the Rustler and gypsum veins in the Dewey Lake. He suggests that none of the gypsum formed from evaporitic fluid such as Permian seawater, but that they all show influence of meteoric water. Nonetheless, Lambert (1991, p. 5-66) also infers that the gypsum D/H is not consistent with modern meteoric water; it may be consistent with earlier meteoric fluids. There is no obvious correlation with depth indicating infiltration. Strontium isotope ratios ($^{87}Sr/^{86}Sr$) indicate no intermixing or homogenization of fluids between Rustler and Dewey Lake (Lambert, 1991, p.5-54), but there may be lateral movement of water within the Dewey Lake. Dewey Lake carbonate vein material shows a broader range of Sr ratios than does surface caliche, and the ratios barely overlap (Lambert, 1991, Figure 5-17). In general, it is possible, but not necessary, to interpret the Sr ratios of Dewey Lake veins as the result of mixing between fluids with Rustler and surficial ratios. There are no analyses of Dewey Lake host rock to further limit this inference because carbonate and sulfate are not common rock mineral constituents: cements have not been separated and analyzed.

3.1.1.6 SANTA ROSA

There have been different approaches to the nomenclature of rocks of Triassic age in Southeastern New Mexico. Bachman (1974) generally described the units as "Triassic, undivided" or as the Dockum Group, without dividing it. Vine (1963) used "Santa Rosa Sandstone," and Santa Rosa has become common usage. Lucas and Anderson (1993b) import other formation names that are unlikely to be useful for WIPP.

The Santa Rosa has been called disconformable over the Dewey Lake (Vine, 1963, p.B25; Lucas and Anderson, 1993b, p. 232). These rocks have more variegated hues than the underlying uniformly colored Dewey Lake. Coarse-grained rocks, including conglomerates are common, and the formation includes a variety or cross-bedding and sedimentary features (Lucas and Anderson, 1993b).

Within the WIPP site boundaries the Santa Rosa is relatively thin to absent. At the Air-Intake Shaft, Holt and Powers (1990, Figure 5) attributed about 2 feet (0.6 meters) of rock to the Santa Rosa. The Santa Rosa is a maximum of 255 feet (78 meters) thick in potash holes drilled for WIPP east of the site boundaries (Jones, 1978, table 20B). The Santa Rosa is thicker to the east.

3.1.1.8 GATUÑA FORMATION

Lang (in Robinson and Lang, 1938) named the Gatuña for outcrops in the vicinity of Gatuña Canyon in the Claystone Basin. Rocks now attributed to the Gatuña in Pierce Canyon were once included in the "Pierce Canyon Formation" with rocks now assigned to the Dewey Lake. The formation has been mapped from the Santa Rosa, New Mexico, area south tot he vicinity of Pecos, Texas. It unconformably overlies different substrates.

Vine (1963) and Bachman (1974) provided some limited description of the Gatuña. The most comprehensive study of the Gatuña is by Powers and Holt (1993), based on WIPP investigations and landfill studies for Carlsbad and Eddy County. Much of the formation is colored light reddish brown. It is broadly similar to the Dewey Lake and Santa Rosa, though the older units have more intense hues. The formation is highly variable, ranging from coarse conglomerates to claystones with some highly gypsiferous sections. Sedimentary structures are abundant. Analysis of lithofacies indicates that the formation is dominantly fluvial in origin with areas of low-energy deposits and evaporitic minerals. It was deposited in part over areas actively subsiding in response to dissolution (Powers and Holt, 1993, p. 280).

The thickness of the Gatuña is not very consistent regionally. Powers and Holt (1993) report thicknesses up to about 300 feet (91 meters) at Pierce Canyon, with thicker areas generally subparallel to the Pecos River. To the east, the Gatuña is thin or absent. Holt and Powers (1990) reported about 9 feet (2.7 meters) of undisturbed Gatuña inn the Air-Intake Shaft.

The Gatuña has been considered to be Pleistocene in age based on a volcanic glass in the upper Gatuña (Bachman, 1980) that has been identified as the Lava Creek B ash dated at 0.6 million years (Izett and Wilcox, 1982). An additional volcanic ash from Gatuña in Texas yields consistent K-Ar and geochemical data, indicating it is about 13 Ma (Powers and Holt, 1993, p. 272). Thus the Gatuña ranges in age over a period of time that may be greater than the Ogallala Formation on the High Plains east of WIPP.

3.1.1.8 MESCALERO CALICHE

The Mescalero caliche is an informal stratigraphic unit apparently first explicitly used by Bachman (1974), though Bachman (1973, p. 17) described the "caliche on the Mescalero Plain." He differentiated the Mescalero from the older, widespread Ogallala caliche or capric on the basis of textures, noting that breccia and pisolitic textures are much more common in the Ogallala. The Mescalero has been noted over significant areas in the Pecos drainage, including the WIPP site area (Bachman, 1981), and it has been formed over a variety of substrates.

Bachman described the Mescalero as a two part unit: (1) an upper dense laminar capric, and (2) a basal, earthy to firm, nodular calcareous deposit. Machette (1985, p.5) classified the Mescalero as having Stage V morphologies of a calcic soil (the more mature Ogallala capric reaches Stage VI).

Bachman (1076, p. 148) provided structure contours on the Mescalero caliche for a large area of southeastern New Mexico, including the WIPP site. From the contours and Bachman's discussion of the Mescalero as a soil, it is clear that the Mescalero is expected to be continuous over large areas. Explicit WIPP data are limited mainly to drillholes, though some drillhole reports do not mention the Mescalero. The unit may be as much as 10 feet (3 meters) thick (Bachman, 1985, p. 19).

The Mescalero was inferred on basic stratigraphic and climatic grounds as having accumulated during the early to middle Pleistocene (Bachman, 1974, 1980). Bachman (1980) reported finding a volcanic ash in the upper Gatuña along Livingston Ridge and underlying the Mescalero. This original report that this was the Pearlette "O" ash was superseded when Izett and Wilcox (1982) reported the ash as Lava Creek B, about 0.6 Ma.

The Mescalero must therefore be younger. Samples of the Mescalero from the vicinity of the WIPP were studied using uranium-trend methods (Rosholt and McKinney, 1980). Based on early written communication from Rosholt, Bachman (1985, p. 20) reports that the basal Mescalero began to form about 510,000 years ago and the upper part began to form about 410,000 years ago; these ages are commonly cited in WIPP literature. The samples are interpreted by Rosholt and McKinney (1980) in the formal report as indicating ages of 570,000 ± 110,000 years for the lower part of the Mescalero and 420,000 ± 60,000 years for the upper part.

Based on morphology of caliche along part of the souther rim of Pierce Canyon, Hawley (1993) has argued that some of the caliche within the Delaware Basin may be Ogallala instead of Mescalero. This question has not been further addressed.

The Mescalero, as a soil, indicates a stable surface on which it can develop (Bachman, 1985, p. 19). It is considered relevant to paleoclimatic considerations and as an indicator of stability or integrity of the WIPP site (Powers et al., 1978, p. 4-8). Bachman (1985, p. 27) considered the Mescalero as an impediment to erosion; the discussion by Bachman indicates the Mescalero is an indicator of surface stability over the last 500,000 years.

3.1.1.9 SURFICIAL SEDIMENTS

Above the Mescalero caliche, the Kermit and Berino soil series have been mapped across the WIPP site (Chugg et al., 1952, sheet number 113). These are sandy soils developed on eolian material (Chugg et al., 1952, pp. 16, 25). The Kermit-Berino soils include active dune areas. The Berino has a sandy A horizon; the B horizons include more argillaceous material and weak to moderate soil structures. A and B horizons are described as non-calcareous, and the underlying C horizon is commonly caliche. Bachman (1980) interpreted the Berino soil as a paleosol that is a remnant B horizon of the underlying Mescalero.

Rosholt and McKinney (1980) applied uranium-trend methods to samples of the Berino

from the WIPP site area. They interpreted the age of formation of the Berino as 330,000 ± 75,000 years. Though this is generally consistent with the age of the underlying Mescalero, it is not understood why the ages are not closer if the Berino formed at the same time as the Mescalero.

3.1.2 Conceptual Models of Groundwater Flow Above the Salado Formation

Summary Statement: There are two conceptual models of groundwater flow in strata above the Salado Formation, the confined model and the groundwater basin model. The confined model considers only flow in individual stratigraphic units with relatively high hydraulic conductivity. The groundwater basin model considers flow in all units, including those with extremely low hydraulic conductivity, as part of a single hydrologic system. In a practical sense, these models are complementary. **The groundwater basin model better represents the real groundwater flow system, but the confined model is a justified, and perhaps necessary, simplification for use in some PA flow and transport calculations.**

Discussion: There are two conceptual models of groundwater flow in strata above the Salado Formation, the confined model and the groundwater basin model. The first, the confined model, focuses on lateral flow in the relatively more permeable units. It is an empirical model in that it is based primarily on hydrologic and geochemical data collected as part of the site characterization process. For example, the present day north to south flow in the Culebra can be established by hydraulic head data without knowing the locations of discharge and recharge areas. This model recognizes that there appears to be a potential for vertical flow across confining layers but assumes that this flow can be neglected except in regions where the confining units have been disturbed and are more permeable. This conceptual model is the basis for the 1992 PA calculations of flow and transport in the Culebra Dolomite. The domain of this conceptual model is thought to be a subdomain of the hydrologic system that controls its behavior and, therefore, calculations based on this model require boundary conditions that represent hydrologic processes outside of the model domain. For example, heads along a portion of the boundary were raised or lowered to simulate the effects of climate change on recharge to the flow system in the 1992 PA (Swift et al., 1994).

The second model is based on the concept of the groundwater basin. This conceptual model has a strong theoretical basis (Hubbert, 1940; Tóth, 1963; Freeze and Witherspoon, 1967) and is widely accepted and applied by hydrogeologists. A groundwater basin is a three-dimensional, closed hydrologic unit bounded on the bottom by an "impermeable" rock unit (actually a stratigraphic layer with much smaller permeability than the layers above), on the top by the ground surface, and on the sides by groundwater divides. The upper boundary of the flow domain is the water table, which may or may not coincide with the land surface. All rocks in the basin have finite permeability, i.e., hydraulic continuity exists throughout the basin. Implicit in this description of the groundwater basin is that the entire length of each flow path is contained within the basin. All recharge to the basin (if it occurs) is by infiltration of precipitation to the water table, and all discharge from the basin (if it occurs) is by flow across the water table to the land surface.

Differences in elevation of the water table across the basin are assumed to generate the hydraulic gradients to drive groundwater flow. Water flows along gradients of hydraulic head from regions of high head to regions of low head. The highest and lowest heads in the basin occur at the water table at its highest and lowest points, respectively. Therefore groundwater generally flows from the elevated regions of the water table, downward across confining layers (layers with relatively low permeability), laterally along conductive layers (layers with relatively high permeability), and finally upward to exit the basin in regions where the water table (and by association, the land surface) is at low elevations. Infiltration is necessary to maintain relief on the water table. If infiltration were to stop for a sufficient period of time, flow from regions of high to low head would "level" the water table, and groundwater would become stagnant. However, a lack of infiltration rarely, if ever, actually results in stagnant conditions because long periods of time are required for groundwater to "drain" from the regions of higher head. The time required for a system to drain is controlled by the thickness, permeability, and compressibility of confining layers in the basin, as well as the initial relief of the water table. The adjustment time could be tens of thousands of years or longer.

The pattern of groundwater flow depends on the lateral extent and depth of the basin, the shape of the water table, and the heterogeneity of the permeability of the rocks in the basin. Field observations and numerical studies have demonstrated that flow in a conductive layer is parallel to the upper and lower surfaces of the layer and flow in a confining layer is approximately vertical. Even extremely slow vertical flow in confining layers is significant on a regional scale because it is summed over very large horizontal surfaces.

3.1.2.1 VERTICAL FLOW THROUGH RUSTLER CONFINING LAYERS

The issue of whether or not vertical flow occurs through confining layers in the Rustler Formation is pertinent to the evaluation of the two conceptual models. Evidence of zero vertical flow would invalidate the groundwater basin model because it based on the concept of hydraulic continuity. Both models are compatible with the existence of extremely slow vertical flow. Pumping tests and geochemical data have been interpreted to show that vertical flow through Rustler confining units is "insignificant". Hydrologic modeling studies support the existence of extremely slow vertical flow through confining layers. These positions are not necessarily contradictory. The fact that vertical flow is too slow to leave a geochemical signature or to be observed during pumping tests does not mean that it is zero. To date, an argument for zero vertical flow has not been presented. The arguments concerning vertical flow are summarized below.

3.1.2.1.1 Possible Role of Karst Dissolution in Vertical Flow in the Rustler

The term karst is usually applied to regions where dissolution of dolomite and/or limestone has resulted in collapse of the surface, forming a distinctive topography. In the vicinity of the WIPP,

however, the term is applied to features formed by dissolution of evaporites such as halite and anhydrite as well as some carbonates (Bachman, 1987). Brinster (1991) has proposed that Nash Draw, the largest karst feature in southeast New Mexico, was formed by movement of water along regional fracture systems related to the Cenozoic tilting of the Delaware Basin. The intersection of fractures with the Capitan Reef aquifer allowed groundwater undersaturated with respect to gypsum and halite to flow southwestward into the fractured evaporites. The collapse of Nash Draw lowered the base level and allowed the draining of the Rustler units. In Brinster's (1991) interpretation, the processes that formed Nash Draw cannot be repeated because of the removal of most of the Rustler and all of the younger units, but the draining of the hydrostratigraphic units east of the draw continues. As discussed in the following paragraphs, evidence suggests that some karst features have developed east of Nash Draw in the past, and may be continuing to form in the Los Medaños area between the WIPP and Nash Draw.

As is typical of both arid to semi-arid regions with surficial deposits of eolian sand and karst regions where dissolution has created subsurface channels for runoff, there is no well-developed surface-water drainage system at the WIPP. Small intermittent streams lead into depressions that are in some cases eolian blowouts and, in at least one location, a dissolution sinkhole. Northwest of the WIPP and outside the land-withdrawal boundary, the WIPP-33 borehole was drilled in a small depression to test the hypothesis that this was the location of a sinkhole that extended downward through the Salado Formation. When the well showed no abnormalities in the upper Salado, drilling was stopped. However, the borehole showed that almost all the anhydrite in the upper Rustler had been altered to gypsum and that no halite was present. The Magenta appeared to have been almost completely dissolved, the Culebra was highly fractured, and anhydrites below the Culebra were altered to gypsum (Sandia National Laboratories and United States Geological Survey, 1981). Circulation was lost intermittently throughout drilling and tool drops of several feet were noted. About 1500 m to the northeast at borehole P-13, driller's records report the Rustler to be completely intact with halite present and the anhydrites mostly unaltered (Jones, 1978).

Sinkholes are also present south of Los Medaños, in the vicinity of the H-7 and H-9 boreholes (see Figure 3.1.1-1). San Simon Swale and San Simon Sink east of the WIPP may also be karst features.

Models of groundwater flow to date have not considered vertical flow through sinkholes, and have instead examined effects of spatially uniform potential infiltration (Corbet and Wallace, 1993; Appendix A of this report), or the effects of selectively varying the location of vertical flow (Haug et al., 1987; Davies, 1989). Sinkholes could affect regional flow by providing point sources for inflow to deeper units or by providing interconnections between conductive layers separated by less conductive units. In both processes, effects would be similar to those discussed in Section 3.4.2 regarding open boreholes through the Rustler Formation.

3.1.2.1.2 Geochemical Evidence Related to Vertical Flow

Siegel et al. (1991a) summarize an effort to interpret the chemical, mineralogical, isotopic, and hydrological data available as of 1989. Siegel et al. concluded that the bulk of the data argues against significant vertical flow. The following paragraph is from the executive summary (page ES-3) of that report:

> Mineralogical and isotopic studies of sulfates in overlying layers also show that no significant amounts of either solutes or water have permeated vertically downward from the surface to recharge the Culebra. Specifically, much of the anhydrite in the Tamarisk member between the Magenta and Culebra members has not been hydrated to gypsum by recrystallization in the presence of fresh water, D/H ratios in gypsum throughout the Rustler are not consistent with a pervasively large water/rock ratio accompanying such hydration, and comparison of $^{87}Sr/^{86}Sr$ ratios of gypsums and carbonates in Rustler, Dewey Lake, and surface rocks shows that secondary sulfates and carbonates in the Rustler did not form in a hydrological regime that was uniformly interconnected with overlying rocks and the surface. Thus, the available mineralogical, hydrological, and isotope data indicate no significant vertical connection between the Culebra and overlying strata.

The results of another geochemical investigation performed by Bodine et al. (1991) suggest instead that groundwater in the Culebra and other conductive layers has been in contact with anhydrites and halites in the intervening confining layers. They presented the distribution of dissolved constituents in groundwater from the Rustler Formation in terms of salt norms. A salt norm (Bodine and Jones, 1986) can be envisioned as the hypothetical assemblage of mineral salts that would have precipitated from an evaporated water sample and would be in equilibrium with the last vestige of the remaining water. The salt norms yield a diagnostic characterization of the water that aids in the interpretation of possible origins of the solutes and past water-rock interactions. Their analysis of the distribution of salt norms of Rustler groundwater suggests that meteoric water has moved into the Magenta, Culebra, and Rustler-Salado contact zone. The salt norms of these waters indicate that they have interacted chemically with the anhydrites and halites in the intervening confining layers. This implies that at least a portion of the water in the conductive units has migrated through the confining units.

3.1.2.1.3 Hydrologic Observations Related to Vertical Flow

Hydrologic observations have also been presented to argue both for and against vertical flow across the Tamarisk Member, a unit of extremely low hydraulic conductivity separating the Culebra and Magenta dolomites. LaVenue et al. (1990, p. 2-15), for example, note that heads in the Magenta do not respond to pumping in the Culebra. They used this observation to support a decision to not consider vertical flow when modeling flow in the Culebra. The lack of drawdown in the Magenta as the Culebra is pumped does confirm that the confining layer is laterally extensive and has low hydraulic conductivity. However, as discussed in the following paragraph, the fact that we do not observe drawdowns in the Magenta during pumping tests in the Culebra should not be used

to infer that flow through the layers does not occur in the undisturbed flow field.

Neuman and Witherspoon (1969a, 1969b) described mathematically the change in hydraulic head with time that would occur in an aquifer as water is pumped from that aquifer, as well as the change in hydraulic head that would occur in a second aquifer and a confining unit separating the two aquifers. Application of this analysis to the Culebra, Magenta, and Tamarisk shows that the decrease in hydraulic head with time, that is the drawdown, in the Culebra would be less if vertical leakage from the Tamarisk occurred than if the no leakage occurred. The leakage would initially come from storage in the Tamarisk. At later times, water could be drawn from the Magenta if the pumping continued long enough that the drawdown of heads in the Tamarisk propagated across its entire thickness. Therefore the effects of leakage would be recognized first in the drawdown response of the Culebra and only much later, if ever, in the Magenta.

3.1.2.1.4 Numerical Modeling of Vertical Flow

Haug et al. (1987) and Davies (1989) used numerical models to investigate the possible importance of vertical flow in the undisturbed flow field. They applied constant-head conditions along the lateral boundaries of a horizontal domain and used source terms to represent vertical flow at specified rates in selected portions of the domain. Results from these studies show that vertical flux can be accommodated, and perhaps is necessary, when calibrating this type of model. For example, Haug et al. (1987) found that it was impossible to calibrate their steady-state confined model with respect to fluid density without adding small but realistic vertical fluxes in selected regions. Haug et al. (1987, p. 8-2) concluded that "... future modeling studies should not attempt to simulate the Culebra dolomite as a completely confined hydraulic system but rather as a leaky-confined aquifer." Davies (1989), also using this approach, performed simulations in which vertical flow accounted for as much as 25 percent of the total flux through the Culebra.

Following a different approach to evaluate the possible importance of vertical flow, Davies (1989), Corbet and Wallace (1993), and Corbet (Appendix A of this report) performed simulations that explicitly include strata that overlie and underlie the Culebra. Davies simulated flow in a vertical, two-dimensional domain, while Corbet and Wallace performed three-dimensional simulations. The relief of the water table over the model domain drives flow in both the two- and three-dimensional simulations. No-flow conditions along the lateral boundaries represent flow divides. These boundary conditions assure that all flow into or out of the Culebra must be by vertical leakage through adjacent confining layers. Just as a model that assumes perfectly confined conditions cannot demonstrate that vertical leakage does not occur, results from these simulations cannot demonstrate that it does occur. These results do, however, demonstrate that simulations based on a conceptual model in which vertical leakage is an important component can reproduce basic features of the regional flow system. For example, modern-day flow within the WIPP-site boundary is toward the south in the Culebra Dolomite, but is to the west in the overlying Magenta Dolomite. The three-dimensional simulations show that this counter-intuitive condition can be

explained as a natural consequence of the regional heterogeneity of the hydrologic system and of slow vertical leakage through the Tamarisk Member.

Given the lack of evidence for zero vertical flow through confining layers and the support for slow vertical flow provided by hydrologic models, the current position is that flow through unfractured confining units in the Rustler Formation is finite but extremely slow. Flow through confining layers can justifiably be neglected in calculations of flow and transport in single conductive units at the scale of the land withdrawal area. However, hydraulic continuity through confining units must be retained in regional three-dimensional flow models.

3.1.2.2 IMPLEMENTATION OF THE CONCEPTUAL MODELS

3.1.2.2.1 Confined Model

Implementation of the confined model for use in the 1992 PA is described in Chapter 7 of Volume 2 and Chapter 6 of Volume 4 of the Preliminary Performance Assessment for the Waste Isolation Pilot Plant, December 1992 (WIPP PA Department, 1992).

3.1.2.2.2 Groundwater Basin Model

The groundwater basin model was first implemented in two dimensions along a a vertical east -west trending cross-section extending from the axis of Nash Draw to a topographically high region east of the WIPP site (Davies, 1989). A three-dimensional numerical representation of the groundwater basin model (SECO3D) is currently being developed and used to investigate long-term regional flow of groundwater in strata above the Salado Formation. The numerical model solves transient or steady-state equations of groundwater flow. This model differs from other three-dimensional models used to simulate regional groundwater flow in that it treats the water table as a free surface which rises and falls in response to groundwater flow and the amount of moisture available for recharge to the saturated zone. Seepage faces (areas where groundwater can discharge from the flow system) form in regions where the water table is maintained at the land surface. Unsaturated flow above the water table is not considered in this numerical representation.

For transient simulations, the model solves

$$\nabla \bullet K \nabla h = S_s \frac{\partial h}{\partial t} \qquad eq.1$$

on the interior of the domain to assure conservation of mass. In this equation, hydraulic head h is the dependent variable, K is a spatially-dependent hydraulic-conductivity tensor, and S_S is specific

storage. No-flow boundary conditions are imposed on the bottom and vertical sides of the domain. The following pair of equations define a kinematic condition which is imposed on the top boundary to represent the free surface:

$$h(x,y,z_{wt}) = z_{wt}(x,y,z) \qquad eq.2$$

$$(K \bullet \nabla h + N) \bullet \nabla (h - z) = S_y \frac{\partial z_{wt}}{\partial t} \qquad eq.3$$

(Bear and Verruijt, 1987).

In these equations, z_{wt} is the elevation of the water table, N is the normal flux due to recharge and/or evapotranspiration, and S_y is the specific yield. The kinematic condition is applied if the elevation of the water table is below the land surface. If the water table is at the land surface, the kinematic condition may need to be converted to a seepage face. The seepage boundary condition is

$$h(x,y,z_{wt}) = z_{ls}(x,y) \qquad eq.4$$

where z_{ls} is the local land surface elevation and t_{wt} is the time at which the water table encounters the land surface. To determine whether the kinematic or the seepage boundary condition should be applied, the vertical speed of the water table, $\partial z_{wt} / \partial t$ is computed. The algebraic sign of the quantity shows whether the water table is falling or rising. The seepage condition is applied at a particular location if the water table there is rising. The kinematic condition is applied if the water table is falling.

The lateral boundary of the numerical model follows groundwater divides that inclose a region that is believed to be sufficiently large to control regional groundwater flow in the supra-Rustler strata (Figure 3.1.2-1). Groundwater divides are assumed to coincide with major topographic highs and depressions. The boundary follows Nash Draw and the Pecos River valley along the west and south and the axis of San Simon Swale to the east. The boundary continues up the San Simon

Swale and dissects topographic highs in the northern part of the model region.

The base of the numerical model is positioned along the top of the Salado Formation. The hydraulic conductivity of the Salado is sufficiently small that its upper surface can be represented in this model as a no-flow boundary. The rocks above the are represented as ten hydrostratigraphic units (Figure 3.1.2-2). Each hydrostratigraphic unit is heterogenous with respect to hydraulic conductivity. Values of hydraulic conductivity are assigned to portions of the model domain to represent the rock type (i.e. whether the rock is a dolomite, anhydrite, halite, mudstone, or siltstone) and the extent to which geologic processes have modified the hydraulic properties of the rocks. Geologic processes considered include dissolution of the upper portion of the Salado Formation and the resulting fracturing and disruption of overlying rocks, dissolution of minerals that previously filled fractures, and plugging of rock pores hy halite cements. These processes are thought to have occurred in distinct regions. Figure 3.1.2-3 shows the approximate extent of the regions as indicated by drillhole and geophysical data. As discussed in Section 3.1.2, karst features extending tens to hundreds of meters might disrupt confining layers and thereby facilitate increased localized recharge. Features of this scale are not currently represented in the hydraulic conductivity distribution used for the groundwater basin model.

Simulations performed using three-dimensional numerical models have enhanced the conceptual understanding of groundwater flow above the Salado in the vicinity of the WIPP (Corbet and Wallace, 1993; Appendix A of this report). This understanding, in turn, has been applied to evaluate several scenarios discussed in this paper, including the change in groundwater flow due to future changes in climate, the impact of subsidence over potash mines, and the effect of shallow boreholes.

Corbet and Wallace (1993) reported on early results of the three-dimensional modeling study. These simulations were performed using a modified version of a computer code, MODFLOW, developed by the United States Geological Survey (McDonald and Harbaugh, 1988; McDonald et al., 1991). Sandia National Laboratories modified this code to represent seepage faces in an approximate way. These simulations did not accurately represent groundwater flow near the WIPP because each hydrostratigraphic unit was assumed to be homogenous with respect to hydraulic conductivity. Nonetheless, these simulations did demonstrate several important aspects of the natural hydrogeologic system. The simulations suggested that groundwater flow in the Culebra Dolomite is strongly influenced by the relief of the water table. A substantial portion of the water flowing in the Culebra is from slow vertical leakage from overlying confining layers. Also flow rates and directions in the Culebra are sensitive to the amount of moisture that infiltrates to the water table.

Results from more recent simulations performed using the SECO3D code confirmed the results of the earlier simulations and provided additional information about the effects of climate change (Appendix A of this report). These simulations incorporate the rigorous treatment of the free surface and seepage face boundary conditions described above, as well as a distribution of hydraulic

properties that reflects the effect of geologic processes. First a steady-state flow field calculated using a value of maximum potential recharge of 0.1 cm/yr was compared to a flow field calculated using a value of 0.01 cm/yr. The maximum potential recharge rate is the fastest rate that moisture is allowed to infiltrate through the unsaturated zone to the water table. Both rates used are a small fraction the present-day annual precipitation, approximately 30 cm/yr, at WIPP. This comparison was done to evaluate whether or not groundwater flow in the Rustler could be sensitive to future changes in climate. The simulation results suggest that even this difference in potential recharge of less than a tenth of a centimeter per year could have an impact on flow patterns. Simulated flow in the Culebra near the WIPP site, for example, is toward the south given the lower rate of recharge, but is toward the west if the higher rate of recharge is assumed. The flow pattern for the lower recharge rate (0.01 cm/yr) is similar to the pattern observed today. The hydraulic gradient is approximately twice as steep in the calculation with higher recharge. Whether or not flow driven to the west by a steeper gradient would actually result in shorter travel times to the accessible environment depends on details of the transmissivity distribution which could not be included in these simulations.

These results show how much a climate change could impact flow in the Culebra if the change persisted long enough for flow patterns to adjust completely to the change. As the second part of this study, a transient simulation was performed to evaluate how fast a climate change could impact groundwater flow patterns. The simulated period of time was the past 14,000 years. Using the estimated precipitation record for this period (Swift, 1993) as a basis for the temporal pattern of recharge, the recharge rate was decreased from 0.1 to 0.01 cm/yr over the period from 14,000 until 8,000 years before the present. The rate remained at 0.01 cm/yr for the rest of the simulation. Flow in the Culebra adjusted slowly enough that the simulated flow pattern for the present-day is more representative of the 0.1 cm/yr recharge rate assumed for 14,000 years ago than the current 0.01 cm/yr rate. This result implies that the undisturbed pattern of groundwater flow in the Rustler Formation will not change much over the next 10,000 years. However, this conclusion must be considered to be tentative because it is based on a single set of model parameters.

These simulations also provide information on how much a change in climate could affect the thickness of saturated zone in the Dewey Lake Red Beds and the Dockum Group. The saturated thickness of these units is an important factor in determining whether or not they could act as lateral pathways for radionuclide migration. Currently, the saturated thickness of these units is not well known but is thought to be a relatively small portion of their total thickness. The simulations suggest that if groundwater flow adjusted to the higher, 0.1 cm/yr, recharge rate, the water table in the vicinity of WIPP would be near the surface and consequently nearly the entire thickness of these units would be saturated. At the lower recharge rate, the simulated thickness of the saturated zone is 45 to 80 meters less. This result suggests that perhaps the most important impact of climate change would be to increase the thickness of saturated sediments above the Rustler Formation.

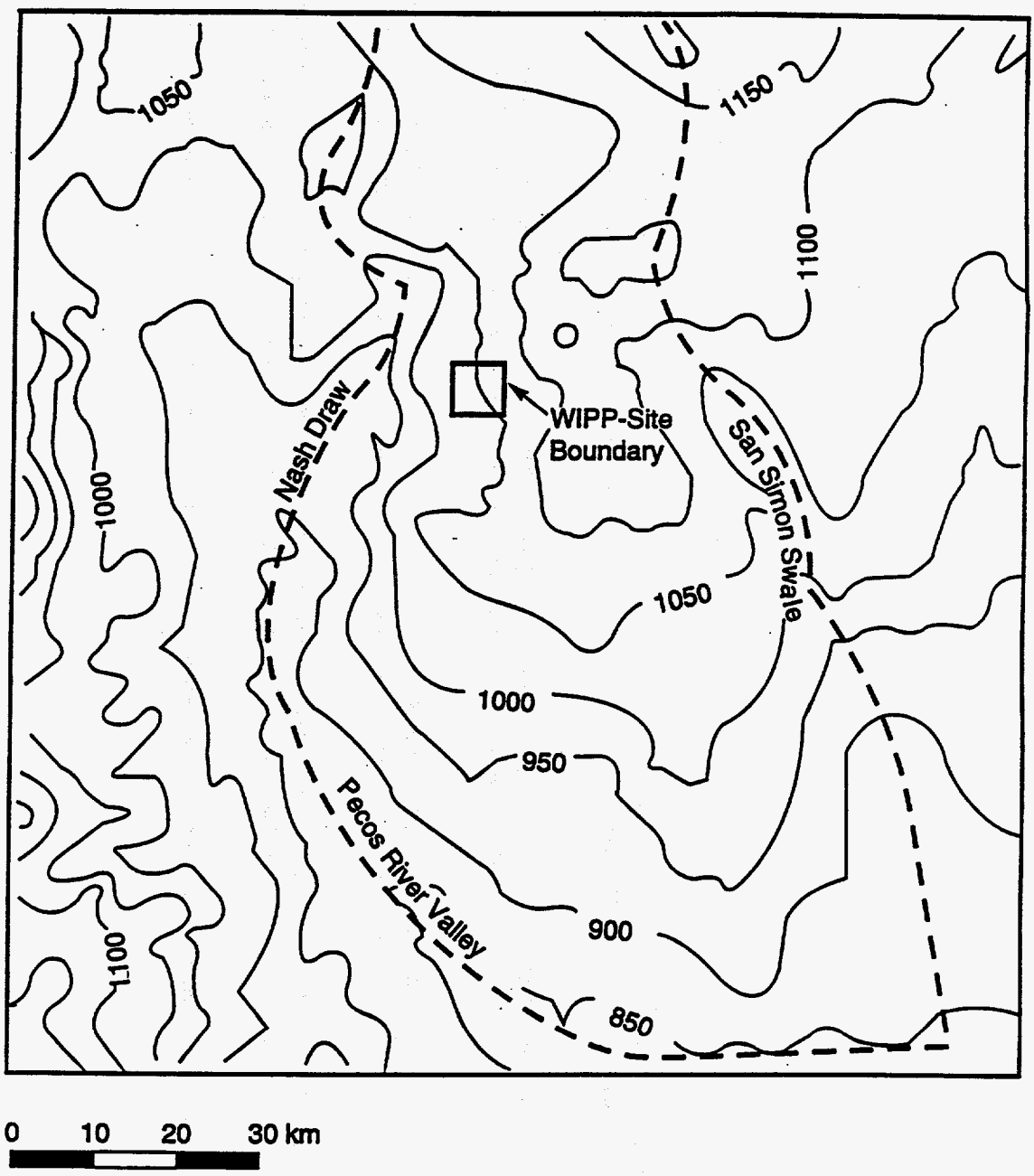

TRI-6116-97-0

Figure 3.1.2-1. Topography of the and surface and the lateral boundary of the regional groundwater flow model. Contour interval is 50 m. Model boundary follows groundwater divides along topographic depressions to the west, south, and east, and dissects topographic highs to the north. No-flow boundary conditions are used along the entire lateral boundary.

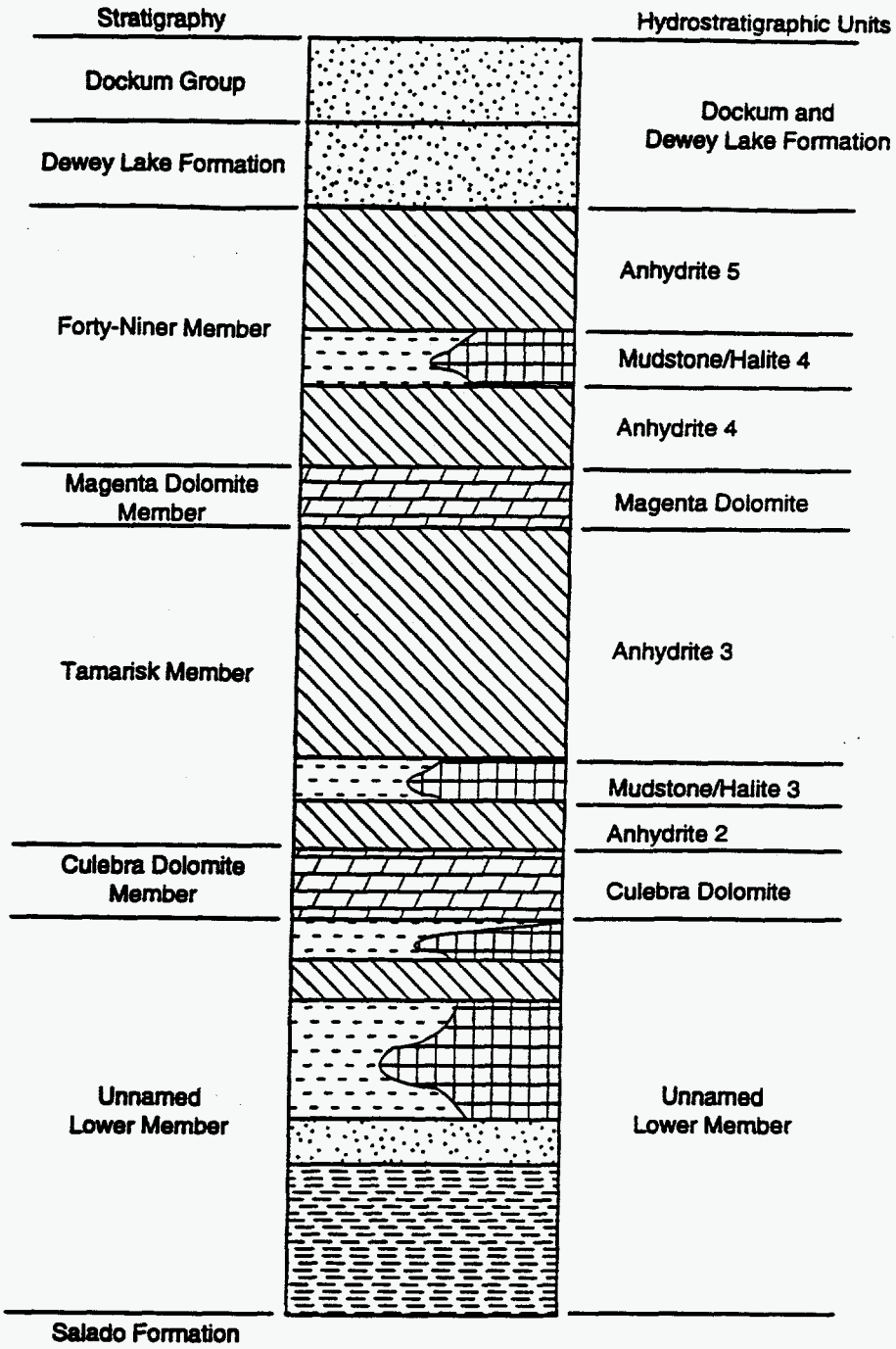

Figure 3.1.2-2. Hydrostratigraphic units for the regional groundwater flow model. See Appendix A for additional discussion.

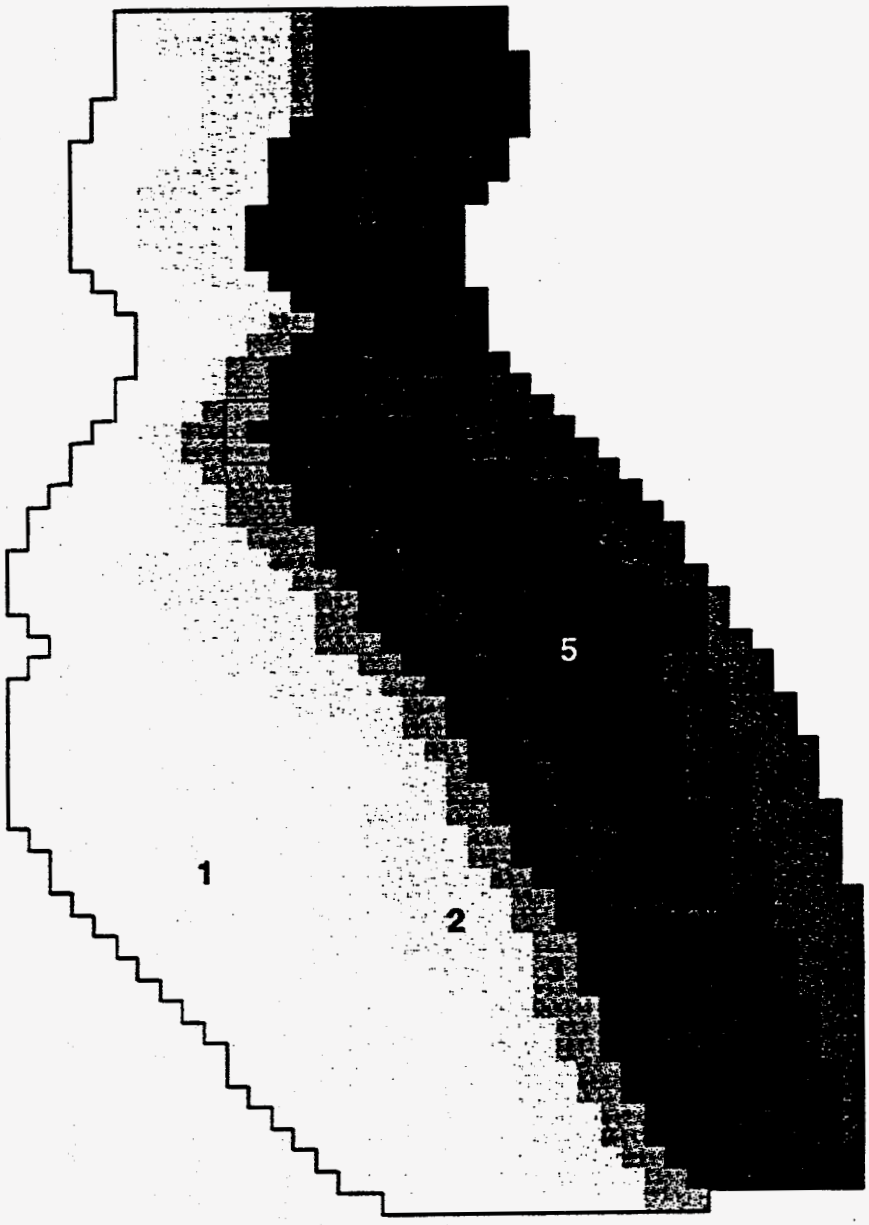

Figure 3.1.2-3. Zonation of hydraulic conductivity in the regional groundwater flow model. See Appendix A for additional discussion.

3.1.3 Groundwater Geochemistry and Regional Groundwater Flow

Summary Statement: Long-term performance assessment calculations to quantify flow and transport of radionuclides in the Culebra Dolomite are currently made using a two-dimensional confined flow model, in which groundwater flow is restricted (i.e., stratabound) within the Culebra and is not influenced by leakage to or from adjacent strata or by recharge from the surface (WIPP Performance Assessment Department, 1992, Vol. 2, Section 7.6 and Appendix A). Calculations using the two-dimensional confined flow model indicate that the flow direction in the Culebra above the repository is southward (LaVenue et al., 1990), a result which is consistent with the calculated flow path based on potentiometric measurements made in the Culebra from wells around the site. During the last ten years, several regional-scale geochemical studies have been conducted with Culebra rocks and groundwaters to evaluate whether inferences made on the basis of hydrogeological observations are consistent with geochemical observations. Interpretations based on those investigations have suggested that flow paths in the Culebra above the repository are not southward. Resolution of that apparent inconsistency is desirable to increase confidence in long-term performance assessment calculations of flow and transport. Results from a three-dimensional modeling effort using the groundwater basin concept (see Section 3.1.2 and Appendix A of this report) suggest that the apparent inconsistency can be resolved with that more comprehensive hydrogeological numerical modeling technique. Until that work is completed, however, the baseline position on this issue is simply that available information is insufficient to explain regional groundwater geochemistry in the context of hydrogeological observations.

Discussion: To evaluate present-day groundwater flow paths in the Culebra, several regional-scale geochemical investigations have been conducted on Culebra rocks and groundwaters over the past decade. A detailed review of that work is beyond the scope of this position paper, and would not add to existing published reviews (refer to Lappin, 1988; Lappin et al., 1989, sections 3.3.2 and 3.3.3; WIPP Performance Assessment Division, 1992, volume 2, section 2.2.3.6; U.S. Department of Energy, 1994, section 2.2.2). The objective of the following discussion is only to provide a brief review of the results of some of the more extensive regional geochemistry investigations, and the interpretations that those authors made.

The most recently completed and published body or work on this topic used results from interpretations based on an extensive compilation of lateral changes in isotopic (stable and radiogenic) ratios of Culebra rock, mineral, and groundwater; solute (major and minor ions) concentrations in Culebra groundwater; and the mineralogy of the Culebra (Lambert, 1987; Lambert and Carter, 1987; Lambert and Harvey, 1987; Bodine et al., 1991; Siegel and Lambert, 1991; Siegel et al., 1991b; Lambert, 1991, 1992; Siegel and Anderholm, 1994). A concise summary of that work can be found in Siegel et al. (1991a, pages ES-1 to ES-5).

Siegel et al. (1991b) refined a hydrogeochemical facies distribution of Culebra

groundwaters using a rather extensive data base of chemical analyses of groundwaters collected from monitoring and irrigation wells near the WIPP site. Siegel et al. showed that Culebra groundwater residing in the eastern half of the WIPP site consists of approximately 2 to 3 molal ionic strength sodium chloride brine whereas groundwater in the western half of the site consists of approximately 0.3 to 1.6 molal ionic strength sodium chloride brine. Groundwater compositions south of the WIPP are relatively dilute calcium sulfate waters, with ionic strengths of about 0.1 molal. Assuming that the ionic strength of a groundwater increases along a flow path, the distribution of groundwater hydrogeochemical facies is not consistent with the southward flow direction calculated by LaVenue et al. (1990) from potentiometric data.

One possible explanation for the apparent inconsistency has been proposed by Chapman (1986, 1988), who coupled an extensive compilation of stable and radiogenic isotope ratios of Rustler Formation groundwaters with isotopic data from regional groundwaters and surficial waters. Chapman cited evidence for shot residence times of Culebra groundwaters and postulated that recharge from the surface could account for the less concentrated groundwaters south of the WIPP Site. That explanation, however, is not supported by the isotopic and solute data described in later work by Lambert, Siegel, and others. Specifically, radiogenic isotopic signatures suggest that the age of the groundwater in the Culebra is on the order of tens of thousands of years (Lambert, 1987; Lambert and Carter, 1987; Lambert and Harvey, 1987). An alternative explanation for the apparent inconsistency was put forth by Siegel et al. (1991a, and references therein). Those authors contend that there has been a change in the location and amount of recharge since the last glacial maximum and that the present distribution of solutes and isotopes in the Culebra is a relict of a flow regime of a wetter climate, in which the recharge area was in the vicinity of Nash Draw resulting in an eastward paleo-flow direction. The current distribution of hydrogeochemical facies, therefore, represents a rock-water system that is still slowly reaching a new chemical and physical equilibrium.

Currently, a detailed resolution of the apparent inconsistency between regional-scale geochemical observations and flow directions calculated from potentiometric data has not been reached. However, preliminary results of three-dimensional calculations using the groundwater basin approach in general support the explanation put forth by Siegel et al. (1991a, and references therein; see also Siegel and Anderholm, 1994), that the flow direction in the Culebra has changed since the wetter climate of the Late Pleistocene, although the Pleistocene flow direction may have been quite unlike that previously proposed (See Sections 3.1.2 and 3.4.1 and Appendix A of this report). On the basis of those preliminary results, the WIPP Project expects that the apparent inconsistency will be resolved.

3.1.4 Castile Brine Reservoirs

Summary Statement: Pressurized brine reservoirs are found at some locations in the uppermost anhydrite layer of the Castile Formation. TDEM surveys indicate the possible presence of three or four of these reservoirs beneath portions of the WIPP disposal rooms. Flow from a brine reservoir through an intrusion borehole into the Culebra dolomite can be modeled by treating the brine reservoir as an exponentially decaying source characterized by the parameters pressure, volume, and storativity. Future calculations of possible flows from brine reservoirs should use values for volume and storativity based on the available data, and should limit the number of independent reservoirs that might be encountered to four.

Discussion: Pressurized brine reservoirs have been encountered within the uppermost anhydrite layer of the Castile Formation in at least 13 boreholes in the Delaware Basin (Figure 3.1.4-1) (Popielak et al., 1983). Two of these boreholes, WIPP-12 and Belco-Hudson, are on or within a mile of the WIPP site. Many more boreholes penetrating the Castile near the WIPP site have not encountered brine reservoirs (e.g., AEC-8, Badger Unit Federal #1, Cabin Baby-1, Cotton Baby, DOE-1, DOE-2, James Ranch #1, WIPP-11, and WIPP-13). Time-domain electromagnetic (TDEM) surveys conducted at the WIPP site have indicated the possible presence of three or four Castile brine reservoirs beneath portions of the WIPP disposal rooms (Earth Technology Corporation, 1988, p. 8).

Based on the TDEM survey, PA has assumed that Castile brine reservoirs underlie 25 to 57% of the WIPP disposal area. Therefore, 25 to 57% of the exploratory boreholes penetrating the WIPP repository in PA human-intrusion scenarios connect the Culebra and the repository to a Castile brine reservoir. The 1992 PA model of the brine reservoir followed the approximation developed by Reeves et al. (1991), summarized below.

Reeves et al. (1991) examined ways to implement a borehole connection between a brine reservoir, the repository, and the Culebra in a numerical model. They conceptualized the brine reservoir as a three-component system: an inner highly fractured ring having a transmissivity between 7×10^{-6} and 7×10^{-2} m^2/s, an outer less fractured ring having a transmissivity between 7×10^{-8} and 7×10^{-4} m^2/s, and an infinite surrounding region of intact anhydrite having a transmissivity between 1×10^{-13} and 1×10^{-9} m^2/s (p. 2-6). They found (p. 5-12) that so long as borehole permeability was in the range from 10^{-14} to 10^{-10} m^2, the only properties of a Castile brine reservoir that were important in calculating flow into the Culebra dolomite were the reservoir pressure, storativity, and outer-ring radius (or reservoir volume); the different transmissivities and the radius of the inner ring were found to be unimportant over the ranges considered. This finding allows a brine reservoir to be treated as an exponentially decaying source term in numerical models.

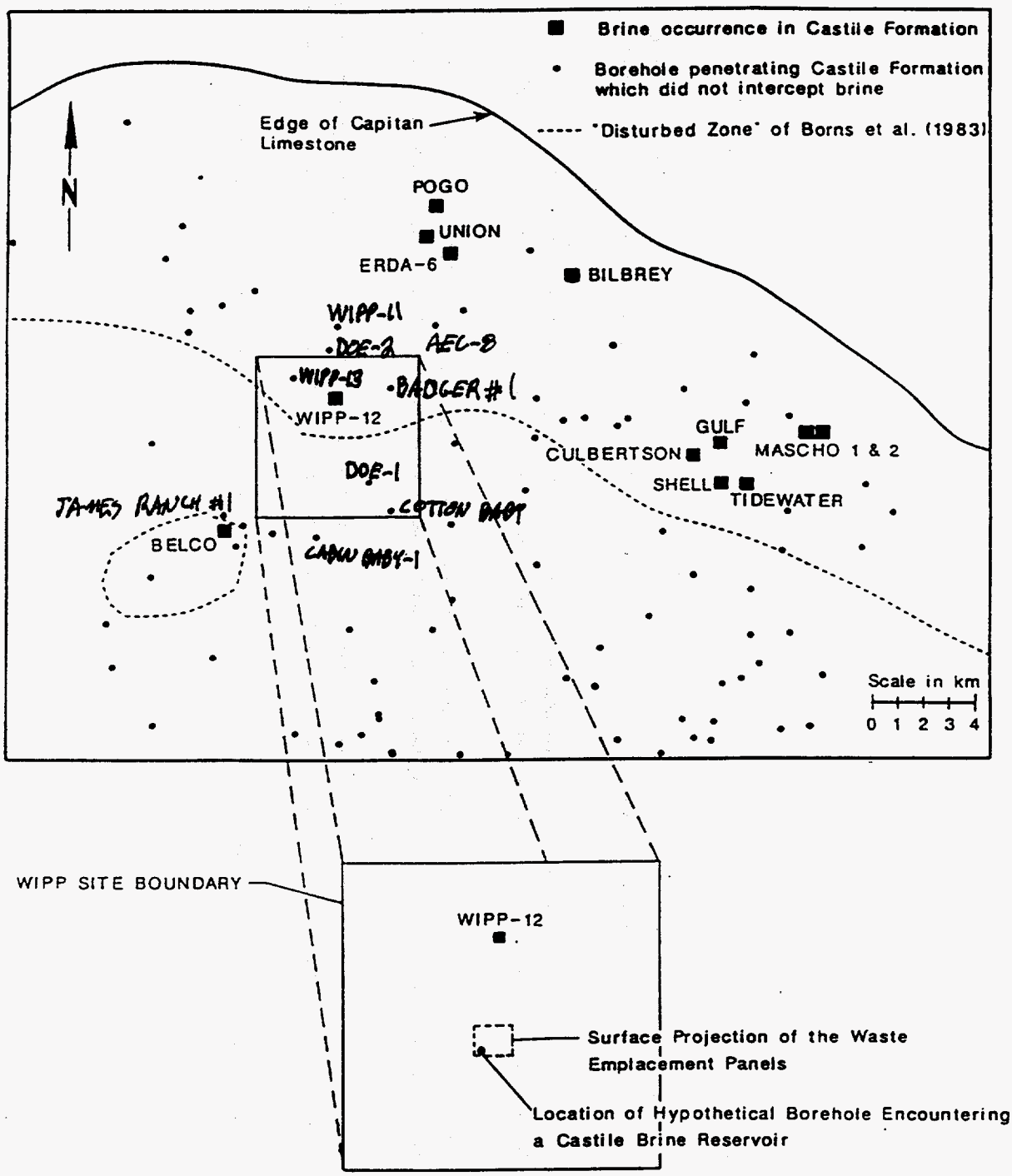

Figure 3.1.4-1. Selected deep boreholes that penetrate the Castile Formation, northern Delaware Basin.

The combination of brine reservoir volume and storativity used in the 1992 PA calculations was such that the initial pressure of the brine reservoir did not appreciably deplete over 10,000 years. In effect, the brine reservoir behaved as a constant-pressure source and the release of brine and radionuclides to the Culebra was overestimated. The 1992 PA calculations assumed a brine reservoir volume of 2×10^8 m^3. Popielak et al. (1983, p. H-54) estimated the WIPP-12 reservoir volume to be about 3×10^6 m^3, with a range of uncertainty from 3×10^5 to 1×10^7 m^3. The ERDA-6 reservoir volume is estimated at 1×10^5 m^3, with a range of uncertainty from 1×10^4 to 5×10^5 m^3 (Popielak et al., 1983, p. H-48). Future calculations should not use reservoir volumes larger than the 1×10^7 m^3 upper limit on the WIPP-12 reservoir volume.

The storativity range used in the 1992 PA calculations was developed from erroneous values presented in Reeves et al. (1991, Table A-1, p. A-2,3) for the volumes of brine produced from the WIPP-12 reservoir during different testing activities. The total volume indicated by Table A-1 of Reeves et al. (1991) is 37,924 m^3, whereas the correct value is only 13,469 m^3 (D'Appolonia, 1982, Figure 4; 1983, p. 3-1). Thus, the storativity range of 2×10^{-2} to 2 m^3/Pa used in the 1992 PA (Sandia WIPP Project, 1992, p. 4-15) should be reduced to 7×10^{-3} to 7×10^{-1} m^3/Pa in future calculations.

The 1992 PA also considered each borehole hitting a Castile brine reservoir to be an independent event, with each hit encountering a fully pressurized and separate brine reservoir. Future calculations should limit the number of brine reservoirs to four, based on the results of the TDEM survey (Earth Technology Corporation, 1988, p. 8).

3.1.5 Multi-Phase Flow

Summary Statement: Numerical evaluations of flow and transport in the Culebra to date have treated the unit as being fully saturated (single-phase liquid only) . No numerical studies have been performed to make a determination of the effect of unsaturated conditions which could occur as a result of gas entering the unit through a borehole either from the Castile brine reservoir or the repository.

Discussion: Two-phase or unsaturated flow conditions in the Culebra and other non-Salado units occurs naturally and may also occur as a result of human intrusion. Two-phase conditions will alter the flow field to an uncertain extent, and may in turn impact transport velocities.

Unsaturated flow occurs naturally in formations above the water table. Due to capillary pressure differences between the units, the various layers above the water table can act as capillary barriers to inflow or infiltration. The natural dip of the layers can divert the flow laterally from its infiltration location, and the storage capacity of the unsaturated units could alter the flow rate at the water table compared to the inflow at the surface.

Human intrusion scenarios may introduce gas into the boreholes either from such sources as the Castile brine reservoirs or from gas in the repository due to gas generation in the waste. Depending on the borehole details including the plugs, some of this gas may be introduced into non-Salado formations or flow to the surface. Because of the lower pressures in the units above the Salado, the gas volume will expand over the volume occupied in the reservoir. Gas bubbles could alter the natural flow patterns and velocities of the brine due to flow blockage and density differences, and the gas bubbles could migrate differently than the brine. Fracture-matrix flow could be significantly changed with the introduction of gas due to the capillary pressure difference between the phases, possibly resulting in gas flow primarily in fractures and brine flow primarily in the matrix. Chemistry could also be changed by the introduction of gas into the non-Salado units, affecting radionuclide retardation.

At the present time, the non-Salado formations are analyzed using single-phase or fully saturated approaches, ignoring the possible influence of unsaturated or two-phase conditions. An evaluation of the possible effects of unsaturated and two-phase conditions, including scoping studies as necessary, could be conducted to assess the potential impact on system performance. For example, it is possible that permeability of the borehole plugs is high enough that any gas released up a borehole would escape to the surface and not enter the Culebra.

3.2 Culebra Flow and Advective Transport

This section contains conceptual and mechanistic models concerning fluid flow and advective transport in the Culebra. Calculations of radionuclide transport in the Culebra are performed in two steps. First, calculations are performed to determine a flow field and its respective specific discharge. Specific discharge is the rate at which groundwater flows through a unit cross-sectional area of rock. Although specific discharge has the units of velocity, it does not represent the actual velocity of flow. The real velocity (interstitial velocity) is faster because the fluid can only flow through the area provided by pores and fractures in the rock, rather than the entire cross-sectional area. A second step is required to transform the specific-discharge field into the interstitial velocity and to account for physical and chemical retardation of the radionuclides. This second step is more difficult because it must take into consideration the fact that the Culebra is fractured and acts as a double-porosity medium.

A critical piece of information required to calculate the specific-discharge field is the distribution of the rock's transmissivity. The transmissivity of the Culebra has been measured at a relatively large number of locations (see Section 4.2.2). The models used to transform these discrete data into a continuous distribution of transmissivity are described in Section 3.2.1. Knowledge of a second parameter, the rock storativity, is required to perform calculations of a flow field that changes with time. As discussed in Section 3.2.2, fewer measurements of rock storativity have been made. Section 3.2.3 considers the effects of the spatial distribution of fluid density in the Culebra on the flow field. Artificial change to the density distribution can be

introduced by leakage from boreholes (Section 3.2.4). Leakage from boreholes could also introduce multi-phase (gas in addition to liquid) flow into the Culebra and, through, rock/water interactions modify the hydraulic and retardation properties of the Culebra. Models that incorporate the effects of fractures, the double-porosity model and the channeling model, are described in Sections 3.2.5 and 3.2.6. Finally, Section 3.7 discusses the role of dispersion in radionuclide solute transport.

3.2.1 Transmissivity

Summary Statement: Measured transmissivity values vary spatially over several orders of magnitude near WIPP. The spatial variations in transmissivity are implemented by numerically generating realizations conditioned on observed head and transmissivity values using the pilot point technique (LaVenue and RamaRao, 1992). This approach of generating transmissivity realizations has been extensively reviewed..

Discussion: Measured transmissivity values (see Section 4.2.2) vary spatially over several orders of magnitude, trending from lower values east of WIPP to higher values west of WIPP. The spatial variations in transmissivity are implemented by numerically generating realizations conditioned on observed head and transmissivity values using the pilot point technique (LaVenue and RamaRao, 1992). Multiple realizations are generated and sampled on to address the uncertainty associate d with the transmissivity field. This approach has been extensively reviewed. Transmissivity is assumed to be constant over time.

3.2.2 Storativity

Summary Statement: Interpreted storativity values vary spatially in the vicinity of the WIPP over a few orders of magnitude. Performance assessments to date have assumed a spatially invariant value for storativity. This assumption results in incorrect Darcy velocities in transient flow simulations, although the uncertainty cannot be quantified at this time.

Discussion: Storativity is an important hydraulic parameter during transient events, such as pumping or injection, because it affects the head gradients that are created, which in turn affect the groundwater velocities. Therefore, accurate calculations of solute transport under transient conditions rely on accurate definition of the storativity (and transmissivity) field. Storativity values interpreted from hydropad-scale pumping tests of the Culebra at the WIPP site range from 3×10^{-6} (Gonzalez, 1983) to 3×10^{-4} (Saulnier, 1987; Beauheim, 1989). Storativity data are sparse, however, and no attempt at defining a storativity field over the WIPP site has been performed.

In the GRASP-INV modeling used to define the transmissivity fields for the 1992 PA

calculations (LaVenue and RamaRao, 1992), a constant storativity value of 2 x 10^{-5} was assigned throughout the modeling domain. Because the transmissivity fields are calibrated to transient events, the assumption of a spatially constant storativity leads to inaccurate definition of transmissivity fields and, hence, inaccurate estimates of the Darcy velocities in calculations based on those transmissivity fields. The magnitude and direction of the flow uncertainties resulting from the approach employed cannot be determined without numerical simulations.

Future GRASP-INV modeling should solve for both the transmissivity and storativity fields that are consistent with the observed transient head data. The resultant storativity and transmissivity fields should be used for any calculations of transient flow and transport conducted for PA. WIPP PA may wish to consider alternative inverse techniques that simultaneously estimate transmissivity and storativity from transient data.

3.2.3 Variable-Density Flow

Summary Statement: The Culebra dips gently from west to east. Variable-density conditions exist naturally within the Culebra due to varying concentrations of total dissolved solids (TDS), with fluid density increasing from west to east. The numerical implementation of a horizontal stratigraphy is strictly correct only for constant-density, single-phase fluid flow and transport. If large fluid density gradients are present, heavier fluids will move preferentially downdip (to the east) relative to lighter fluids, and horizontal models may underestimate the eastward component of transport. The effects of stratigraphic dip are expected to be insignificant, but supporting simulations have not been performed to date. The effects of enhanced migration of heavier fluids to the east cannot be incorporated into a horizontal model because density gradients may be in a different direction than pressure (hydraulic head) gradients.

Discussion: The Culebra varies in thickness from about 4 to 12 m and dips an average of 0.44 degrees (Davies, 1989) from west to east. Variable-density conditions exist naturally within the Culebra, with fluid density increasing from west to east. Additional density variations may be introduced by fluid from an intrusion borehole (see Section 3.2.4).

A rigorous implementation of variable-density flow and transport in a non-horizontal unit must consider pressure and density gradients independently. Pressure gradients drive flow from high pressure to low pressure whereas density gradients drive flow from high elevation to low elevation. The directions of these two gradients are not coincident. For horizontal flow, density gradients are zero, and pressure gradients define the direction of flow. In this case pressure gradients can be represented by equivalent freshwater heads. However, for non-horizontal flow, equivalent freshwater heads cannot be used because the effects of density gradients are not properly reproduced.

The west to east fluid density gradients enhance transport of higher density fluids (such as

contaminated brine from the repository) downdip (to the east). This effect on transport is expected to be insignificant, but supporting simulations have not been performed to date. Davies (1989) concluded that ignoring the impact of density-driven flow may be acceptable in some areas of the WIPP domain but it is not acceptable in others, particularly in the southern portion. However, over the modeling periods of concern, flow deviations due to density effects are expected to be minimal.

3.2.4 Fluid from an Intrusion Hole

Summary Statement: Connection of the Culebra with the Salado and a Castile brine reservoir through an intrusion borehole could allow brine to flow into the Culebra. This could cause the head in the Culebra to increase, locally inducing radial flow from the borehole. The area affected will depend on the local transmissivity and storativity of the Culebra, as well as on the flow rate into the Culebra. Reeves et al. (1991) predicted a decrease in radionuclide travel time to the site boundary of up to 7.4% due to a fluid disturbance from an intrusion borehole. This effect can be implemented in an undisturbed flow field by increasing hydraulic heads in the vicinity of the borehole. Potential density, chemical, and multiphase effects from the intrusion fluid are discussed in other sections.

Discussion: The fluid from an intrusion borehole could have the following four effects on flow and transport in the Culebra:

1) Increase hydraulic gradients and flow velocities in the vicinity of the borehole.

2) Change the density of the Culebra fluid.

3) Result in rock/water interactions that alter flow and transport properties in the Culebra.

4) Result in multiphase flow conditions in the Culebra.

Reeves et al. (1991, p. 3-12 to 3-18) quantify the impact of an intrusion borehole on the Culebra flow field. At 10,000 years, the disturbed flow field is predicted to be only 12.5 m wide downstream from the well. Conditional on the assumptions of their model, for a borehole permeability of 10^{-10} m^2, the travel time to the site boundary is predicted to be 7.4% faster than the undisturbed case. For lower borehole permeabilities, the impact on travel time is less.

The other affects listed above are discussed in Sections 3.2.3, 3.3.1, and 3.1.5.

3.2.5 Double Porosity

Summary Statement: At some locations on and around the WIPP site, the Culebra dolomite is a double-porosity medium. In this usage, double porosity simply means that the Culebra has two porosities, matrix and fracture. Observations from core samples and the results of hydraulic and tracer tests provide evidence for areas where the Culebra responds as a double-porosity medium and other regions where it responds as a single-porosity, matrix-only medium.

The double-porosity conceptualization used by WIPP PA Department (1992) assumes that advective transport occurs only in fractures, with diffusion of radionuclides and contaminants occurring between the fractures and matrix. Sensitivity studies (Helton et al., 1992; WIPP PA Deparment, 1993, v. 4) have shown that cumulative release can be reduced if radionuclides that are transported in the fractures can diffuse into the matrix. In the double-porosity conceptualization as implemented by PA, one of the most important parameters for transport is the effective surface area for diffusion which is represented by the fracture spacing (matrix block size). This parameter is not well characterized.

It is acceptable to model the entire Culebra as a double-porosity medium. This may cause calculated velocities to be slightly too high in the lower transmissivity zones where the Culebra actually behaves as a single-porosity medium, leading to slight overestimates of radionuclide transport.

Discussion: At some locations on and around the WIPP site, the Culebra is a double-porosity medium. By double porosity we simply mean the Culebra has two porosities. The primary porosity or original porosity is the porosity within the rock matrix. Analysis of core samples suggests that the matrix porosity (or volume of void space between grains divided by total volume) is in the range of .03 to .30 (Kelley and Saulnier, 1990). The secondary porosity is the void space of the fractures divided by total volume. A critical issue for transport in a fractured medium is the degree to which fractures and matrix interact.

In a double-porosity, fractured medium, flow is generally conceptualized as occurring primarily in the fractures because flow velocities are usually orders of magnitude higher in the fractures than the matrix. However, diffusive (or advective) transport of radionuclides or contaminants from fractures into the matrix can act as an important physical retardation process.

The double-porosity conceptualization used by WIPP PA Department (1992) assumes that advective transport occurs only in fractures, with diffusion of radionuclides and contaminants occurring between the fractures and matrix. Sensitivity studies (Helton et al., 1992; WIPP PA Department, 1993, v.4) have shown that cumulative release can be reduced if radionuclides that are transported in the fractures can diffuse into the matrix. In the double-porosity conceptualization as implemented by PA, one of the most important parameters for transport is the effective surface area for diffusion per unit volume of fluid, which is represented by the fracture spacing (matrix block size). This parameter is not well characterized.

Field tests near the WIPP site have provided evidence for areas where the Culebra appears to respond as a double-porosity medium and other areas where it appears to respond as a single-porosity (matrix-only) medium. Conservative tracer tests have been conducted within the Culebra at several locations for transport scales ranging from approximately 20 to 40 m. Convergent-flow and two-well recirculating tracer tests provide data that can be used to characterize the flow and transport process. The observed long time period required for initial (detectable) tracer breakthrough (74 to 316 days) for the H-2 and H-4 tracer tests suggests the prevalence of single-porosity, matrix-only transport at these locations. Hydraulic-test responses at these two hydropads also indicate single-porosity, matrix-only conditions. Interpretations of pumping tests and tracer tests at the H-3, H-6 and H-11 hydropads suggest that the Culebra behaves as a double-porosity (fracture plus matrix) medium at these locations. Significant fracture participation in transport is evidenced by rapid initial tracer breakthrough (1 to 21 hrs) on one travel path at the H-3, H-6, and H-11 hydropads (Jones et al., 1992).

Values of two so-called "double-porosity" parameters have been interpreted from the convergent-flow tracer tests conducted at the H-3, H-6, and H-11 hydropads (Jones et al., 1992): fracture porosity and fracture spacing (matrix-block length). The values presented by Jones et al. (1992), however, are specific to the numerical model used for test interpretation and do not represent intrinsic or exact properties of the Culebra. The fracture porosity values, for example, were calculated assuming that tracer traveled in a straight line from the tracer-injection well to the tracer-recovery well under radial flow conditions. Within the numerical model used for the test interpretations (SWIFT II), this fracture porosity was assumed to exist within three orthogonal fracture sets with equal and uniform apertures. In actuality, the fracture porosities presented by Jones et al. (1992) represent the effective flow porosity for any fracture geometry, but always under the assumptions of continuous, isotropic radial flow.

The fracture spacings presented by Jones et al. (1992) are also specific to the assumed cubic fracture geometry, as well as to assumptions made about the flow rate along the various flow paths. The fracture spacings cannot be considered separately from other parameters used in the tracer-test analyses. That is, fracture spacing is directly correlated with matrix tortuosity and free water diffusion coefficient through the characteristic matrix diffusion time (τ) given by:

$$\tau = L^2/\Theta D$$

where: L = one-half the fracture spacing
Θ = matrix tortuosity
D = free water diffusion coefficient.

In the interpretations presented in Jones et al. (1992), values of Θ and D were specified based on laboratory data and values for L were determined for each tracer test through curve matching. In effect, the uncertainty in all three parameters was lumped into the estimate of fracture spacing.

The parameter defined through tracer-test interpretations, however, is not fracture spacing but the ratio of fracture surface area to matrix volume. The tracer-breakthrough behavior in a tracer test would be the same for any fracture geometry having the same surface to volume ratio, so long as the tracer does not diffuse all the way to the center of the matrix block. That is, the breakthrough curve produced by a test of a system with cubic matrix blocks would be identical to the curve produced by a test of a system with slab blocks with one-third the thickness of the cubic blocks, until the tracer reached the center of the slabs. The time at which this occurs is given by the characteristic matrix diffusion time defined above. Tracer tests provide no information on fracture geometry until the characteristic matrix diffusion time is exceeded and matrix saturation effects begin to be observed. Jones et al. (1992) assumed cubic (or spherical) matrix blocks in their tracer-test interpretations. If their results are to be used to simulate transport through a system having a different assumed geometry, their calculated fracture spacings would have to be adjusted to create the correct surface to volume ratio in the new geometry.

For any fracture geometry, the characteristic matrix diffusion times for radionuclides would be different than those determined for the benzoate tracers used in the tracer tests at WIPP because of different free water diffusion coefficients. The other two parameters contributing to the diffusion time, fracture spacing and matrix tortuosity, can be used to simulate radionuclide transport so long as the ratio of the specific values used, as given in the above equation, does not change. That is, fracture spacing and matrix tortuosity are correlated parameters and should not be sampled independently of one another.

It isappropriate to model the entire Culebra as a double-porosity medium even though portions of it appear to be single porosity. This may cause calculated velocities to be slightly too high in the lower transmissivity (single-porosity) zones, leading to slight overestimates of radionuclide transport.

3.2.6 Channeling

Summary Statement: Fracture channeling in the Culebra may result in up to a factor of 10 increase in radionuclide release relative to uniform flow over entire fracture planes due to higher velocities and reduced matrix diffusion in a numerical implementation of double-porosity transport.

Discussion: Fracture channeling occurs through discontinuous networks of relatively high-conductivity channels within individual fractures planes. Typically these channels represent areas where fracture apertures and fracture connectivity are greatest. Areas where fracture apertures are smaller, or where flow paths run into dead ends, represent relatively stagnant areas that may provide temporary storage of solutes. Observations by Holt and Powers (1990, p. 3-19) of the Culebra in the Air Intake Shaft indicate that flow is concentrated within a 1.7-m-thick

horizon that is more extensively fractured than the rest of the Culebra. However, all fractures are not equally productive and individual fractures do not produce water uniformly over their entire lengths. Rasmuson and Neretnieks (1986, p. 1247) report that 90% of the water flowing through a fracture typically passes along only 5 to 20% of the fracture plane.

Relative to the case of uniform flow over the entire fracture plane, channeling increases the fluid velocity and reduces the fracture surface area available for matrix diffusion. Increasing fluid velocity decreases both travel time and matrix diffusion. Reducing the surface area available for diffusion likely would not be significant for regional-scale transport because the travel time would be larger than the time required for fracture and matrix solute concentrations to reach equilibrium (Dykhuizen, 1992, p. 2450), provided that the fractures and channels were no more than approximately a meter apart. Given that fracture and channel spacings are not known to be less than one meter, fracture channeling in the Culebra may result in up to a factor of 10 increase in radionuclide release relative to uniform flow over entire fractures planes in a numerical implementation of double-porosity transport.

3.2.7 Plume Dispersion

Summary Statement: Rapid pressure responses to pumping observed over large distances in wells suggest extensive connectivity of fractures in portions of the WIPP land-withdrawal area. Tests that reveal delayed yield from storage under such fractured conditions dictate the use of either a double-porosity or double-medium (double permeability) model to represent Culebra transport.

Discussion: Large-scale dispersion of contaminants in such situations is controlled to various degrees by the following mechanisms (see Figure 3.2.7-1):

1) Dispersion of solute moving within individual fractures of the system. This is dispersion that occurs within the fracture due to longitudinal velocity variations imposed by laminar flow modified by transverse diffusion and the effect of variations of aperture, roughness, and channeling.

2) Dispersion of the plume due to the divergent, intersecting network of variable aperture conduits that comprise the fracture geometry. This dispersion is very dependent on the statistical properties of the heterogeneous fracture network (fracture orientations, spacings, extent, connectivity, and the mechanism of partitioning of flow).

3) Advective flow from fracture to matrix and matrix to fracture. This mechanism, coupled with matrix diffusion greatly increases the effective dispersion of the plume.

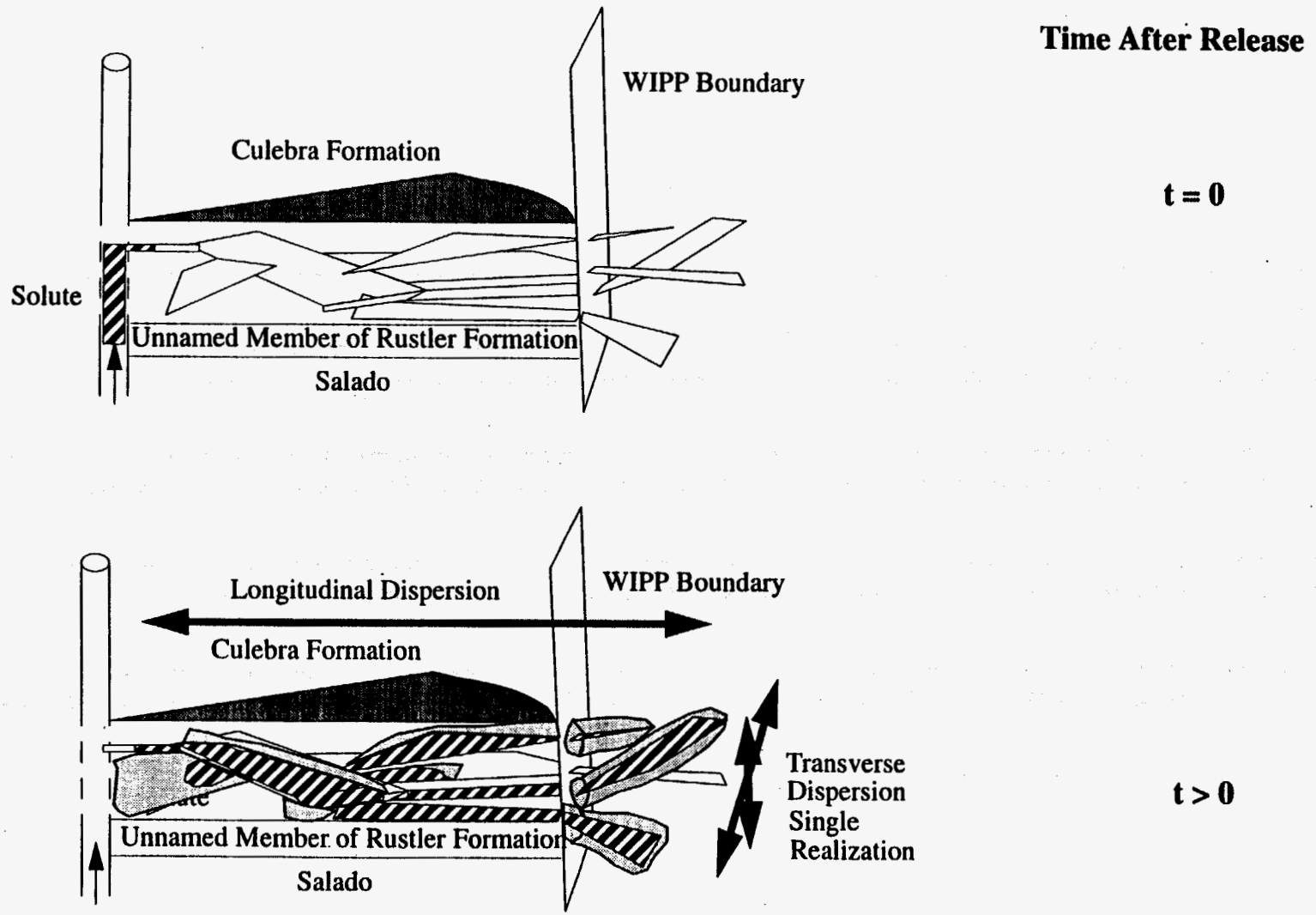

Figure 3.2.7-1. Dispersion due to a confined fracture network with matrix advection.

4) Macroscopic dispersion of the plume in matrix transport. This type of dispersion has been well studied and is controlled largely by the variability of the matrix permeability, its associated correlation scales and the initial size of the plume.

5) Local dispersion in matrix transport. This dispersivity is typically measured in tracer tests of non-fractured media and is important in the calculation of the variability of a plume in a single realization of transport in the matrix.

The most complete model (here referred to as the Fracture Network Model) possible for transport would include separate flow models for the matrix and fracture systems with continuity imposed at their boundaries. Transport between the fracture network and matrix would be carried out via advective flow and diffusion between these two systems. The fracture network would be generated using statistical parameters observed in outcrops and from well logging as well as parameters inferred from tracer tests, while the matrix parameters would be obtained from laboratory core tests as well as pump and tracer tests at the wells that do not show a significant amount of fracture behavior. A less extensive model (referred to as the Matrix Advection Extension to PA Models) may be suitable for use in future performance assessments.

3.2.7.1 MATRIX ADVECTION EXTENSION TO PA MODELS

This proposal starts with the existing PA flow and transport models (SECO-FLOW and SECO-TRANSPORT). Both models are modified to include matrix advection. Transmissivities that were previously derived from pump tests in double-porosity and matrix media are then re-analyzed to separate matrix and fracture transmissivities and to deduce fracture porosities. First and second moments of their distributions and correlation lengths are estimated from these data. The proposed flow and transport model will include a spatially-variable fracture porosity, diffusion coefficient, and matrix permeability but will use a two-dimensional horizontal fracture geometry. Solute may be transported to the matrix via advection or diffusion. Advection may result from local dead-end fractures or, where the number or width of fractures diminish, due to decreases in fracture porosity. Realizations of the specific discharge and velocity fields are calculated using matrix and fracture permeabilities and fracture porosity realizations generated from their respective distributions. This step may require modifications to an existing inverse code to generate both fracture and matrix permeability fields as well as a fracture porosity field consistent with slug, pump and tracer test data. The specific discharge and velocity fields are then used to simulate flow and transport within the fracture and matrix network. Gradients computed through the matrix between the fractures produce advective flow and transport of the contaminant between matrix and fracture and vice-versa. Spatially-variable local parameters control dispersion within the fracture system and within the matrix.

Discussion: Matrix Dispersivity

Modern stochastic theory in single-porosity (matrix) media has shown large-scale transmissivity variability and its associated correlation length to be the controlling factors in the macroscopic dispersion of a solute plume in matrix flow problems. In the 1992 PA, all mass transport was conducted through a fracture system with constant fracture aperture (double-porosity model) and there was no advective transport within the matrix. Although transmissivity data exist to adequately describe large-scale transmissivity variations and consequent macroscopic plume dispersion in single porosity simulation, the present double-porosity numerical model permits no advective flow in the matrix and, hence, no macroscopic matrix dispersion. On the other hand, the local specific discharge calculated from transmissivity realizations using the SECO2D FLOW code is used to calculate local flow velocities within the fractures. These velocities, variable in the plane of bedding, disperse the solute confined within a single fracture in a manner that is supposed to represent the entire matrix/fracture system. Actual dispersion within a single "real" fracture system is dominated by the distribution of fracture apertures as well as the parabolic velocity profile and so may differ significantly from the system modeled in the 1992 PA. Lack of variability in the modeling of geometric parameters describing the fracture system will tend to underestimate fracture dispersivity. Dispersion is probably modeled overly-conservatively in the 1992 PA.

A more realistic representation of the true behavior in the Culebra entails the use of a model that includes matrix advection, matrix permeability and porosity estimated from wells exhibiting matrix flow with additional estimates of matrix permeability from dual porosity test data where the matrix permeability and fracture permeability are estimated separately. The computation of dispersion in the double-porosity media may be more faithfully modeled thereby.

Discussion: Fracture porosity variability

The use of the 1992 PA double-porosity model presents a dilemma in that radionuclide transport is principally conducted through a series of parallel 2D horizontal fractures, which is an unlikely, albeit conservative, conceptualization of the actual mixed fracture/matrix flow system. It is particularly important to identify geometric fracture parameters from field data because the objective of field tests is to characterize qualitatively the geologic mechanisms important to transport at the WIPP site. It has been noted that different sets of geometric parameters and even different conceptual models (Gelhar, 1993, p. 216) may produce reasonable fits to concentration breakthrough curves. The matching of a single geometric parameter, namely spacing of a cubic system of fractures, using SWIFT II simulations as done in Jones et al. (1992) is believed to be as good as is possible given the present state of the art in analysis of tracer test data. Other models, using site-specific geologic data could provide alternate interpretations, as noted elsewhere.

Because the double-porosity conceptual model used in the 1992 PA permits no advective flow in the matrix, it is not possible to take credit for dispersion produced by the great contrasts

in local velocity between fracture flows and matrix flows, nor is credit taken for macroscopic dispersion within the matrix via its permeability variations. Instead, the local specific discharges from a single porosity flow model (using GRASP-INV transmissivity realizations which are derived using data from both single and double-porosity pump tests) are used with fracture spacings with ranges derived from Jones et al. (1992). The conservation of specific discharge models all transport through the fracture system, an overly-conservative assumption. The velocity field generated from the overall transmissivity data is likely to have less spatial variability than the velocity field generated from consideration of flow through fractures only. Gelhar (1993, p. 275) calculates the asymptotic longitudinal fracture macrodispersivity, A_{fract} with the relation,

$$A_{fract} = \left(4 + 0.205\sigma_\beta^2 + 0.16\sigma_\beta^4 + \ldots\right)\sigma_\beta^2\lambda_\beta$$

where σ_β^2 and λ_β are the variance and correlation length of the natural logarithm of the apertures. Noting that the variance of the log of apertures is related to the variance of the log of fracture porosity by

$$\begin{aligned} Var(\ln(\phi_{fract})) &= Var\left(\ln\left(\frac{b}{b+B}\right)\right) \\ &\cong Var\left(\ln\left(\frac{b}{B}\right)\right) \\ &= Var(\beta) \end{aligned}$$

where β is the variability of the natural log of the aperture, we may calculate $Var(\beta) = \sigma_\beta^2 = 0.97$ using the fracture porosity data from the 1992 PA. Calculating the longitudinal fracture macrodispersivity from Gelhar's equation gives $A_{fract} = 4.1\lambda_\beta$. The asymptotic longitudinal macroscopic dispersivity for the Culebra as simulated in 1992 PA is approximately

$$A = \sigma_f^2\lambda \cong 2.25\lambda$$

where σ_f^2 and λ are the variance and correlation scales for the porous medium transmissivity as derived from pump and tracer tests showing both matrix and double-porosity nature. Previous analysis of WIPP data indicate a correlation length of about 1600 meters. The point of this exercise is to show that the macroscopic dispersivity of the present PA model is

dependent upon a length scale associated with the set of matrix and double-porosity pump tests. Actual dispersion within a fracture should be dictated by the fracture porosity length scale. This scale is probably smaller that obtained in pump tests.

3.2.7.2 FRACTURE NETWORK MODEL

The most realistic model for transport in the Culebra is a full fracture model that includes advective flow in both the matrix and fractures and that incorporates the variability of both the matrix and fracture transmissivity and the variability of the fracture geometric parameters. The variability of these parameters would be conducted in the same manner as the realizations of the transmissivity field are currently carried out; that is, as a set of realizations conditioned on observed transmissivities from pump tests and heads in wells. Statistical moments associated with fracture geometric parameters could be estimated from outcrop and from slant-hole cores..

The fracture network model could be either 3D or quasi-3D in nature. Implementation of this model would require a considerable amount of effort and risk. An inverse code to properly generate self-consistent realizations of both the fracture network and matrix transmissivity would have to be developed. A transport code exists in which a fracture network, each fracture being of infinite extent, has been simulated under the influence of a constant gradient. All flow in this model is assumed laminar and takes place only within the fractures. The results of simulations using this model show a linear increase of dispersivity with distance of flow. No ergodic behavior (no asymptotic limit) was seen in this study, however, limiting behavior may be possible at a larger scale. It is clear that the significant lateral dispersion induced by a stochastically-oriented fracture network will significantly lower concentrations at the WIPP outflow boundaries. This Fracture Network Model (without matrix diffusion) would probably also yield somewhat less integrated discharge at WIPP outflow boundaries due to the fact that a significant portion of the plume is transported in directions not aligned with the mean gradient. However, due to the fact that the WIPP outflow boundary is approximately equidistant from the point of release and that no retardation mechanism exists in this model, we would not expect a great deal of reduction in the integrated discharge at the site boundary. Compliance is based on the integrated discharge, not concentration, at the WIPP boundary for disturbed scenarios which result in a release into the Culebra. The incorporation of mechanisms of retardation, such as radioactive decay, matrix diffusion, advective flow in the matrix, and dead-end fractures would lead to a much more significant decrease in release.

The WIPP Project is unaware of any public-domain model that combines a stochastically-oriented fracture network with the above release mechanisms. Furthermore, the proper use of a Fracture Network Transport code would require significant expenditures and time to identify the geometric fracture parameters over significant length scales.

3.3 Culebra Chemical Retardation

PA calculations and sensitivity analyses (Helton et al., 1991; WIPP PA Department, 1992; Bertram-Howery et al., 1990) have identified the radionuclide retardation factor (relative transport rate of radionuclides with respect to the ambient fluid flow velocity) in the Culebra as a key parameter for the WIPP facility compliance with regulations. Radionuclide retardation could result from both physical and chemical factors. Physical retardation due to matrix diffusion has been demonstrated through double-porosity models (Reeves et al., 1991). However, no experimental data for actinides exist on physical retardation due to matrix diffusion under conditions expected to be present in the WIPP waste. Chemical retardation is caused by various chemical reactions that may occur between the chemical species in the solution and at the solid/solution interface. The chemical retardation phenomenon has been observed both in laboratory and field tests associated with groundwater pollution studies involving organic pollutants (Mackay et al., 1986) and inorganic pollutants (Weber et al., 1991, and references therein). This phenomenon also forms the basis for chromatographic methods for chemical separation (Heftmann, 1961).

3.3.1 Rock-Water Interaction in the Culebra

Summary Statement: The conceptual model of chemically retarded transport in the Culebra is dependent on several flow and transport related parameters, which are affected by the nature of fluid flow within the Culebra and the distribution of minerals in the Culebra. Evidence available to date indicates that chemically retarded transport in the Culebra will occur and will attenuate the cumulative radionuclide release. Some of the numerical models used to simulate retarded transport may incorrectly predict the cumulative releases, however, due to incorrect assumptions about the distribution of minerals and the nature of fluid flow within the Culebra. Currently, the potentially large amount of sorption on the proposed "clay mineral linings" on fracture surfaces is not included in performance assessment models. The baseline conceptual model for chemically retarded transport is advective flow through high-angle fracture sets that do not have a concentration of clay minerals adjacent to them (and are not clay "lined"), coupled with diffusive transport of solutes into a matrix with a mineralogy equivalent to the bulk mineralogy of the Culebra (i.e., about 95 wt. % dolomite and 5 wt. % clay minerals).

Discussion: In constructing a conceptual model for chemical and physical retardation of actinide elements in the Culebra, two critical factors must be considered: (1) the nature of the substrates that are present in the flow path; and (2) the amount of surface area available for mineral-solute interaction. In implementing the conceptual model using experimentally determined parameters with a numerical code, consideration must be given to geometric scaling issues and chemical equilibrium (e.g., adsorption kinetics). Obviously, numerical codes to evaluate solute transport must adequately represent the system and produce accurate predictions. But because of the potentially very large number of variables that would be required in an exact solution of the

conceptual model, simplifying assumptions based on experimental results and observations must be made.

Foremost in developing a conceptual model for chemically retarded transport is consideration of the rock fabric and the nature of the fluid flow through that rock fabric. An accurate and concise description of geologic aspects of the Culebra that are pertinent to chemical and physical retardation can be found in the 1992 WIPP preliminary performance assessment documentation (WIPP PA Department, 1992, Volume 2, p. 2-16 through 2-23, and references cited therein) and in other parts of this position paper. Some specific points warrant discussion here.

The two major minerals that are considered to be important for adsorption in the Culebra are dolomite, which is a potentially important adsorbent because of the vast amount present in the Culebra, and clay minerals, which are not nearly as abundant as dolomite, but are typically quite powerful adsorbents. Most of the clay minerals in the Culebra are detrital in origin, deposited along bedding planes while the evaporite minerals, such as dolomite, were forming. The clay minerals are concentrated in discontinuous lenses or are present as anastomosing networks, but are generally concentrated along sub-horizontal planes. The mineralogy of some of the clay minerals (e.g., what is now present as corrensite) were diagenetically altered, but their spatial distribution did not change since deposition. Bioturbation apparently was not substantial enough to homogenize the distribution of minerals as is observed in some carbonate rock types. In many carbonate rocks, pressure-solution produces stylolites, which usually appear as jagged surfaces where insoluble residue is concentrated. Stylolites are not observed in the Culebra . Petrographic and visual observation of the Culebra demonstrates that the distribution of clay minerals has not changed appreciably since deposition. Further, authigenic clay minerals are not present in appreciable quantities: the clay minerals are detrital, and were present before fracturing. Because clay minerals are so important to chemically retarded transport, substantial effort has been made on evaluating them.

Fractures in the Culebra can be divided into two categories based on their orientation. One category are those caused by parting along the sub-horizontally oriented planes of relative weakness in the rock resulting from the concentrations of clay minerals at bedding planes. Sub-horizontal fractures, therefore, have a relatively greater concentration of clay minerals adjacent to them. There is typically not a discrete clay mineral layer (i.e., "clay lining") that uniformly coats the surfaces of the fractures, and conceptual models involving discrete clay mineral "linings" cannot currently be supported.

Concentrations of clay minerals <u>adjacent</u> to sub-horizontal fracture surfaces can be supported, however. Unfortunately, the incomplete core coverage coupled with the mineralogic heterogeneity of the Culebra makes it difficult to defend the concept of advective fluid flow solely through sub-horizontal fractures with concentrations of clay minerals adjacent to them. Further, documenting the concentrations and lateral distributions of clay minerals adjacent to

fractures, as well as physico-chemical parameters necessary to calculate transport (e.g., porosity, diffusion constants, thickness), would be a difficult task.

The second set of fractures observed in the Culebra are high-angle fractures (greater than 45 degrees from horizontal) and are not distinctly controlled by distribution of clay or other minerals. Detailed examination of core samples of the Culebra has shown that many of the high-angle fractures are filled to various extents with gypsum. Beauheim and Holt (1990, Figure 2-13) demonstrated that the percentage of high-angle fractures that are filled with gypsum crystals increases eastward across the site. The presence of post-depositional gypsum fill indicates that groundwater has flowed through those high-angle fracture sets in the past, but the age of these fillings is not known.

Lines of evidence that have been used to deduce which fracture set is currently the active flow path include visual observations in the air intake and waste handling shafts, examination of post-depositional gypsum fill, and examination of a rust-colored coating (possibly iron oxyhydroxide) on fracture surfaces. Those observations support fluid flow in both the sub-horizontal fractures as well as the high-angle fractures (refer to 3.2.5), and it is not clear which fracture set is currently the preferred groundwater flow path. It is not likely that the fluid flow path can be elucidated without substantial work. It may also be difficult to defend flow through a particular fracture set across the entire WIPP site, because of the heterogeneity in Culebra rock fabric.

Results of field tracer tests conducted within the WIPP land-withdrawal boundary suggest that, on at least local scales (approximately 1 to 100 m), fluid flow in the Culebra is controlled by the double-porosity nature of the rock, in that groundwater flows through fracture porosity by advection and dissolved solutes move into the intercrystalline pores in the matrix by aqueous diffusion (refer to 3.2.5). Transport in this region may occur, however, by matrix advection or matrix advection coupled with fracture advection. An investigation of matrix advection has been proposed as an activity for evaluation by the SPM process. For purposes of evaluating the conceptual model of rock-water interaction in the Culebra, a critical issue is the mineral surface area available for retardation; whether a solute is transported to a mineral surface in the rock matrix by diffusion or advection is of secondary importance. Regardless of the mechanism of transport, movement of solutes through the matrix will increase chemical retardation. However, in the absence of the matrix diffusion component, significant levels of chemical retardation may occur on minerals in close proximity to fracture surfaces. This may be particularly true if advective fluid flow is primarily through the sub-horizontal fractures, which have a greater concentration of clay minerals adjacent to them.

On the basis of the properties of the Culebra described above, thirteen alternative conceptual models for flow and transport are possible (Table 3-1). The thirteen cases are constructs that result from possible combinations of advective and diffusive flow, matrix or fracture transport, flow through high-angle or sub-horizontal fractures, and differences in

distributions of clay minerals within the rock. It is recognized that many of the conceptual models are not very probable, and may be eliminated from serious consideration for reasons described. Implicit in this discussion is an assumption that K_d values suitable for use in a compliance application will be available.

The link between the nature of fluid flow in the Culebra and chemical retardation is a fundamental part of constructing a conceptual model for retarded transport. In other words, chemical retardation is conditional on the mechanism(s) of fluid transport. Conceptual models numbers 1-6 in Table 3.3-1 represent cases in which fracture advection-matrix diffusion is the operative solute transport mechanism, and is by far the most likely mechanism according to results to date. Conceptual models numbers 7-12 represent cases in which no matrix diffusion occurs and that flow occurs solely by fracture advection. Conceptual model number 13, included for completeness, is a case in which the dominant flow mechanism is by matrix advection. This case will not be considered further for the baseline used in the current iteration of the SPM, because it is not consistent with currently supported conceptual models.

For each of the two main groups of conceptual models (1-6 and 7-12), the fracture advection component of fluid flow may be <u>dominated</u> by flow through sub-horizontal fractures, high-angle fractures, or both. The conceptual models within those two groups reflect the possible alternatives. Conceptual models numbers 1 and 7 represent the "fall-back" positions for cases involving fracture advection-matrix diffusion and fracture advection, respectively, in which no retardation occurs (i.e., K_ds are defined as 0). Available information on actinide sorption in the Culebra demonstrate that sorption will occur, but those early scoping data do not provide sufficient quantification of K_ds (refer to 3.2.4).

Because we do not know whether the dominant advective flow path in the Culebra is through high-angle or sub-horizontal fractures, and because we do not know the connectivity of those fracture sets, the current baseline assumption is that advective flow occurs through the high-angle fracture set only, which do not have detrital clay minerals in close proximity to them (conceptual model number 2). To simulate retardation for this conceptual model, a weighted distribution coefficient is used in SP calculations, calculated from the expert panel estimates of K_ds. The apparent bulk rock K_d for each actinide is estimated by combining a 95% weighting of the matrix (i.e., dolomite) K_ds with a 5% weighting of the clay mineral K_ds. The five weight % clay mineral figure was estimated based on the bulk concentration of clay in the Culebra as described in work by Sewards (1991) and Powers and Holt (1990). For this conceptual model, concentrations of clay minerals adjacent to fractures are not recognized.

Table 3.3-1. Alternative Conceptual Models for Rock-Water Interaction in the Culebra Dolomite Member of the Rustler Formation.

conceptual model number (arbitrary)	localized solute transport	potential solute/rock interactions			closest 1992 P.A. sensitivity analysis section	estimated chemical retardation potential
	mechanism	surfaces exposed	mineral distribution*	distribution coefficient(s)		
1	fracture advection; matrix diffusion	fractures + matrix	not important (Kd = 0)	Kd = 0 (no retardation)		none
2**	fracture advection; matrix diffusion	high-angle fractures + matrix	homogenous	weighted clay + dolomite Kd		moderate to high
3	fracture advection; matrix diffusion	sub-horizontal fractures + matrix	concentrations of clay-minerals in matrix adjacent to fractures	clay Kd; dolomite Kd	see text	high to very high
4	fracture advection; matrix diffusion	sub-horizontal fractures + matrix	clay-mineral "lined" fractures	clay Kd; dolomite Kd	section 8.4.4; Figures 8.4-12 to 8.4-13	very high
5	fracture advection; matrix diffusion	high-angle fractures + matrix	concentrations of clay-minerals in matrix adjacent to fractures	weighted clay + dolomite Kd		high
6	fracture advection; matrix diffusion	sub-horizontal + high-angle fractures + matrix	concentrations of clay-minerals in matrix adjacent to fractures	alternate between [weighted clay + dolomite Kd] and [clay Kd; dolomite Kd]	section 8.4.3; Figures 8.4-7 to 8.4-11	high
7	fracture advection; no matrix diffusion	fractures	not important (Kd = 0)	Kd = 0 (no retardation)		none
8	fracture advection; no matrix diffusion	high-angle fractures	homogenous	weighted clay + dolomite Kd		low
9	fracture advection; no matrix diffusion	sub-horizontal fractures	concentrations of clay-minerals in matrix adjacent to fractures	clay Kd	see text	low to moderate
10	fracture advection; no matrix diffusion	sub-horizontal fractures	clay-mineral "lined" fractures	clay Kd	section 8.4.2; Figures 8.4-2 to 8.4-6	moderate
11	fracture advection; no matrix diffusion	high-angle fractures	homogenous	weighted clay + dolomite Kd		low
12	fracture advection; no matrix diffusion	sub-horizontal + high-angle fractures	homogenous	alternate between [weighted clay + dolomite Kd] and [clay Kd; dolomite Kd]		low
13	matrix advection	matrix	homogenous	weighted clay + dolomite Kd		extremely high

* the possibility of Fe-oxyhydroxide coatings on fracture surfaces has not been considered in these scenarios

** baseline conceptual model, with $K_d = 0$

3.3.2 Adsorption

Summary Statement: The 1992 preliminary performance assessment assumed that adsorption of solutes on solid phases obeys a linear isotherm with local chemical equilibrium between solute and solid phases. Conclusive data in support of these assumptions are not currently available. The impact of these assumptions on radionuclide release cannot be estimated at this time due to the lack of relevant information. Therefore, a bounding position at this time with regard to adsorption is to take no credit for adsorption.

In addition, the 1992 performance assessment assumed that K_d values based on batch experiments are applicable to advective and/or diffusive transport and they are not sensitive to model cell size chosen in the numerical implementation of the transport model.

Discussion: Currently, chemical retardation factors (R) in PA analyses are calculated using the following equation (Freeze and Cherry, 1979):

$$R = 1 + \rho_b K_d (1-\phi)/\phi \qquad (1)$$

where K_d is the distribution coefficient for each radionuclide and ϕ and ρ_b are the porosity and bulk density of the rock, respectively. This equation can be derived from the advection-dispersion equation assuming local equilibrium for adsorption and a linear relationship between the amount of a solute adsorbed on the unit amount of the solid, S, and the concentration of the solute, C.

$$S = K_d C \qquad (2)$$

This is the linear isotherm model called the K_d-model. However, other forms of isotherms are quite common (Fetter, 1993). These other forms of isotherms show saturation effects at higher solute concentrations, i.e., isotherms level off at higher concentrations. In some cases, as the solute concentration is further increased, adsorption increases rapidly due to additional processes such as surface precipitation (as monolayers on surfaces) coming into play, and the isotherm takes on the S-shape. Note that currently the linear isotherms for some of the actinides are based on single measurement (Dosch, 1980, 1981; Dosch and Lynch, 1978; Lynch and Dosch, 1980; Nowak, 1980; Serne et al., 1977; Tien et al., 1983). These single-point isotherms are obviously not absolutely correct because one could connect the zero-point and the measured non-zero point of an isotherm using an infinite number of possible curves, including a straight line (i.e., the linear isotherm). Not knowing what the actual isotherms for various actinides look like, it is difficult to assess if the PA calculations based on linear isotherms are conservative.

Another assumption made by PA is that local chemical equilibrium always exists between

solutes and solid phases. However, chemical nonequilibrium is quite common for many organic solutes (see Brusseau et al., 1989 and references therein), and some of the actinides may also exhibit nonequilibrium. Since the equilibration times for relevant actinides are not known, it is not possible to assess the impact of the assumption of local chemical equilibrium on radionuclide release.

Because the assumptions of isotherm linearity and local chemical equilibrium are not fully supported and the impact of these assumptions on radionuclide release cannot be estimated at this time due to the lack of relevant information, the bounding position at this time with regard to adsorption is to take no credit for adsorption, i.e., K_d is assumed to be zero. It should be noted that this is an overly conservative position because Dosch and other workers (see references cited earlier) have clearly established that the Culebra rock significantly adsorbs various actinides, although actual K_ds are not quantifiable at this time.

When additional measured-retardation factors and/or K_d values are available, will they be valid for any conceptual model and are they sensitive to the scale of the experiments? The K_d values are applicable to advective and/or diffusive flow because K_d is inherently a property of a solution-solid interface for an adsorbate-adsorbent pair and, therefore, does not depend on the conceptual model being employed for chemical transport. Adsorption of an actinide, and consequently its chemical retardation, is not affected by whether the brine flow is advective, diffusive, or both, but rather by what minerals the actinides encounter during their transport. Similarly, in a homogeneous medium, K_d is a function of the chemical composition of the medium, but not the size of the medium (e.g., core sample size). This is implicit in the definition of K_d based on Eq. (2); the scale independence of K_d is valid even when the adsorption isotherm is nonlinear. The same conclusions are applicable to the distribution coefficient Ka on a per-unit-surface-area basis because Ka is defined in the same way as K_d (Freeze and Cherry, 1979) in the case of chemical transport through fractures. Therefore, K_d values for a given actinide based on laboratory mechanistic adsorption experiments (core size: 20 - 100 micrometer), or laboratory column experiments (core size: up to 100 cm), or field tracer tests (sample size in tens of meters) should be approximately the same if the physical-chemical conditions are comparable and can be used for any model cell size. K_d values obtained from these different experiments may vary to some degree from sample to sample and their size. Since K_d is expected to be scale-independent, as explained above, these variations could be due to several factors:

1) The Culebra is highly heterogeneous at both micro and macro scales. One approach to incorporate these variabilities is through a cumulative distribution function (CDF) for K_d as in the 12/92 PA.

2) Chemical equilibration time for some or all reactions is comparable or greater than liquid transit time through a model cell. In these cases, chemicals move from one location to the next before local chemical equilibrium is established, as implied in Eqs. (1) and (2).

3) K_d variations observed in different samples could be due to different processes (adsorption, ion exchange, and/or precipitation) being responsible for sorption in different samples.

3.3.3 Colloid-Facilitated Radionuclide Transport

Summary Statement: The presence of actinide-bearing colloidal particles in the WIPP system have the potential to accelerate or retard the transport of actinides relative to transport of dissolved species. For long-term performance assessment calculations conducted to date, the impact of colloidal particles on actinide transport were not quantified. Because there is a possibility that colloidal particles can increase transport rates relative to dissolved species, not including colloids in transport calculations for assessment is not necessarily conservative. For example, some colloidal particles are sufficiently large to be excluded from participating in matrix diffusion. Actinides sorbed on the surfaces of those colloidal particles will not be physically retarded, and actinide transport by colloids therefore must be considered. Results from a recently initiated experimental program have reduced the potential impact of colloid particles on actinide transport. Specifically, "hard-sphere" carrier colloids are not mobile, regardless of whether they have sorbed radionuclides on their surfaces, and so are eliminated from participation in actinide transport. Actinide intrinsic colloids and "soft-sphere" carrier colloids (e.g., humic materials) may be mobile, but are sufficiently small to undergo matrix diffusion in the Culebra and so will be physically retarded. Actinides that are bioaccumulated by or sorbed on microbes, however, will be transported primarily by fracture advection because the relatively large sizes of microbes precludes them from entering the intercrystalline pores of the Culebra matrix.

Discussion: Quantification of actinide transport by colloidal particles requires coupling of various aspects of hydrogeology, geochemistry, and colloid chemistry (see, e.g., McDowell-Boyer et al., 1986; Hwang et al., 1991; Nuttall et al., 1991; Bennett et al., 1993; van der Lee et al., 1993). Those aspects may be grouped into the following categories: (1) the physico-chemical behavior of colloidal particles in the dispersent, including the formation of the particles and their kinetic and chemical stabilities; (2) interaction of the colloidal particles with actinides; and (3) the hydrologic behavior of colloidal particles in the subsurface environment. The potential importance of colloid-facilitated radionuclide transport has only been recognized for about a decade (see, e.g., Avogadro and de Marsily, 1983) and rigorous transport models and computer codes suitable for long-term performance assessment of the WIPP Site are not yet available. However, by focusing on concepts included in the three categories above with specific consideration to the WIPP environment, quantifying the impact of colloidal particles on actinide transport has been simplified to the point where it is a tractable problem.

The following text includes a brief review of different types of actinide-bearing colloids and their behavior in WIPP environments.

3.3.3.1 PHYSICO-CHEMICAL BEHAVIORS OF COLLOIDAL PARTICLES

Carrier colloids, which are ordinarily non-radioactive, are colloidal-sized particles which may act as substrates for sorption of actinides as well as other metals (carrier colloids with sorbed actinides are referred to in the published literature as pseudocolloids, Type II colloids, and Fremdkolloide) (Lieser et al., 1986a, 1986b, 1990; Buddemeier and Hunt, 1988; Kim, 1991). The carrier colloid category is further subdivided on the basis of known physico-chemical behaviors of those colloidal particles.

"Hard-sphere" carrier colloids, traditionally referred to as hydrophobic colloids in colloid chemistry, have discrete well-defined particle-fluid boundaries and are stabilized in very low ionic strength solutions by electrostatic effects caused by the electric double surrounding the particles (Heimenz, 1986). At high ionic strengths (which are actually quite low relative to brines associated with the WIPP), however, the electric double layer surrounding the "hard-sphere" colloids collapses, and virtually eliminates electrostatic repulsion between particles (Gregory, 1978; van Olphen, 1991, p. 24; see also Derjaguin and Landau, 1941; Verwey and Overbeek, 1948; Matijević, 1973). Forces of attraction between the particles (i.e., van der Waals forces) causes agglomeration of particles to form clusters large enough to settle by gravity. This phenomenon has been known empirically for well over a century (see, e.g., Hardy, 1900) and was theoretically explained in the middle of this century (Derjaguin and Landau, 1941; Verwey and Overbeek, 1948).

The WIPP Site is unique among proposed nuclear waste repositories in that groundwaters in both the near-field (i.e., the disposal room) and the far-field (i.e., the Culebra) environments consist of high ionic strength brines (refer to Brush, 1990; Siegel et al., 1991b). Experiments at Sandia National Laboratories (SNL) have confirmed that dispersions of "hard-sphere" carrier colloids are not kinetically stable in Culebra brine simulants (hydrogeochemical facies "A" and "C;" Siegel et al., 1991b), Salado Formation-like brine simulants (Brine A; Molecke, 1983; Brush, 1990), and Castile Formation brine simulants (ERDA-6; Brush, 1990). Therefore, "hard-sphere" carrier colloids have been eliminated from further consideration in quantifying transport of actinides. This group of colloids includes many of the colloidal particles identified at other sites (see McCarthy and Degueldre, 1993, their Table 6). Colloidal particles that can be eliminated from consideration in transport of actinides at the WIPP Site include iron(III)-(hydr)oxides, clay minerals, and mineral constituents of the host rock. Further, colloidal particles produced from drilling (i.e., cuttings) and mineral precipitates formed from brine mixing will not be kinetically stable.

Sterically stabilized "hard-sphere" carrier colloids are coated with compounds capable of modifying the colloids' surface behavior so that electrostatic attraction and repulsion forces are overcome, rendering them kinetically stable. An example of this colloid type are colloidal particles stabilized by organic compounds in sea water (Honeyman, 1991; Honeyman and

Santschi, 1992). Microbes are probably best placed in this category, although their cell walls are not rigid. At the WIPP Site, concentrations of naturally occurring microbes are on the order of 10^9 to 10^{10} cells per liter (Francis and Gillow, 1994, their Table 1). In the presence of nutrients provided by WIPP waste constituents, those concentrations are likely to increase. Microbes are important for actinide transport because they may act as substrates for sorption of actinides, but also may bio accumulate actinides. In addition to microbes, it is well known from industrial research that colloidal dispersions can be sterically stabilized in electrolytes by the addition of some types of polymers (see, e.g., Theng, 1976; Sato, 1980). It is unlikely, however, that potential steric compounds such as alcohols and carboxylic acids produced as by-products of microbial degradation of WIPP waste, could be present in large enough concentrations to have an impact on stability of "hard-sphere" carrier colloids in the extremely high ionic strength brines associated with the WIPP. Until results from the ongoing colloid experimental program are available, sterically stabilized "hard-sphere" carrier colloids (i.e., microbes) should be included in transport calculations.

"Soft-sphere" carrier colloids are flexible particles with rather indistinct particle-fluid boundaries, and are essentially dissolved macromolecules. They are not affected by ionic strength in the same way as "hard-sphere" carrier colloids. "Soft-sphere" carrier colloids are closest in form and behavior to particles referred to as hydrophilic colloids in the traditional colloid chemistry literature (Lyklema, 1978; Heimenz, 1986); examples include humic and fulvic acids (Choppin, 1988; Tiller and O'Melia, 1993). Because this type of colloid is not destabilized by high ionic strengths, "soft-sphere" carrier colloids may be important in transport of actinides at the WIPP. Humic and fulvic materials (high-molecular weight organic macromolecules) are of particular concern because of their well-known capability of complexing with metal cations, including actinides (Choppin, 1988, Dearlove et al., 1990; Vlassopoulos et al., 1990; Tipping, 1993; van der Lee et al., 1993). The concentrations of humic materials in deep subsurface groundwaters is typically quite small, because of the long periods of time available for oxidation of those materials. Existing information on total organic carbon (TOC) concentrations in Culebra groundwaters, for example, shows that TOC is on the order of 1 mg/L (Myers et al., 1991) which is quite low. An additional potential source of humic materials is from soil constituents of WIPP waste (U.S. Department of Energy, 1994b, Table 4-1, Waste Matrix Code Group 4200), or perhaps from long-term microbial degradation of cellulosic constituents in the waste. Experiments are in progress at SNL to investigate this type of colloid.

Actinide intrinsic colloids (also known as true colloids, Type I colloids, and Eigenkolloide) are thought to form by condensation reactions of hydrolyzed actinide ions (Maiti et al., 1989), to form macromolecules, or "polymers," of colloidal size. It is believed that the actinide ions are bridged by hydroxyl groups or oxygen ions (Kim, 1991). Following the oxidation state analogy described earlier in this paper, the tendency of actinides to hydrolyze and to form intrinsic colloids follows the order: $M^{4+} > M(VI)O_2^{2+} > M^{3+} > M(VI)O_2^{2+}$ (Choppin, 1983; Kim, 1991). The tendency for formation of one particular actinide intrinsic colloid, the Pu(IV)-polymer, is enhanced by increased concentrations of Pu(IV), temperature, and basic conditions

(Toth et al., 1981). Examples can be found the literature of polymeric species of most of the actinides of importance to WIPP (see e.g., Baes and Mesmer, 1976; Kim, 1991). It is important, however, to note the sizes of polymers described in the literature. It is well known that as polyvalent metals, the actinides can form lower polymers such as dimers, trimers, tetramers, and hexamers. However, in terms of physical transport behavior, the lower polymers will behave no differently than dissolved monomeric species. In contrast, the higher polymers, such as the Pu(IV)-polymer, may reach colloidal sizes (1 nm to 1 μm) and will have different hydrodynamic properties than the sub-colloidal-sized dissolved species.

The most well-known and well-studied actinide intrinsic colloid is the Pu(IV)-polymer. Most of the knowledge about the Pu(IV)-polymer comes from research at relatively high Pu concentrations in highly acidic solutions (e.g., Kraus, 1956; Costanzo et al., 1973; Bell et al., 1973a, b; Lloyd and Haire, 1978; Toth et al., 1981), which was conducted to help improve processing techniques. Investigations focusing on chemical conditions relevant to environmental concerns have been conducted more recently (Cleveland, 1979; Rai, 1981; Kim, 1991; Nitsche et al., 1992). A conclusive demonstration of the mechanisms of formation of the Pu(IV)-polymer has not yet been made, but there is a preponderance of evidence that shows that polymerization is strongly linked to hydrolysis (see e.g., Kim, 1991), and that the initial polymerization produces an amorphous macromolecule that becomes crystalline with time (see Cleveland, 1979, and references therein). Lloyd and Haire (1978) showed that the aged polymer actually consists of nanometer-sized mineral crystallites. Rundberg et al. (1988) and Triay et al. (1991) used different analytical methods to confirm the particulate nature of the Pu(IV)-polymer, and also estimated that the size was on the order of nanometers. In terms of implications for transport at the WIPP, if the Pu(IV)-polymer is indeed a crystalline colloidal particle, rather than a "soft-sphere"-like (hydrophilic) colloid, it would behave like a "hard-sphere" (hydrophobic) colloid. As such, it would be destabilized by high ionic strength solutions, such as WIPP brines. Critics may point out that they are familiar with Pu(IV)-polymer solutions that have remained stable for years. That observation is not necessarily inconsistent with the notion that the Pu(IV)-polymer is a "hard-sphere" type colloid. For example, Overbeek (1982) reported that some of the gold sols (dispersions of 3 nm diameter metallic gold, a "hard-sphere" type colloid) used in historically important experiments by Michael Faraday in the mid-1800's were still in existence at the time of Overbeek's publication. Experiments are in progress to evaluate the formation and behavior of actinide intrinsic colloids, including the Pu(IV)-polymer, at Lawrence Livermore National Laboratory (LLNL). Until such results are available, however, actinide intrinsic colloids should be considered to be dissolved macromolecules which are not destabilized by high ionic strength WIPP brines.

In summary, "hard-sphere" carrier colloids can be eliminated from further consideration because of the destabilizing effects of the high ionic strength brines associated with the WIPP. The remaining subtypes, sterically stabilized "hard-sphere" carrier colloids (microbes), "soft-sphere" (humic materials) carrier colloids, and actinide intrinsic colloids cannot be eliminated. The remaining portion of this discussion focuses on the sources and transport behaviors of those

colloids.

3.3.3.2 SOURCES OF COLLOIDAL PARTICLES

In an intrusion scenario, there are two potential sources of actinide-bearing colloids: the disposal room environment (which also includes colloids introduced to the disposal room from Castile Fm. groundwaters), and colloids formed in situ within the Culebra. In an undisturbed situation, the types of colloids that could be present in Culebra and Castile Fm. brines are "hard-sphere" carrier colloids, microbes, and "soft-sphere" carrier colloids (humic materials). As described above, the high ionic strengths of the brines will destabilize the "hard-sphere" carrier colloids; actinides may sorb onto those colloids, but they will be immobilized. Because of the presence of soils in WIPP waste (U.S. Department of Energy, 1994b, Table 4-1, Waste Matrix Code Group 4200), the concentration of humic materials in disposal room brines is likely to exceed the concentration of humic materials in Castile Fm. or Culebra brines. Likewise, because of the nutrients provided by organic components of the waste, the concentrations of microbes in the disposal room environment will exceed the concentration of microbes in Castile Fm. or Culebra brines. Actinide intrinsic colloids are more likely to form in environments of greater actinide concentrations such as the disposal room environment, rather than the Culebra. The source of colloidal particles that may participate in transport of actinides is clearly dominated by those introduced from the disposal room environment. It follows that investigation of colloid-facilitated actinide transport in the Culebra has close ties to the characterization and quantification of mobile colloidal actinides for the Actinide Source Term Program (refer to the Source Term position paper for details).

3.3.3.3 TRANSPORT BEHAVIORS

Because the sizes of colloidal particles are significantly greater than the sizes of dissolved species, colloidal particles behave differently in terms of transport. In quantifying colloid-facilitated actinide transport in the Culebra, the primary distinction in colloid subtypes is whether the sizes of colloidal particles are larger or smaller than the mean pore throat diameters (0.63 μm; Kelley and Saulnier, 1990, p. 4-10) of the intercrystalline pores in the Culebra matrix. Colloidal particles that are smaller than the pore throats will be transported into the rock matrix by physical diffusion, and, therefore, transport will be retarded physically. In contrast, colloidal particles that are larger than pore throats will be excluded from the matrix and will be transported by advection and diffusion in fractures (see, e.g., Vilks, 1994). The subtypes of colloidal particles included in the current baseline fall into two categories in terms of hydraulic properties: (1) actinide intrinsic colloids and "soft-sphere" carrier colloids (humic materials) behave as dissolved macromolecules that are small enough to enter the pore throats in the Culebra, but are sufficiently larger than other dissolved species to have reduced physical diffusion rates; and (2) microbes, which are larger than the mean pore throat diameter in the Culebra, and will not undergo matrix diffusion.

Conservative estimates of the effective diffusion constants for the macromolecular-type colloidal particles have been made on the basis of their sizes (the free water diffusion constant for a solute in a liquid is inversely proportional to the radius of the diffusing particle; see Bird et al., 1960; Heimenz, 1986, p. 81).

The WIPP Project recognizes that there are other phenomena, such as surface (physical) filtration, chemical filtration by sorption of colloids themselves onto fixed substrates, and equilibrium sorption and desorption of actinides on surfaces of carrier colloids, that will affect the transport of actinides by colloidal particles (see Bennett et al., 1993). Rigorous quantification of the effects of those phenomena, however, is not tractable at the current time for long-term performance assessment calculations for a system as complex as the WIPP. Disregarding those phenomena, however, will not result in greater releases. Furthermore, those phenomena which are being disregarded are expected to be of secondary importance on reducing releases compared to other phenomena, such as the kinetic and chemical stability behavior of colloids in WIPP brines.

3.3.4 Actinide Coprecipitation From Brine Mixing

Summary Statement: In an intrusion scenario, mixing of disposal room brines with Culebra brines are likely to result in a non-equilibrium condition resulting in precipitation of actinide-bearing minerals (coprecipitation) or in dissolution of Culebra minerals. The 1992 preliminary performance assessment did not evaluate effects due to brine mixing. Coprecipitation will decrease radionuclide release and reduce transmissivity in proximity of the borehole, whereas rock dissolution will increase transmissivity by opening clogged fractures or widening existing fractures. Coprecipitation may result in the formation of relatively large crystals in the rock matrix, or it may result in the formation of "hard-sphere" type colloids (see Section 3.3.3). In the latter case, those colloidal particles will be destabilized by the high ionic strengths of the Culebra brines, rendering them and any coprecipitated actinides immobile. Adequate experimental results or models are not currently available to quantify a reduction in actinide transport by coprecipitation. However, it is reasonable to assume that disregarding the effects of coprecipitation or dissolution is a conservative assumption.

Discussion: In most natural environments, mixing of groundwaters in equilibrium with different subsurface environments produces non-equilibrium conditions resulting in precipitation of solids or dissolution of minerals in the host rock.

Scoping calculations using chemical equilibrium modeling have demonstrated that at the WIPP site, mixing of disposal room brines (which may be dominated by Castile or Salado brines) with Culebra brines may result in precipitation of sulfate or carbonate minerals. On the basis of published literature, actinide elements are often readily incorporated into the crystal lattices of carbonate minerals (see e.g., the review by Stout and Carroll, 1992). Precipitation of actinide-

bearing minerals or immobile colloidal particles is an appealing prospect in terms of performance of the WIPP, because this retardation mechanism is not reversible like adsorption. Once the mineral forms, it is not likely to dissolve unless new non-equilibrium conditions are introduced. In addition to providing a potentially immobile sink for actinides, precipitation of minerals due to brine mixing may also reduce the transmissivity of the Culebra in proximity of the intrusion borehole.

Alternatively, brine mixing could result in dissolution of the host rock until equilibrium is reached. If the pH of the disposal room brine is outside the stability range of dolomite (about pH6 to pH9), dissolution of dolomite in the Culebra is likely to occur. However, equilibrium would be reached in a very short time because of the reactivity of dolomite. Any dissolution required for the brine to reach a new equilibrium would, therefore, occur near the borehole, and increases in transmissivity due to dissolution would be localized. Because of the relatively high ionic strengths of possible disposal room brines, dissolution of the host rock may also occur due to ionic strength effects (see, e.g., Freeze and Cherry, 1979, p. 107-108). However, that effect is expected to be secondary compared to dissolution due to exceeding the pH stability range of dolomite.

In summary, mixing of disposal room brines with Culebra brines are likely to produce a non-equilibrium condition. Localized dissolution of the host rock may occur to neutralize the pH of the brine mixture, but because of the rapid dissolution kinetics of dolomite, dissolution is expected to be limited to the proximity of the intrusion borehole. If precipitation occurs, actinides are likely to be included in mineral precipitates, and will be immobile, regardless of whether they are colloidal particles or relatively large crystals. Unfortunately, quantifying retardation of actinides due to coprecipitation is complicated by the need to consider precipitation kinetics, the effects of complexes on actinide coprecipitation, and coupling solute flow rates with coprecipitation. Consequently, whereas benefit could be gained if actinide coprecipitation were quantified, it is conservative to disregard the effects of brine mixing.

3.4 Long Term Processes

This section contains conceptual and mechanistic models concerning processes that potentially could act over thousands of years to alter patterns of groundwater flow in strata above the Salado Formation.

3.4.1 Climate Change

Summary Statement: Climate in southeastern New Mexico may be wetter and cooler at some times during the next 10,000 years than it is at present. A wetter and cooler climate may result in an increase in the amount of water infiltrating to the saturated zone, thereby raising the water

table. A rise in the elevation of the water table could increase the hydraulic gradient or change its direction in the Culebra or other members of the Rustler Formation. Three-dimensional modeling work to date suggests that the hydrologic system may respond too slowly for significant changes in the hydraulic gradient in the Culebra to occur within 10,000 years. A rise in the water table could also affect performance by increasing the extent of the saturated zone in the rocks above the Rustler Formation

Discussion

Paleoclimates and Climatic Variability

Geologic data from southeastern New Mexico and the surrounding region show repeated alternations of wetter and drier climates throughout the last 1.5 million years, corresponding to global cycles of glaciation and deglaciation. Data from plant and animal remains and paleo-lake levels permit quantitative climate reconstructions for the region only for the last glacial cycle, and confirm the interpretation that conditions were coolest and wettest during glacial maxima (Swift, 1993). The hottest and driest conditions since the last glaciation have been similar to those of the present. Modeling of global circulation patterns suggests that these changes resulted from the disruption and southward displacement of the winter jet stream by the ice sheet, causing an increase in the frequency and intensity of winter storms throughout the American Southwest (COHMAP Members, 1988). Mean annual precipitation 22,000 to 18,000 years ago, when the last North American ice sheet reached its southern limit roughly 1500 km north of the WIPP, was approximately twice that of the present. Mean annual temperatures may have been as much as 5°colder than at present.

Glacial periodicities have been stable for the last 800,000 years (Hays et al., 1976; Imbrie et al., 1984; Imbrie, 1985). Barring anthropogenic changes in the Earth's climate, relatively simple modeling of climatic response to orbital changes in insolation suggests that the next glacial maximum will occur in approximately 60,000 years (Imbrie and Imbrie, 1980). The extent to which unprecedented anthropogenic climate changes may alter this conclusion is uncertain, but presently available models of climatic response to an enhanced greenhouse effect (e.g., Mitchell, 1989; Houghton et al., 1990) do not predict changes of a larger magnitude than those of the last 1.5 million years. Furthermore, published models do not suggest significant increases in precipitation in southeastern New Mexico following global warming (Washington and Meehl, 1984; Wilson and Mitchell, 1987; Schlesinger and Mitchell, 1987; Houghton et al., 1990). Even allowing for anthropogenic change, climate variability at the WIPP can be bounded by extremes of the last 1.5 million years (Swift, 1993).

Relatively shorter-term climatic fluctuations have occurred throughout the last 1.5 million years with periodicities on the scale of hundreds to thousands of years. The causes of these nonglacial fluctuations are , in general, unknown, but paleoclimatic data indicate that precipitation may have approached glacial highs at some times during the last 10,000 years

(Swift, 1993). Based on the past record, fluctuations of this sort are probable during the next 10,000 years, and must be included in long-term assessments.

Hydrologic Modeling of Climate Change

In regions with dry climates, such as present-day southeastern New Mexico, the water table (i.e the top of the saturated zone) is at some depth below the land surface. Only a few percent of the total precipitation infiltrates and percolates downward through the unsaturated zone. If the climate were to become cooler and wetter, the amount of moisture that infiltrates to the water table could be somewhat greater, and consequently the water table could rise. A conceptual model based on the concept of the groundwater basin described in Section 3.1.2 is used to evaluate possible changes in groundwater velocities in strata overlying the Salado Formation that could occur if the climate becomes wetter. According to this conceptual model, the elevation and shape of the water table determine to a large extent the patterns of groundwater flow in the basin. This conceptual model assumes that there is sufficient vertical flow through confining layers that the water table influences flow at depth.

Maximum gradients of hydraulic head are predicted to occur when the infiltration rate is sufficient to raise the water to table to the ground surface at all locations. This is because the energy available to move groundwater in a basin depends on the difference in elevation between the highest and lowest positions of the water table. In regions with wet climates, the water table tends to be close to the ground surface everywhere. In regions with drier climates, the water table tends to remain near the land surface in topographically low areas but its elevation fluctuates under topographically high areas in response to changes in infiltration. The difference between the high and low parts of the water table, and consequently the gradient driving groundwater flow, is therefore maximized if the water table is everywhere near the land surface. On a regional scale these gradients will be similar to the slope of the land surface. At a local scale, however, hydraulic gradients can be greater or less than the slope of the overlying land surface.

The possible impact of climate change on flow in confined layers can be demonstrated by considering the Culebra. Present-day flow in the Culebra is toward the south and driven by hydraulic gradients of approximately 3.25 m/km. If flow in the Culebra equilibrated with a water table at the land surface, the flow direction would change to the west and the average hydraulic gradient would be approximately three times greater. Flow rates would be faster given the larger hydraulic gradients if the average transmissivity of the Culebra were the same to the west of the repository as it is to the south. However, an examination of the transmissivity fields used for the 1992 Performance Assessments (LaVenue and RamaRao, 1993) suggests that flow to the west would encounter regions of lower transmissivity than would flow to the south. If calculations confirm that flow to the west would actually pass through regions of low transmissivity, then increased gradients might not result in increased flow rates.

Groundwater will fill an open hole in unconfined units to the level of the water table if the units have a sufficiently large hydraulic conductivity. The present-day position of the water table in the vicinity of the WIPP is not well-known because the Dewey Lake produces very little water to most test holes. The observation that only a small amount of water can be produced from a given drill hole indicates either that the penetrated rock is unsaturated or that its conductivity is small. Brine from an intrusion hole could flow into both saturated and unsaturated portions of the Dewey Lake and the overlying Dockum Group, but could only be transported laterally for long distances toward the accessible environment in the saturated portion. Therefore a wetter climate could impact transport in the Dewey Lake and Dockum Group in two ways. First, it could increase the thickness or lateral extent of the saturated region. Second, the wetter climate could change flow directions and rates in the previously saturated portion.

Results of a three-dimensional modeling study (Section 3.1.2 and Appendix A) suggest that the hydrologic system responds too slowly for increased infiltration at the land surface to significantly modify gradients of hydraulic head in the Culebra over 10,000 years if the confining layers remain undisturbed. However, the greater infiltration could increase the saturated thickness of the Dewey Lake by tens of meters over that period of time.

3.4.2 Drill Holes That May Affect Regional Flow

Summary Statement: Drill holes that do not intersect the waste may still have an affect on long-term performance by altering groundwater flow in strata above the Salado Formation. According to the groundwater basin conceptual model (see Section 3.1.2), the effect on flow in confined units of enhanced vertical communication between hydrostratigraphic units would be to make gradients of hydraulic head more similar to the slope of the ground surface overlying the WIPP site. The effect on performance may be similar to that suggested for climate change (Section 3.4.1).

Discussion: Boreholes have the potential to alter groundwater flow patterns in strata above the Salado by locally increasing the rate of flow across confining layers. We applied the groundwater basin conceptual model (Section 3.1.2) and current knowledge about the shallow flow regime to evaluate the possible impacts of these boreholes.

Pertinent knowledge about the shallow flow regime includes:

Sufficient head data exist to determine horizontal flow directions in the vicinity of WIPP for the Culebra and Magenta dolomites. Flow in the Culebra is generally directed to the south, and flow in the Magenta is toward the west and southwest.

Within the controlled area, fresh-water heads in the Magenta are higher than those in the

Culebra. This suggests, but does not prove, downward flow because heads and fluid densities in the thick confining layer between the Culebra and Magenta (Tamarisk Member) are not known.

Given the concepts of groundwater basin flow described in Section 3.1.2, the differing directions of flows within the Culebra and the Magenta make hydrologic sense. Because of the low conductivity of the Tamarisk Member, there is a significant head loss between the Magenta and the Culebra. Flow in the Magenta more closely reflects the imprint of the local topography, which slopes from east to west within the controlled area. Flow in the Culebra more closely reflects the imprint of the regional land slope, which is generally north to south, paralleling the overall topography of the northern Delaware Basin.

The effect of a leaky borehole in this system will be to increase the vertical conductivity of all units. In those units that already have a relatively high conductivity, this increase may be nominal, but in tighter units (such as the Tamarisk) this increase can be dramatic. An increase in vertical conductivity leads to a decrease in head loss across the thickness of the unit. Given sufficient boreholes connecting the Magenta and the Culebra, differences in head across the Tamarisk be significantly reduced. Heads and gradients in the Culebra would become more like those in the Magenta, and flow in the Culebra would pivot from a southerly direction to a west-southwest direction. Such a west by southwest direction would lend itself to analysis by the same model proposed for climate change issues in section 3.4.1.

3.4.3 Subsidence Over Potash Mines

Summary Statement: Potash ore occurs in the middle portion of the Salado Formation (above the repository horizon) under nearly 2070 km^2 of the Delaware Basin, including some portions of the WIPP controlled area. Subsidence has occurred over potash mines in the past and will continue to occur over the regions that are already mined. An unknown amount of additional mining may occur in the future. Although regional subsidence is expected to lower the absolute elevation of the land surface by up to a few meters and may create local irregularities, it is not likely to alter the relative topography over the area that controls flow over the WIPP.

Regional subsidence may alter the hydraulic conductivities (K) of the Rustler units. If the conductivities of the lower-K units (Tamarisk and Forty-niner) are enhanced to a greater degree than the conductivities of the higher-K units (Culebra, Magenta) then the hydraulic gradients that generate the current north-to-south flow pattern in the WIPP land withdrawal boundary could be diverted towards the southwest. If the conductivities of all units are raised to an equal degree, then the current flow direction would not be altered.

Discussion: The WIPP land withdrawal area occupies a portion of the southeastern quadrant of the federally managed Potash Area. This Potash Area covers approximately 2070 km^2 and

overlaps the boundaries of the regional flow system identified by Corbet and Wallace (1993). The potash zones (specifically the McNutt Potash Zone) occupy a portion of the middle member of the Salado Formation. Subsidence has occurred over mined areas in the past and continues to occur.

Although the land surface in subsiding areas is lowered and there may be local changes in drainage patterns, the overall topographic features that have the primary affect on the location of the water table will remain similar to those of the present. However, subsidence may have impacts other than lowering of the land surface, including possible fracturing of units that overlie the potash zone. This fracturing could lead to an increase in conductivity for those units. The degree of increase and the relative change in conductivity from unit to unit could have an effect on the long-term groundwater flow behavior for Rustler units.

Because the Tamarisk and Forty-niner members presently have very low conductivities, fracturing may cause larger increases in conductivity in those units than in the Culebra and Magenta. The effect on flow would be similar to that described for boreholes that do not intrude the repository (see Section 3.4.2), for the same fundamental reasons. That effect would be a change in the direction of the hydraulic gradients in the land withdrawal area. Currently they direct flow in the Culebra from north to south. If the scenario were to occur, they would direct flow in the Culebra towards the southwest.

4.0 CURRENTLY AVAILABLE DATA FOR ASSESSMENT OF LONG-TERM PERFORMANCE

Data and information relevant to non-Salado containment include flow and transport parameters and their distributions in the non-Salado hydrostratigraphic units. Sections 4.1 through 4.4 briefly summarize the interpreted hydraulic head, transmissivity, storativity, fluid density, porosity, and retardation parameters for the non-Salado units. The raw data used to calculate these parameter values are referenced in Section 4.5. References to documentation in previous performance assessments (WIPP PA Division, 1991; Sandia WIPP Project, 1992) are made where possible.

4.1. Supra-Rustler Units

As discussed in Section 3.1.1, properties of the supra-Rustler units are less well understood than those of other units because of the lack of long-term hydraulic tests and the difficult of making those measurements. Two tests have been attempted in the lower portion of the Dewey Lake Red Beds, at DOE-2 (Beauheim, 1986) and H-14 (Beauheim, 1987a). In both cases, transmissivities were too low to be measured.

4.2 Rustler Formation

As discussed in Section 3.1.1, the Rustler Formation contains five members. Extensive well testing has only been performed on the most transmissive Rustler unit, the Culebra Dolomite Member. Few tests have been performed in units other than the Culebra.

4.2.1 Unnamed Lower Member and Contact Zone with Upper Salado Formation

Mercer (1983) reports values of transmissivity for the "Rustler-Salado contact residuum" from 20 locations in the vicinity of the WIPP site. These values and an additional value (from well H-16) reported by Beauheim (1987a) are shown, along with the locations of the wells at which the measurements were made, in Figure 4-1. A summary of test information from these locations is presented in Table 4-1. This summary was compiled from data contained in Mercer and Orr (1979), Mercer et al. (1981), Dennehy (1982), Dennehy and Mercer (1982), Mercer (1983), Richey (1986; 1987a), and Beauheim (1987a). Table 4-1 indicates that the tests at wells H-8c, WIPP-25, WIPP-27, WIPP-28, and WIPP-29 were conducted over intervals contained entirely within the residuum of the upper Salado. This indication is somewhat misleading, because at these locations, the contact between the Rustler and Salado is not a discrete horizon. At all of these locations, blocks of the unnamed lower member have been translated downward and mixed with Salado residue/breccia, and the contact has been arbitrarily defined as the uppermost occurrence of clasts of the red-tinted gypsum found at the top of the Salado in undisturbed sequences. Thus, the transmissivity values reported for these locations apply to a mixture of disrupted upper Salado and lower Rustler components.

The test intervals at the other wells varied in length between 22 and 143 ft with different stratigraphic coverages, but all included at least the lower 8 ft of the Rustler and the upper 4 ft of the

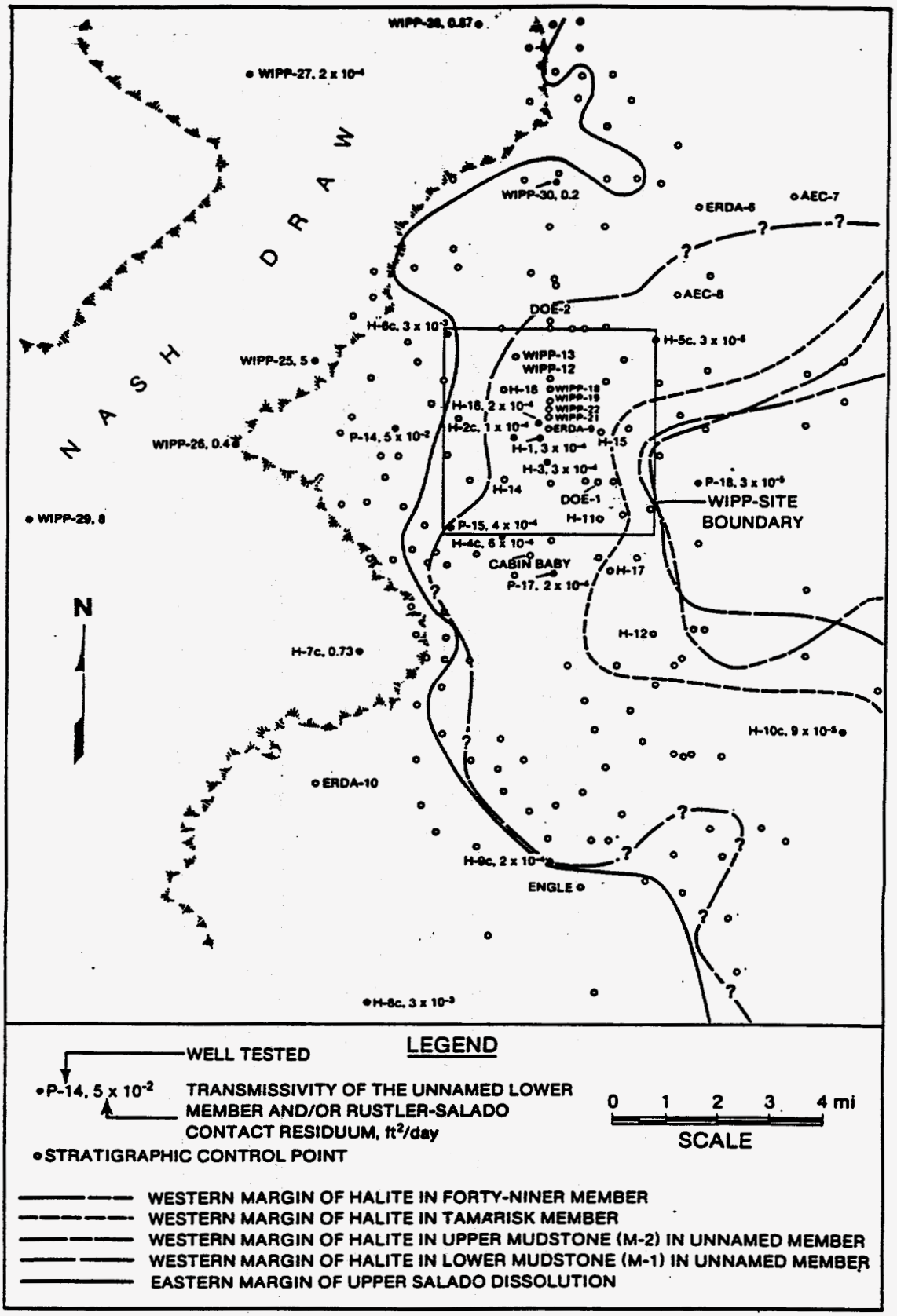

Figure 4-1. Distribution of Rustler halite and unnamed lower member and/or Rustler-Salado contact residuum transmissivity around the WIPP site.

Table 4-1. Summary of Information on Hydraulic Testing of the Unnamed Lower Member and/or Upper Salado.

WELL	UNNAMED LOWER MEMBER DEPTH INTERVAL (ft)[a]	DEPTH INTERVAL TESTED (ft)	COMPLETION INTERVAL (ft)	TRANSMISSIVITY (ft^2/day)[a]	COMMENTS[a]
H-1	699-818[b]	699-842[c]	803-827[c]	3×10^{-4}	
H-2c	645-764	743-795[c]	743-795[c]	1×10^{-4}	
H-3(b1)	694-821	800-868[c]	813-837[c]	3×10^{-4}	
H-4c	516-626	610-661[d]	610-661[d]	6×10^{-4}	
H-5c	924-1041	1025-1076[e]	1025-1076[e]	3×10^{-5}	
H-6c	627-721	699-741[f]	699-741[f]	3×10^{-3}	top of Salado salt at 723 ft
H-7c	274-380[b]	356-420[g]	356-420[g]	7.3×10^{-1}	top of Salado salt at 405 ft
H-8c	614-733	734-808[g,h]	734-808[g]	3×10^{-3}	top of Salado salt at 798 ft
H-9c	677-791	783-816[g]	783-816[g]	2×10^{-4}	
H-10c	1391-1501	1483-1538[g]	1483-1538[g]	9×10^{-5}	
H-16	724-842[i]	739-851[i]	738-851[i]	2×10^{-4} [i]	
P-14	595-687	676-700[c]	676-700[c]	5×10^{-2}	top of Salado salt at 695 ft
P-15	435-542	532-560[c]	532-560[c]	4×10^{-4}	
P-17	583-715	702-726[c]	702-726[c]	2×10^{-4}	
P-18	938-1088	1076-1100[c]	1076-1100[c]	3×10^{-5}	
WIPP-25	472-565	579-608[h,j]	579-608[j]	5×10^{0}	top of Salado salt at 600 ft
WIPP-26	209-309	228-329[j]	228-329[j]	4×10^{-1}	top of Salado salt at 320 ft
WIPP-27	318-416	426-460[h,j]	426-460[j]	2×10^{-4}	top of Salado salt at 508 ft
WIPP-28	446-531	549-589[h,j]	549-589[j]	8.7×10^{-1}	top of Salado salt at 589 ft
WIPP-29	42-143	216-250[h,j]	216-250[j]	8×10^{0}	top of Salado salt at 251 ft
WIPP-30	654-749	731-753[j]	731-753[j]	2×10^{-1}	

[a] Data from Mercer (1983) except as noted
[b] Revision of published depth by R.P. Snyder, USGS, personal communication
[c] Data from Mercer and Orr (1979)
[d] Data from Mercer et al. (1981)
[e] Data from Dennehy and Mercer (1982)
[f] Data from Dennehy (1982)
[g] Data from Richey (1986)
[h] No Rustler tested
[i] Data from Beauheim (1987a)
[j] Data from Richey (1987a; OFR 87-37)

Salado. Most of the transmissivity values for the Rustler-Salado contact zone range from 3 x 10^{-5} to 6 x 10^{-4} ft^2/day. No correlation is evident between test-interval thicknesses and transmissivities, indicating varying hydraulic conductivity. If the measured transmissivities are considered to be derived entirely from whatever portions of the lower siltstone of the unnamed member were included in the test intervals, the average hydraulic conductivity of the siltstone ranges from about 2 x 10^{-6} to 4 x 10^{-5} ft/day. Transmissivities higher than 6 x 10^{-4} ft^2/day were measured at five locations. Dissolution of the upper Salado has occurred at four of these locations (wells H-6c, H-7c, P-14, and WIPP-26; Figure 3-2), and the test intervals included 13 to 40 ft of the upper Salado and residuum which probably contributed the increased transmissivity. Only the value from WIPP-30 (0.2 ft^2/day), where no dissolution of the upper Salado is believed to have occurred, cannot be explained by dissolution/collapse-related transmissivity enhancement.

Water levels take months to years to stabilize in wells completed in low- transmissivity zones such as the unnamed member. Most of the wells in which the lower Rustler and/or upper Salado were tested did not remain completed to those zones long enough for water levels to stabilize, but were instead recompleted to allow testing/monitoring of overlying units. As a result, reliable water-level data are available only from those wells where unnamed member or Rustler-Salado transmissivities greater than 6 x 10^{-4} ft^2/day were measured.

Richey (1987b) presents the water-level data collected from the Rustler- Salado contact zone by the USGS between 1977 and 1985. Stabilized water levels were attained only in wells H-6c, H-7c, H-8c, P-14, WIPP-29, and WIPP-30. Water levels rose slowly in WIPP-25, WIPP-26, and WIPP-28 during their monitoring periods; the last measurements made can be used as minimum water-level elevations at those locations. Of the other wells where Rustler- Salado water levels were measured, only the data from H-2c and P-17 are adequate to place lower bounds on the stabilized water-level elevations that are useful in understanding flow directions. A similarly useful lower bound can be placed on the stabilized water-level elevation at H-16 using fluid- pressure data presented by Beauheim (1987a).

Figure 4-2 presents the water-level elevations measured in the 12 wells listed above. The water-level elevations measured at the wells completed entirely in the residuum of the upper Salado (H-8c, WIPP-25, WIPP-28, and WIPP-29) do not appear to be significantly different from the water-level elevations at the wells completed across the Rustler-Salado contact, indicating probable good hydraulic communication between the brine aquifer in the upper Salado residuum and the lower Rustler siltstone. Drawing conclusions about flow directions from the water-level data is difficult, however, because the density of the Rustler-Salado water varies between the wells. One basis for evaluating general directions of groundwater flow is provided when the water-level elevations are converted to freshwater-head elevations (the elevation to which a column of freshwater would stand while exerting the same pressure at the midpoint of the well-completion interval as the actual water in the well). Because of the dip of the Rustler, however, freshwater-head elevations calculated from the midpoints of the well- completion intervals do not share a common elevation datum and, therefore, interpretation of potential flow directions may be misleading (Davies, 1987). Moreover, any calculation of freshwater head is only as good as the measurement or estimate of the density (or specific gravity) of the water in the well at the time of the water-level measurement.

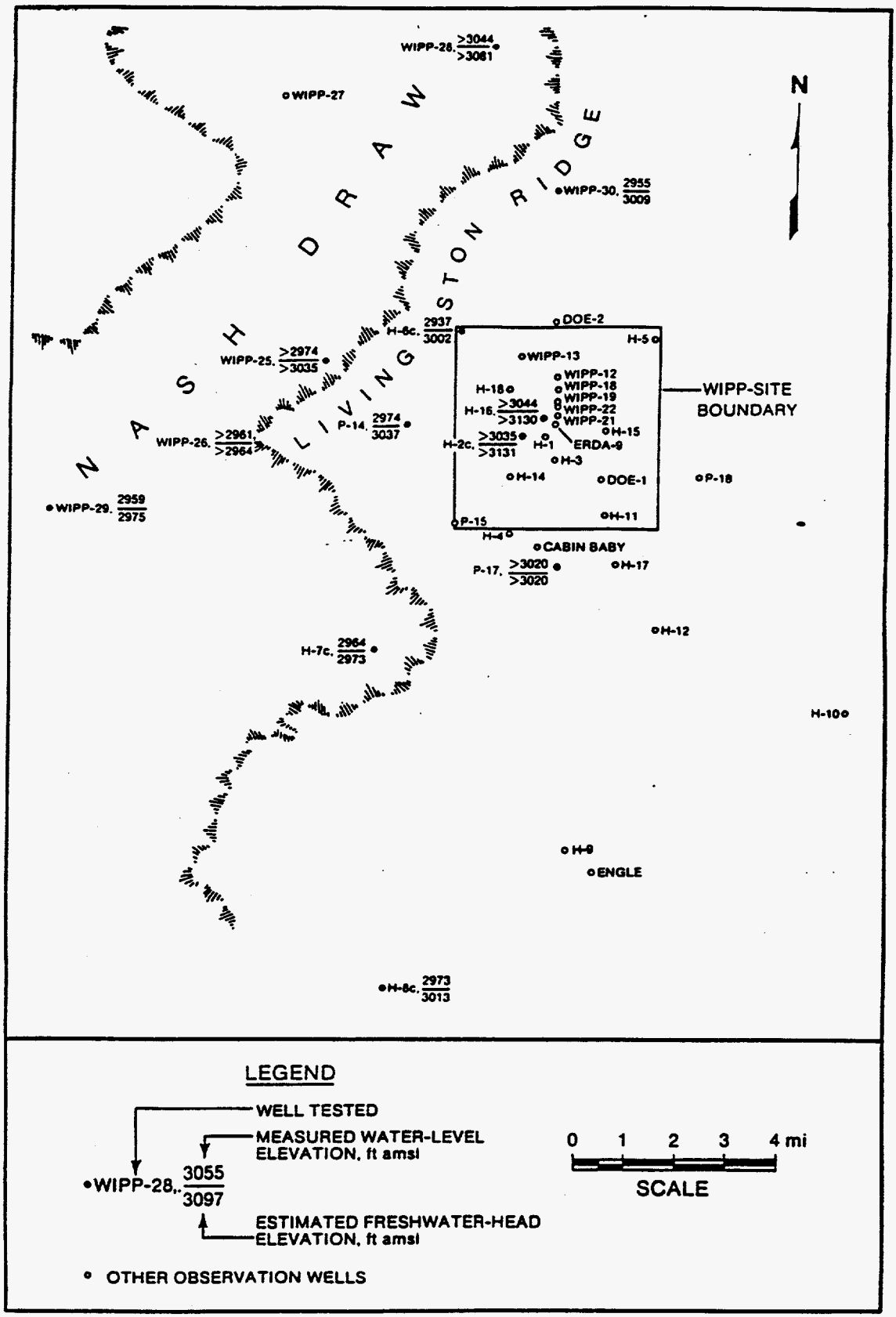

Figure 4-2. Measured water levels and estimated freshwater heads of the unnamed lower member and/or Rustler-Salado contact zone.

The freshwater-head elevations shown on Figure 4-2 were estimated using fluid-density or specific-gravity data presented by Mercer (1983), Richey (1986; 1987a), and Beauheim (1987a) (see Table 4-2). Most of the density/ specific-gravity measurements were made in connection with water-quality- sampling exercises that involved purging the wellbores, and the water-level measurements were made following recovery from those exercises. Because these wells were in general poorly developed, the waters entering the wellbores following the sampling exercises may have had slightly different densities from the waters removed. Thus, the density measurements were assumed to have an uncertainty of ± 0.02 g/cm^3 when used to calculate freshwater heads. The uncertainty in density is higher at WIPP-26, but only in the direction of higher density, because of apparent density stratification in the wellbore (Richey, 1987a). No fluid-density measurements were made on Rustler-Salado water from P-17 during the period from 1981 to 1982 when the only reliable water-level measurements were made. The only conclusion that can be drawn from the P-17 data is that the freshwater head cannot be lower than the measured water level. Table 4-2 summarizes the hydraulic-head data available for the unnamed lower member and/or upper Salado. Geochemical analyses from testing in the unnamed lower member are tabulated in Table 4-3. Concentrations of major chemical constituents in the unnamed lower member are shown in Figure 4-3.

4.2.2 Culebra Dolomite Member

Mercer (1983) reported values for Culebra transmissivity at 20 locations. Beauheim (1987a) provided values for Culebra transmissivity at 15 new locations, and new estimates at seven locations for which values had previously been reported. Combined with testing performed for Project Gnome (Cooper and Glanzman, 1971) and other recent work performed at DOE-2 (Beauheim, 1986), H-3 (Beauheim, 1987c), H-11 (Saulnier, 1987), WIPP-13 (Beauheim, 1987b), AEC-7 (Beauheim et al., 1991), and D-268 (Beauheim et al., 1991), the Culebra has been tested at 41 locations in the vicinity of the WIPP (Table 4-4). Figure 4-4 shows these 41 locations and the most-recent transmissivity values at each provided by the reports referenced above, as well as the distribution of halite within the Rustler over the same area. In general, the highest Culebra transmissivities (tens to thousands of ft^2/day) are found in areas where no halite is present in the Rustler, and the lowest transmissivity (≤ 0.004 ft^2/day) is found at P-18 where halite is present in all three non- dolomite Rustler members. At the two wells (H-12 and H-17) where halite is absent from the Forty-niner but present in the Tamarisk and unnamed member, the transmissivity of the Culebra is about 0.2 ft^2/day. Where halite is present only in the unnamed lower member, Culebra transmissivity ranges from 0.07 to 89 ft^2/day.

Culebra transmissivities of about 1 ft^2/day or greater appear to be related to fracturing. Where the transmissivity of the Culebra is less than 1 ft^2/day, few or no open fractures have been observed in core and the Culebra's hydraulic behavior during pumping or slug tests is that of a single-porosity medium. Where transmissivities are between 1 and at least 100 ft^2/day, numerous open fractures are observed in core and the hydraulic behavior of the Culebra during pumping tests is that of a double-porosity medium. Where the transmissivity of the Culebra is greater than approximately 100 ft^2/day, Culebra core is heavily fractured to the point of brecciation. Double-porosity hydraulic behavior is less apparent in these highly transmissive areas, perhaps because matrix-block size decreases as fracture frequency increases, decreasing the time lag observed between the hydraulic response of the fractures and that of the matrix.

Table 4-2. Hydraulic-Head Information for the Unnamed Lower Member and/or Upper Salado.

WELL	GROUND-SURFACE ELEVATION (ft amsl)[a]	STABILIZED DEPTH TO WATER (ft)[b]	DATE OF WATER-LEVEL MEASUREMENT	DEPTH TO MIDDLE OF COMPLETION INTERVAL (ft)[c]	BOREHOLE-FLUID DENSITY (g/cm^3) (±0.02)	FRESHWATER-HEAD ELEVATION (ft amsl)	MIDDLE OF COMPLETION INTERVAL PRESSURE (psi)
H-2c	3378	<343	2/79	769	1.225[c]	>3131±9	>226.1±3.7
H-6c	3348	411	7-12/80	720	1.21[c]	3002±6	162.0±2.7
H-7c	3163	199	'79-'80	388	1.048[c]	2973±4	85.8±1.6
H-8c	3433	460	11-12/80	771	1.13[d]	3013±6	152.3±2.7
H-16	3410	<366[e]	12/87	795[f]	1.2[f]	>3130±2	>223.3±1.0
P-14	3360	386	'79-'80	688	1.21[g]	3037±6	158.3±2.6
P-17	3336	<316	5/82	714	unknown	>3020	>172.5
WIPP-25	3212	<238	6/80	593	1.173[c]	>3035±7	>180.4±3.1
WIPP-26	3152	<191	6/80	278	1.04[h,i]	>2964+4	>37.7+1.9
WIPP-28	3347	<303	6/80	569	1.140[c]	>3081±5	>131.4±2.3
WIPP-29	2977	18	3-6/80	233	1.072[h]	2975±4	99.9±1.9
WIPP-30	3428	473	6/80	742	1.202[h]	3009±5	140.1±2.3

[a] Data from Gonzales (1989)
[b] Data from Richey (1987b; OFR 87-120) except as noted
[c] Data from Mercer (1983) except as noted
[d] Data from Richey (1986)
[e] Converted from pressure data presented in Beauheim (1987a)
[f] Data from Beauheim (1987a)
[g] Calculated from water analysis presented in Mercer (1983) and Figure E.1 of Haug et al. (1987)
[h] Data from Richey (1987a; OFR 87-37)
[i] Uncertainty = +0.05

1 Table 4-3. Geochemical Analyses from the Unnamed Lower Member and/or Upper Salado.

Well	Date of Sample	Geologic Unit	Density (gm/ml at 20 C)	Ph Units	Alkalinity Field (mg/L as $CaCO^3$)	Bicarbonate FET-FLD (mg/L as CO^3)	Carbonate FET-FLD (mg/L as HCO^3	Nitrogen NO^2+NO^3 Dissolved (mg/L as N)	Sulfide Total (mg/L as S)	Hardness (mg/L as $CaCO^3$)
H-1	77-02-23	312RSLRL	–	7.9	554	675	0	.29	–	160000
H-2C	77-02-23	312RSLRL	–	5.9	163	199	0	1.1	–	130000
H-3	77-02-23	312RSLRL	–	7.6	383	467	0	.77	–	150000
H-4C	79-03-16	312RSLRL	–	–	1	1	0	.27	–	130000
H-5C	79-05-16	312RSLRL	–	–	180	300	–	–	–	340000
H-6C	79-04-09	312RSLRL	–	–	1	–	–	–	–	97000
H-7C	80-03-20	312RSLRL	1.048	6.8	35	–	–	.03	–	10000
H-8C	80-09-06	312RSLRL	–	7.6	21	–	–	.00	.6	4800
H-9C	80-05-20	312RSLRL	1.202	7.0	24	–	–	1.1	–	6800
H-10C	80-05-19	312RSLRL	1.198	6.3	53	–	–	.84	–	49000
P-14	77-02-24	312RSLRL	–	7.2	182	222	0	.34	–	6400
P-15	79-04-03	312RSLRL	–	–	45	–	–	–	–	3400
P-17	79-05-11	312RSLRL	–	–	650	–	–	.04	–	200000
P-18	79-05-11	312RSLRL	1.266	5.35	400	–	–	.06	.0	–
WIPP-25	80-03-19	312RSLRL	1.173	7.2	80	–	–	.04	–	15000
WIPP-26	80-03-18	312RSLRL	1.078	8.5	160	–	–	.05	–	12000
WIPP-27	80-05-21	312RSLRL	1.205	7.8	–	–	–	–	–	–
WIPP-28	80-03-20	312RSLRL	1.140	7.0	–	–	–	–	–	–
WIPP-29	80-03-18	312RSLRL	1.068	7.3	130	–	–	.23	–	10000
WIPP-30	80-03-19	312RSLRL	1.201	7.0	320	–	–	.04	–	12000

Well	Hardness, Noncar-bonate (mg/L $CaCO^3$)	Calcium Dissolved (mg/L as Ca)	Magnesium, Dissolved (mg/L as Mg)	Sodium, Dissolved (mg/L as Na)	Potassium, Dissolved (mg/L as K)	Chloride, Dissolved (mg/L as Cl)	Sulfate Dissolved (mg/L as SO^4)	Fluoride, Dissolved (mg/L as F)	Silica, Dissolved (mg/L as SiO^2)	Boron, Dissolved (UG/L as B)	Solids, Residue at 105 Deg. C., Dissolved (mg/L)
H-1	160000	13000	30000	56000	17000	210000	520	–	<.1	110000	480000
H-2C	130000	9200	25000	66000	9100	200000	1300	–	2.0	150000	450000
H-3	150000	18000	25000	59000	14000	210000	37	–	1.0	1900	327000
H-4C	130000	8300	27000	66000	8600	210000	1400	1.7	1.3	360000	322000
H-5C	340000	2100	82000	14000	21000	290000	2000	<.1	1.6	67000	412000
H-6C	97000	4200	21000	80000	8000	200000	2000	1.0	1.4	200000	316000
H-7C	10000	2600	910	22000	210	41000	2900	.8	7.2	3100	79800
H-8C	4700	1200	430	46000	660	70000	5300	.4	.8	1300	130000
H-9C	6800	1300	870	130000	1200	190000	2600	.1	3.8	19000	326000
H-10C	49000	1500	11000	100000	4000	190000	3300	.7	3.2	120000	323000
P-14	6200	570	1200	120000	1300	180000	10000	–	2.0	1700	350000
P-15	3300	770	350	24000	1400	38000	2800	1.3	1.3	3700	–
P-17	20000	15000	40000	23000	8800	180000	1200	3.8	15	880	–
P-18	–	10000	37000	48000	12000	220000	480	2.3	.4	160000	–
WIPP-25	15000	650	3200	90000	2400	130000	12000	.0	2.6	35000	252000
WIPP-26	12000	2700	1300	52000	1000	88000	7600	.0	2.5	30000	153000
WIPP-27	4700	1160	1040	102000	2570	154000	5190	.2	.1	1300	363000
WIPP-28	13000	615	2070	65000	2070	102000	11000	.2	6.0	54000	–
WIPP-29	10000	850	2000	32000	1000	49000	12000	.9	3.5	21000	129000
WIPP-30	11000	850	2300	120000	1500	170000	7000	.0	3.5	77000	302000

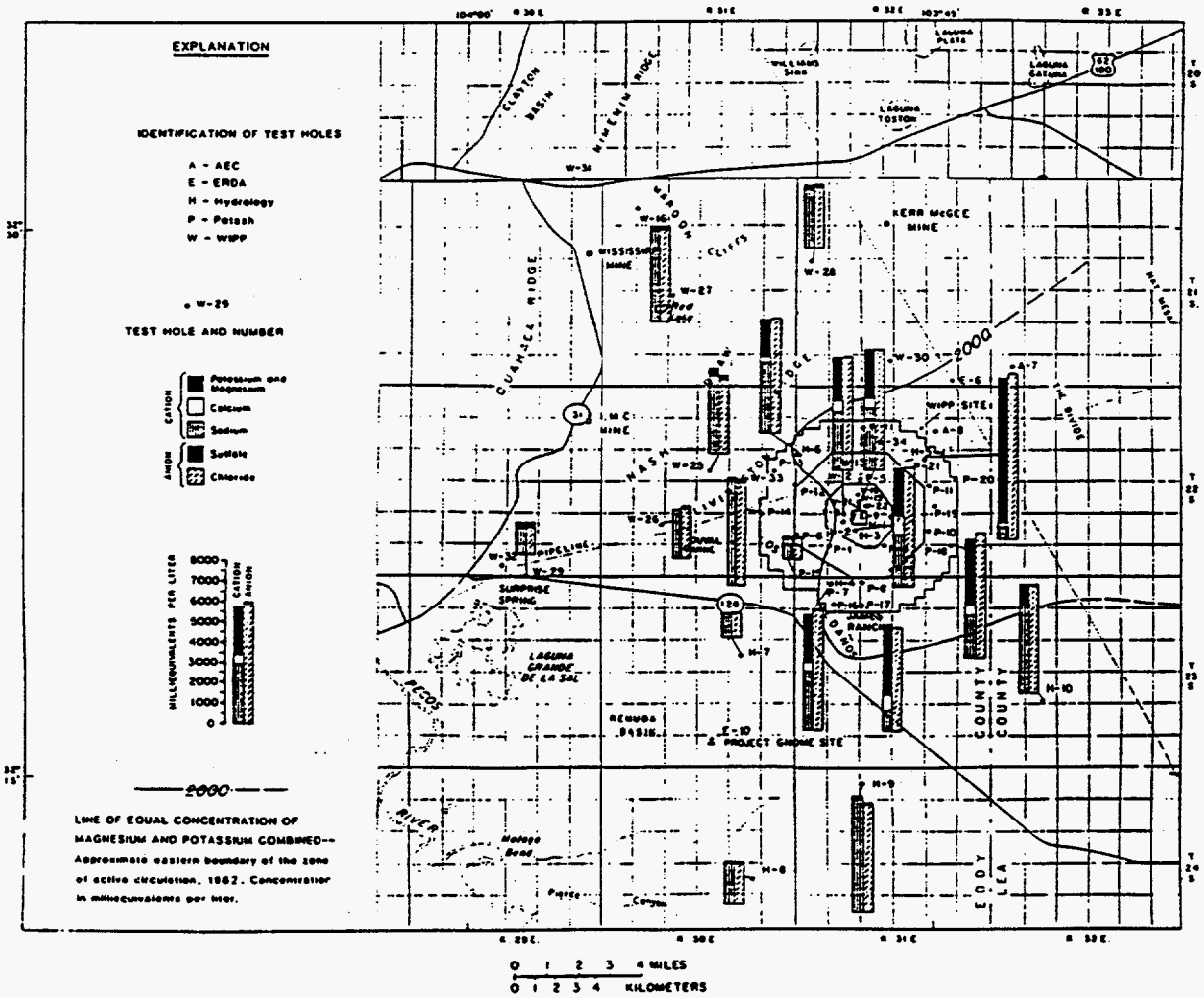

Figure 4-3. Concentrations (meq/L) of major chemical constituents in the unnamed lower member and/or upper Salado (from Mercer, 1983)).

Table 4-4. Summary of Transmissivity Data for the Culebra Dolomite Member of the Rustler Formation.

WELL	CULEBRA DEPTH INTERVAL (ft)	TRANSMISSIVITY (ft^2/day)	REFERENCE
AEC-7	870-896	1.8×10^{-1}	Beauheim et al. (1991)
Cabin Baby-1	503-529	2.8×10^{-1}	Beauheim (1987a)
D-268	370-392	2.2×10^{0}	Beauheim et al. (1991)
DOE-1	821-843	1.1×10^{1}	Beauheim (1987a)
DOE-2	824-846	8.9×10^{1}	Beauheim (1986)
Engle	659-681	4.3×10^{1}	Beauheim (1987a)
ERDA-9	704-727	4.6×10^{-1}	Beauheim (1987a)
H-1	676-699	8.7×10^{-1}	Beauheim (1987a)
H-2	623-645	4×10^{-1}	Mercer (1983)
H-3	672-694	2.3×10^{0}	Beauheim (1987b)
H-4c	490-516	6.5×10^{-1}	Beauheim (1987a)
H-5	897-920	2×10^{-1}	Mercer (1983)
H-6	492-511	7.3×10^{1}	Mercer (1983)
H-7	237-283	$>1 \times 10^{3}$	Mercer (1983)
H-8b	588-614	8.2×10^{0}	Beauheim (1987a)
H-9	647-677	2.3×10^{2}	Mercer (1983)
H-10b	1360-1391	7×10^{-2}	Mercer (1983)
H-11	730-756	2.7×10^{1}	Saulnier (1987)
H-12	823-850	1.8×10^{-1}	Beauheim (1987a)
H-14	545-571	3.0×10^{-1}	Beauheim (1987a)
H-15	861-883	1.3×10^{-1}	Beauheim (1987a)
H-16	702-724	8.0×10^{-1}	Beauheim (1987a)
H-17	706-731	2.2×10^{-1}	Beauheim (1987a)
H-18	689-713	2.0×10^{0}	Beauheim (1987a)
P-14	573-595	1.4×10^{2}	Mercer (1983)
P-15	413-435	9.1×10^{-2}	Beauheim (1987a)
P-17	558-583	1.0×10^{0}	Beauheim (1987a)
P-18	909-938	$<4 \times 10^{-3}$	Beauheim (1987a)
USGS-1	517-549	4.7×10^{2}	Cooper and Glanzman (1971)
WIPP-12	810-835	1×10^{-1}	Beauheim (1987a)
WIPP-13	703-726	6.9×10^{1}	Beauheim (1987c)
WIPP-18	787-808	3.0×10^{-1}	Beauheim (1987a)
WIPP-19	756-779	6.0×10^{-1}	Beauheim (1987a)
WIPP-21	729-753	2.5×10^{-1}	Beauheim (1987a)
WIPP-22	742-764	3.7×10^{-1}	Beauheim (1987a)
WIPP-25	447-472	2.7×10^{2}	Mercer (1983)
WIPP-26	186-209	1.25×10^{3}	Mercer (1983)
WIPP-27	292-318	6.5×10^{2}	Mercer (1983)
WIPP-28	420-446	1.8×10^{1}	Mercer (1983)
WIPP-29	12-42	1×10^{3}	Mercer (1983)
WIPP-30	631-653	1.8×10^{-1}	Beauheim (1987a)

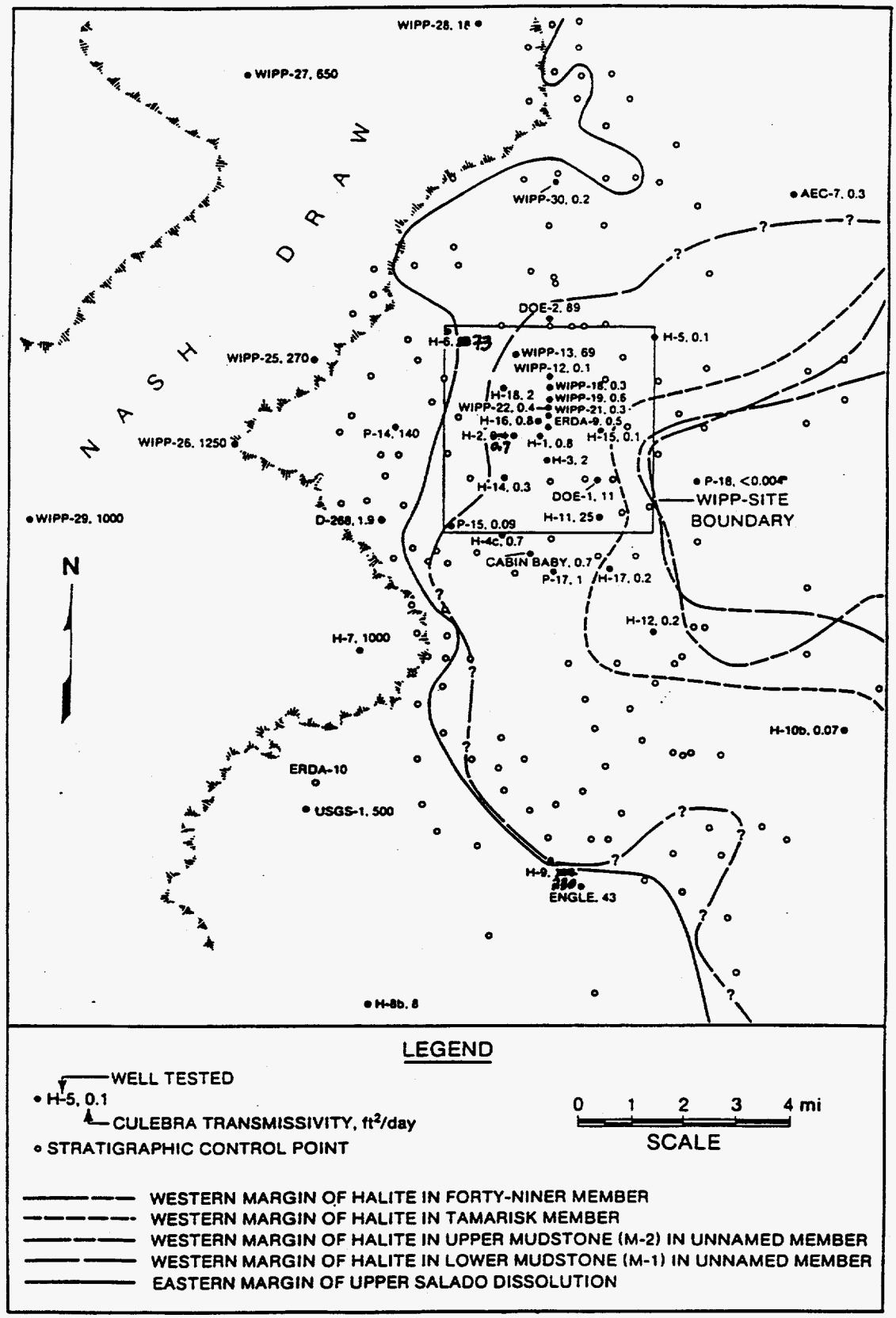

Figure 4-4. Distribution of Rustler halite and Culebra transmissivity around the WIPP site.

In most of the wells completed to the Culebra, water levels have been measured on a regular basis since the wells were constructed. Thus, with about 60 wells at 41 drilling-pad locations currently or once completed to the Culebra, abundant water-level data are available. Culebra water levels at and around the WIPP site have been affected, however, by continuous drainage into one or more WIPP shafts since the construction of the Exploratory Shaft (now the Salt Handling Shaft) in late 1981, as well as by numerous pumping tests and water-quality sampling exercises conducted since 1980. Thus, definition of the potentiometric surface of the Culebra undisturbed by WIPP activities is non-trivial.

Cauffman et al. (1990) performed a thorough review of Culebra water-level data, borehole- and formation-fluid-density data, and WIPP-related hydraulic stresses, and derived estimates of the undisturbed freshwater heads at 35 wells. These estimates are presented in Table 4-5, and are shown contoured (freehand) on Figure 4-5. The freshwater-head contours indicate a southwesterly flow direction down Nash Draw, a southerly flow direction across the WIPP site, and an area of low gradients with apparent westerly flow south of the WIPP site. Davies (1989) reports that flow directions in this southern area of low hydraulic gradients are difficult to define reliably because density-related flow-driving forces may be larger than pressure-related flow-driving forces within this part of the Culebra, suggesting that flow in this area may have a larger easterly, down-dip component than is predicted considering only equivalent freshwater heads.

Currently, no experimental data are available on partitioning coefficients, K_d, for the Culebra Dolomite. A limited amount of data for some of the actinides is available from Dosch (1980, 1981), Dosch and Lynch (1978), Lynch and Dosch (1980), Nowak (1980), Serne et al. (1977), and Tien et al. (1983). However, these K_d data are not representative of actual conditions for the following reasons:

1) Brine used in the majority of these experiments are not representative of Culebra brines (Novak, 1992). Only a limited amount of brine composition data was available when these measurements were performed. Since then, an extensive amount of data on brine composition in the Culebra has become available (Siegel et al., 1991b) which shows that all of the brine simulants except one used in the above-mentioned measurements do not match any of the measured brine compositions.

2) Most of the K_d data available in the above-mentioned references are based on single-point isotherms from batch experiments, i.e., K_ds are obtained based on one measurement of the solute concentration in solution versus the sorbed amount of solute per unit mass of the sorbent (rock powder).

3) It is not known that the equilibrium was established when the final concentrations of the solute were measured in the batch experiments.

Table 4-5. Hydraulic-Head Information for the Culebra Dolomite Member of the Rustler Formation.

WELL	GROUND-SURFACE ELEVATION (ft amsl)[a]	FRESHWATER-HEAD ELEVATION (ft amsl)[b]	DEPTH TO MIDDLE OF CULEBRA (ft)[c]	MIDDLE OF CULEBRA PRESSURE (psi)	CULEBRA FLUID DENSITY (g/cm^3)[b]
AEC-7	3657	3058±3	883	123.1±1.3	?
Cabin Baby-1	3327	2989±2	516	77.1±0.9	?
D-268	3279	3002±1	381[d]	45.1±0.4	?
DOE-1	3465	2998+9,-7	832[e]	158.2+3.9,-3.0	1.088
DOE-2	3418	3069±5	835[f]	210.6±2.2	1.041
H-1	3398	3029±7	688	138.2±3.0	1.022
H-2c	3378	3029+6	634	123.5+2.6	1.006
H-3b1	3389	3009+6	683	131.3+2.6	1.035
H-4b	3333	2995±4	510	74.5±1.7	1.014
H-5b	3505	3064±5	908	202.8±2.2	1.102
H-6b	3348	3060±3	616	142.1±1.3	1.038
H-7b	3164	2994±2	260	39.0±0.9	0.999
H-8b	3434	2992+2	601	68.9+0.9	1.000
H-9b	3406	2978+4	662	101.4+1.7	1.000
H-10b	3687	3023±7	1376	308.5±3.0	1.047
H-11b2	3412	2994+5,-3	743[g]	140.8+2.2,-1.3	1.078
H-12	3426	2998±4	837[h]	177.2±1.7	1.095
H-14	3345	3003+2	558[h]	83.6+0.9	1.010
H-15	3480	2999+9	872[h]	169.4+3.9	1.154
H-16	3410	>3008±1[i]	713[h]	>134.0±0.6	1.037[j]
H-17	3384	2989±3	719[h]	140.4±1.3	1.100
H-18	3413	3057+5,-4	701[h]	149.5+2.2,-1.7	1.017
P-14	3360	3041±3	584	114.8±1.3	1.018
P-15	3310	3008±3	424	52.9±1.3	1.015
P-17	3336	2991±2	571	97.9±0.9	1.061
USGS-1	3426	2985+1	533[k]	39.9+0.4	1.000
USGS-4	3413	2985	489[k]	26.4	1.000
USGS-8	3410	2989	477[k]	24.3	1.000
WIPP-12	3471	3059±4	823	178.1±1.7	?
WIPP-13	3405	3064±4	713	161.2±1.7	1.046
WIPP-18	3456	3051±4	798	170.3±1.7	?
WIPP-25	3212	3047±3	460	127.8±1.3	1.009
WIPP-26	3152	3016±1	198	26.9±0.4	1.009
WIPP-27	3177	3078±2	305	89.3±0.9	1.093
WIPP-28	3347	3075+3,-4	433	69.8+1.3,-1.7	1.032
WIPP-29	2977	2970±1	27	8.7±0.4	?
WIPP-30	3427	3069+6,-7	642	123.1+2.6,-3.0	1.018

[a] Data from Gonzales (1989)
[b] Data from Cauffman et al. (1990) except as noted
[c] Data from Mercer (1983) except as noted
[d] Data from Beauheim ~~and Saw~~ et al. (1991)
[e] Data from Freeland (1982)
[f] Data from Mercer et al. (1987)
[g] Data from Mercer (1990)
[h] Data from Beauheim (1987a)
[i] Lowered by drainage into WIPP shafts; converted from pressure data presented in Stensrud et al. (1988a)
[j] Specific-gravity value from Culebra in Air-Intake Shaft (Lyon, 1989)
[k] Data from Cooper and Glanzman (1971)

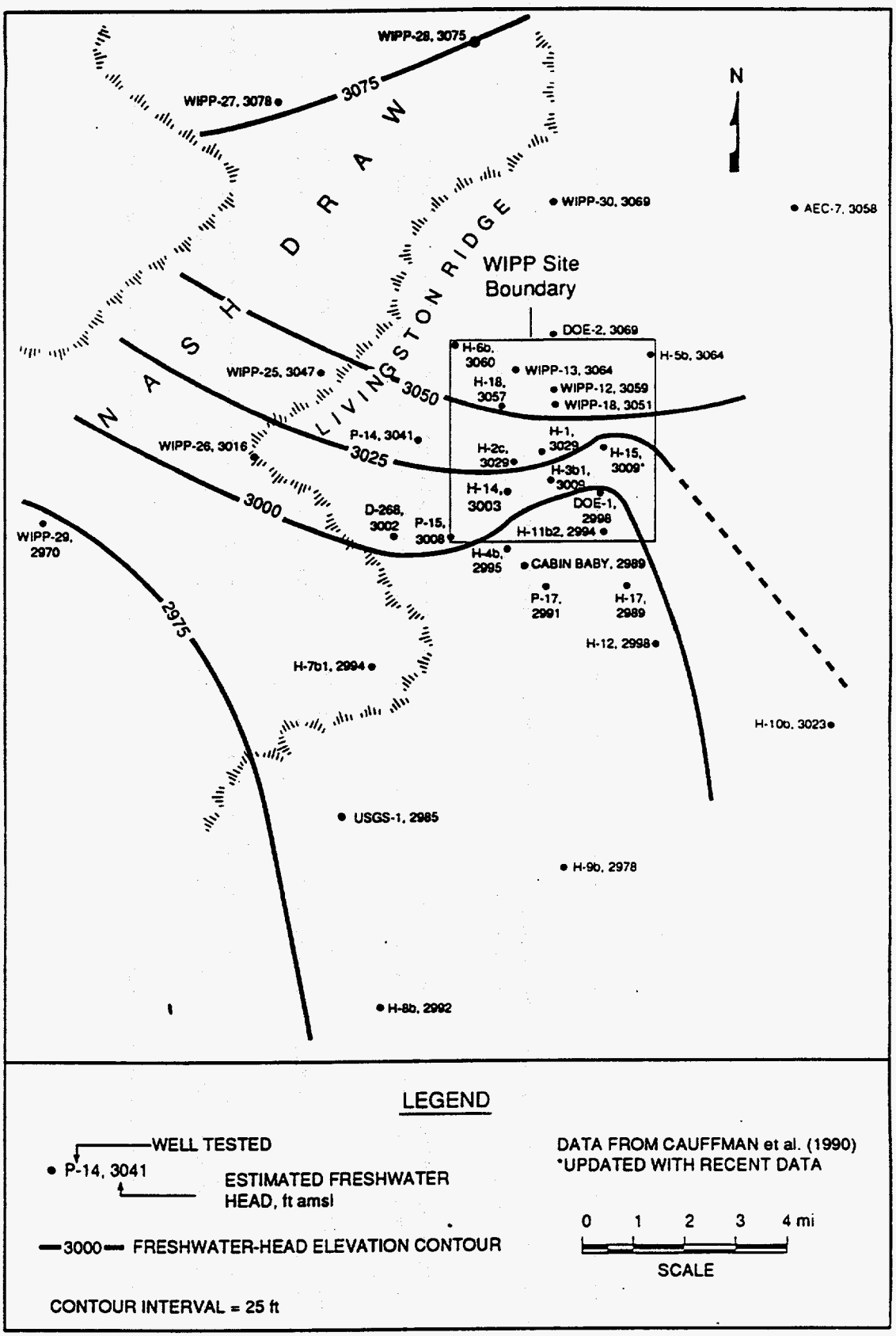

TRI-6115-1-0

Figure 4-5. Estimated freshwater heads of the Culebra.

4.2.3 Tamarisk Member

Less is known about the hydraulic properties of the Tamarisk than about those of the other Rustler members. No hydraulic tests of the Tamarisk anhydrites (A-2 and A-3) have ever been performed because of apparent low transmissivity. Hydraulic tests of the Tamarisk claystone have been attempted at only four locations: H-3b3 (1984 unpublished field notes), DOE-2 (Beauheim, 1986), H-14 (Beauheim, 1987a), and H-16 (Beauheim, 1987a). Drillstem and/or pulse tests failed at all four locations, as the transmissivities were apparently too low to measure over a period of several days. Based on the interpretation of similar tests performed successfully on the unnamed lower member at H-16, Beauheim (1987a) concluded that the transmissivity of the Tamarisk claystone is likely 10^{-5} ft^2/day or less. The transmissivity of the Tamarisk claystone might be expected to be greater west of the WIPP site in Nash Draw where dissolution of the upper Salado and Rustler has occurred, but no direct measurements have been made in this area. The transmissivities of the Tamarisk anhydrites in Nash Draw may also have been increased by dissolution and subsidence-induced fracturing.

No measurements of the undisturbed hydraulic head within the Tamarisk claystone have ever been made. The same low transmissivity that prevented successful hydraulic testing of the Tamarisk at H-3b3, DOE-2, H-14, and H-16 also prevented measurements of hydraulic heads at those locations.

4.2.4 Magenta Dolomite Member

Hydraulic tests have been performed on the Magenta dolomite at 16 locations (Mercer, 1983; Beauheim, 1986, 1987a; Beauheim et al., 1991). The transmissivity values obtained from these tests are shown on Figure 4-6 and in Table 4-6. Most of the transmissivity values are less than or equal to 0.1 ft^2/day. Higher values of transmissivity, 0.3 and 1.0 ft^2 /day, are found at H-6a and H-9a, respectively. No halite is present in the Rustler at either of these two locations. The two highest values of Magenta transmissivity, 375 and 53 ft^2/day, are found in Nash Draw at WIPP-25 and WIPP-27, respectively, where dissolution of the upper Salado has caused collapse and fracturing of the overlying Rustler. Mercer (1983) noted that the transmissivity of the Magenta at WIPP-25 may have been overestimated because of possible leakage from the Culebra along fractures during hydraulic testing. Dissolution of the upper Salado has apparently not affected the Magenta at all locations where it has occurred, however, as the transmissivity of the Magenta is very low at H-8, and could not be measured at WIPP-28.

Between 1979 and 1981, stabilized water levels were measured in 13 wells completed to the Magenta (Richey, 1987b). Figure 4-7 shows the elevations of these stabilized water levels, along with estimated freshwater-head elevations calculated using borehole-fluid-density (or specific-gravity) data presented in Mercer et al. (1981), Dennehy and Mercer (1982), Mercer (1983), Lambert and Robinson (1984), Richey (1986), and Richey (1987a). The contours of the freshwater heads indicate a southwesterly flow direction within the Magenta in the northern portion of Nash Draw, and a generally westward flow direction toward Nash Draw over the rest of the region.

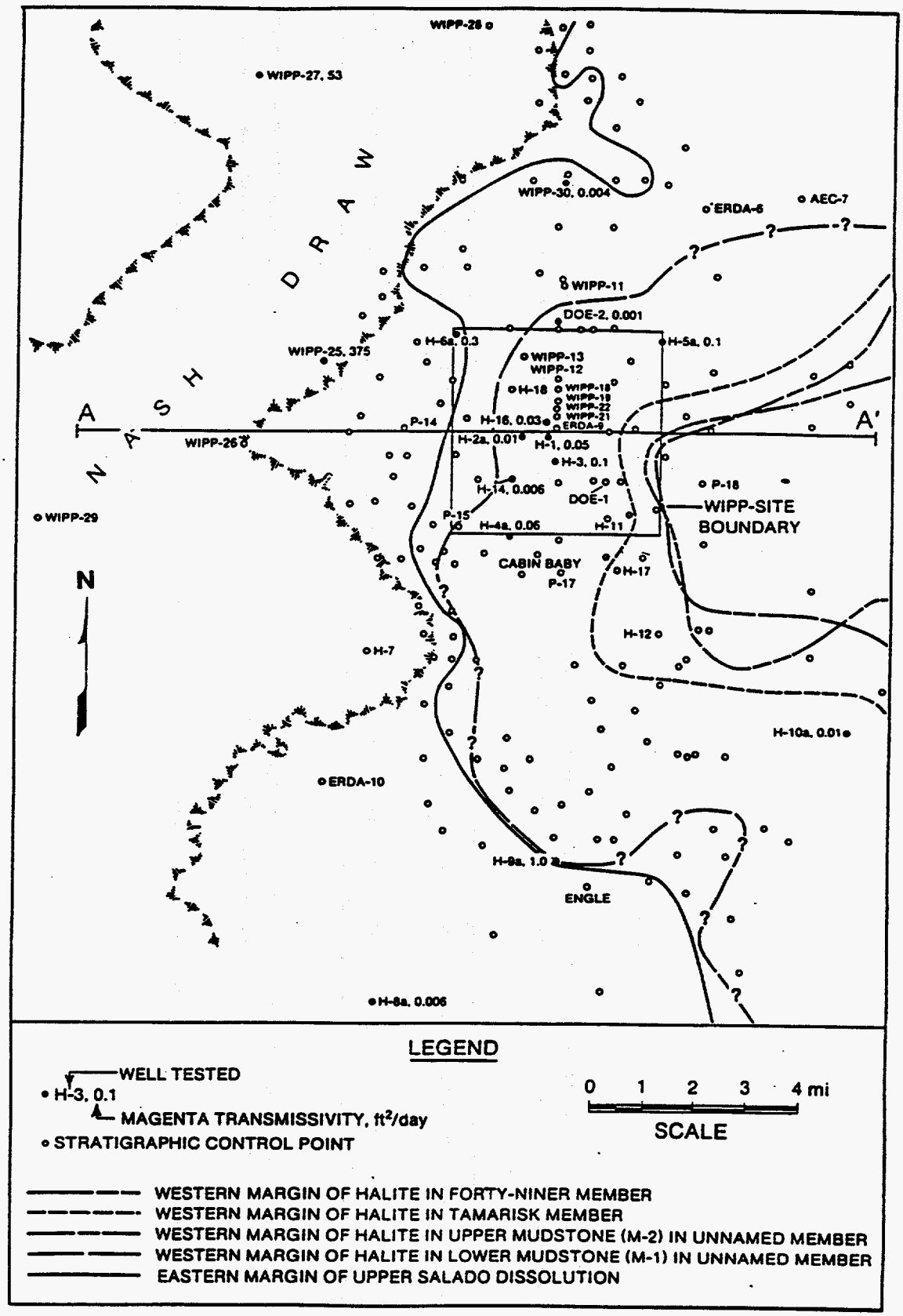

Figure 4-6. Distribution of Rustler halite and Magenta transmissivity around the WIPP site.

Table 4-6. Summary of Transmissivity Data for the Magenta Dolomite Member of the Rustler Formation.

WELL	MAGENTA DEPTH INTERVAL (ft)[a]	TRANSMISSIVITY (ft^2/day)[a]	COMMENTS
DOE-2	699-722[b]	1×10^{-3} [c]	
H-1	563-589	5×10^{-2}	
H-2a	515-543	1×10^{-2}	
H-2b1	515-540[d]	2.4×10^{-3} [d]	
H-3b1	559-584	1×10^{-1} 1.6×10^{-1} [d]	
H-4a	375-400	6×10^{-2}	
H-5a	783-810	1×10^{-1}	
H-6a	492-511	3×10^{-1}	
H-8a	466-488	6×10^{-3}	
H-9a	523-554	1×10^{0}	
H-10a	1256-1280	1×10^{-2}	
H-14	424-448[e]	6×10^{-3} [e]	
H-16	590-616[e]	3×10^{-2} [e]	
WIPP-25	302-328	3.75×10^{2}	
WIPP-27	176-194	5.3×10^{1}	
WIPP-28	285-310	low	testing unsuccessful
WIPP-30	513-537	4×10^{-3}	

[a] Data from Mercer (1983) except as noted
[b] Data from Mercer et al. (1987)
[c] Data from Beauheim (1986)
[d] Data from Beauheim et al. (1991)
[e] Data from Beauheim (1987a)

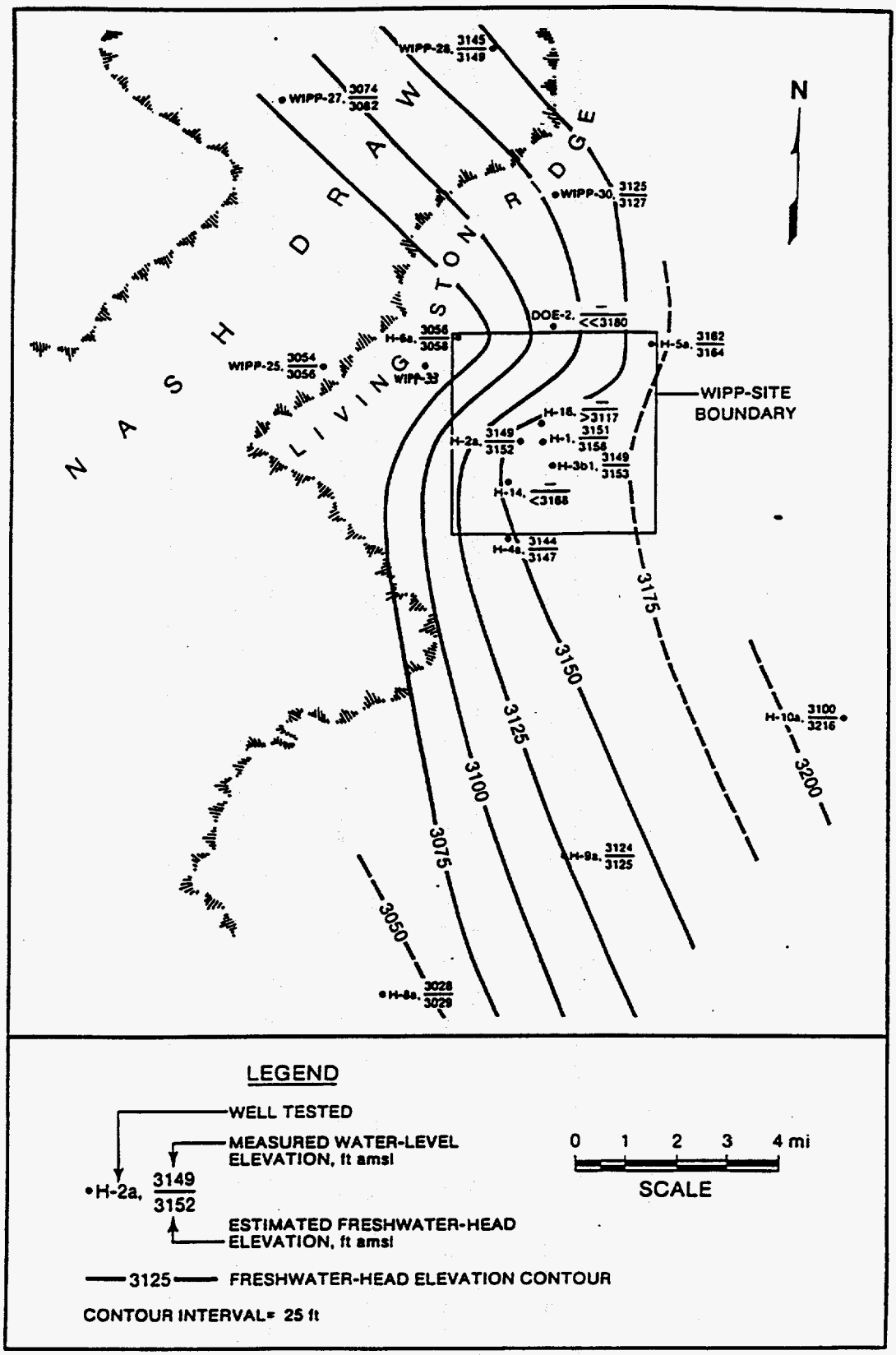

Figure 4-7. Measured water levels and estimated freshwater heads of the Magenta dolomite member.

The hydraulic head at H-6a shown on Figure 4-7 seems anomalously low compared to that at surrounding wells, and causes a flexure in the contour lines across the northern portion of the WIPP site. The low head at H-6a may be related to drainage into dissolution cavities in the upper Rustler such as those encountered at WIPP-33 (Sandia and USGS, 1981). If so, it may be a relatively localized perturbation in the Magenta potentiometric surface, and not affect heads as far to the east as is indicated on Figure 4-7.

Also shown on Figure 4-7 are freshwater heads estimated from pressure measurements made at DOE-2, H-14, and H-16. The pressure measurements at DOE-2 and H-14 were reported by Beauheim (1986 and 1987a) to represent upper bounds on the stabilized formation pressures, while the pressure measurement at H-16 reflects drainage from the Magenta into the nearby WIPP shafts since 1981 (Beauheim, 1987a). With these caveats, the estimated freshwater heads at DOE-2, H-14, and H-16 are in qualitative agreement with the pattern of freshwater heads derived from the water-level data. Table 4-7 summarizes the hydraulic-head data available for the Magenta dolomite. Geochemical analyses from testing in the Magenta are tabulated in Table 4-8. Concentrations of major chemical constituents in the Magenta are shown in Figure 4-8.

4.2.5 Forty-niner Member

The claystone water-producing unit (M-4) of the Forty-niner has been hydraulically tested at only four locations: DOE-2 (Beauheim, 1986), H-3d (Beauheim et al., 1991), H-14 (Beauheim, 1987a), and H-16 (Beauheim, 1987a). At these locations, the interbed thickness ranges from 10 to 15 ft. Transmissivities reported for the claystone interbed are summarized in Table 4-9. As is the case with the other Rustler members, the transmissivity of the Forty-niner claystone might be assumed to be higher west of the WIPP site in Nash Draw as a result of subsidence and fracturing, but no direct measurements have been made in that area. Where the H-4 halite unit is found with the M-4 claystone east of the WIPP site, the transmissivity of the claystone is probably less than where the halite is absent.

Testing of a Forty-niner anhydrite/gypsum alone has been attempted only in H-14 (Beauheim, 1987a). At H-14, a drillstem test was performed in the upper 25 ft of the upper Forty-niner anhydrite (A-5). This test was qualitative in nature, and showed only that the transmissivity of the anhydrite must be several orders of magnitude lower than that of the Forty-niner claystone. Where still present in Nash Draw, the Forty-niner anhydrites/gypsums may have very high transmissivities as a result of dissolution and subsidence-induced fracturing.

Measurements of the hydraulic head of the Forty-niner claystone have been made at wells H-3d, H-14, H-16, and DOE-2. Beauheim (1987a) summarizes these observations, and presents estimates of static fluid pressures at the midpoint of the claystone. The greatest uncertainty in these estimates was attached to the measurement from DOE-2. Re-examination of the original data from DOE-2 (Beauheim, 1986) indicates that a "static" pressure 12 psi lower than that reported by Beauheim (1987a) probably provides a more accurate upper bound on the Forty-niner head at that location. The Forty-niner hydraulic-head data are summarized in Figure 4-9 and Table 4-10.

Table 4-7. Hydraulic-Head Information for the Magenta Dolomite Member of the Rustler Formation.

WELL	GROUND-SURFACE ELEVATION (ft amsl)[a]	STABILIZED DEPTH TO WATER (ft)[b]	DATE OF WATER-LEVEL MEASUREMENT	DEPTH TO MIDDLE OF MAGENTA (ft)[c]	BOREHOLE-FLUID DENSITY (g/cm^3) (± 0.01)[c]	FRESHWATER-HEAD ELEVATION (ft amsl)	MIDDLE OF MAGENTA PRESSURE (psi)
DOE-2	3418	>>310[d]	10/84	711[e]	1.18[e,f]	<<3180±8	<<205.0±3.5
H-1	3398	247	2-3/79	576	1.021	3158±3	145.6±1.4
H-2a	3378	229	7-9/81	529	1.012	3152±3	131.6±1.3
H-3b1	3389	240	'78-'79	572	1.010	3153±3	145.3±1.4
H-4a	3333	189	'79-'80	388	1.017	3147±2	87.7±0.9
H-5a	3506	344	'78-'80	797	1.008	3164±5	197.9±2.0
H-6a	3347	291	'78-'80	502	1.007	3058±2	92.1±0.9
H-8a	3433	405	'80-'84	477	1.008[g]	3029±1	31.4±0.3
H-9a	3406	282	'80-'83	539	1.006[g]	3125±3	112.0±1.1
H-10a	3687	587	'80-'82	1268	1.171[f,g]	3216±14	345.6±5.9
H-14	3346	>221[h]	10/86	436[i]	1.2[f,i]	<3168±4	<111.8±1.9
H-16	3410	<344[j,k]	11/87	603[i]	1.2[f,i]	>3117±1[j]	>134.5±0.6
WIPP-25	3212	158	'80-'84	315	1.010	3056±2	68.7±0.7
WIPP-27	3177	103	'81-'82	185	1.095[f]	3082±2	38.9±0.7
WIPP-28	3347	202	'81-'82	298	1.048[f]	3149±2	43.6±0.8
WIPP-30	3428	303	'82-'83	525	1.01[l]	3127±2	97.2±1.0

[a] Data from Gonzales (1989)
[b] Data from Richey (1987b; OFR 87-120) except as noted
[c] Data from Mercer (1983) except as noted
[d] Converted from pressure data presented in Beauheim (1986)
[e] Data from Beauheim (1986)
[f] Uncertainty = ±0.02
[g] Data from Richey (1986)
[h] Converted from pressure data presented in Beauheim (1987a)
[i] Data from Beauheim (1987a)
[j] Lowered by drainage into WIPP shafts
[k] Converted from pressure data presented in Stensrud et al. (1988b)
[l] Data from Lambert and Robinson (1984)

1 Table 4-8. Geochemical Analyses from Testing in the Magenta.

Well	Date of Sample	Geologic Unit	Density (gm/ml at 20 C)	Ph Units	Alkalinity Field (mg/L as $CaCO^3$)	Bicarbonate FET-FLD (mg/L as CO^3)	Carbonate FET-FLD (mg/L as HCO^3	Nitrogen NO^2+NO^3 Dissolved (mg/L as N)	Sulfide Total (mg/L as S)	Hardness (mg/L as $CaCO^3$)
H-1	76-06-04	310MGNT	–	7.4	75	92	0	–	.0	3300
H-2A	77-02-22	310MGNT	–	8.6	61	74	0	.04	–	2700
H-3	77-05-10	310MGNT	–	8.0	42	51	0	.08	–	5000
H-4A	78-12-14	310MGNT	–	8.0	52	63	–	.01	–	2200
H-5A	78-12-14	310MGNT	–	7.8	41	50	–	.01	–	1300
H-6A	78-12-20	310MGNT	–	7.3	42	51	–	.03	–	2000
H-8A	80-02-12	310MGNT	1.006	9.3	26	–	–	.06	–	2200
H-9A	80-02-05	310MGNT	1.003	8.5	35	–	–	.02	–	2100
H-10A	80-03-21	310MGNT	1.175	7.1	0	–	–	.03	–	17000
WIPP-25	80-09-04	310MGNT	1.010	7.5	150	–	–	.64	1.2	3300
WIPP-27	80-07-24	310MGNT	1.080	6.8	57	–	–	.32	–	11000
	80-09-20	310MGNT	–	6.5	180	–	–	.40	1.8	17000
WIPP-30	80-09-24	310MGNT	–	8.8	62	–	–	00	.0	2400

Well	Hardness, Noncar-bonate (mg/L $CaCO^3$)	Calcium Dissolved (mg/L as Ca)	Magnesium, Dissolved (mg/L as Mg)	Sodium, Dissolved (mg/L as Na)	Potassium, Dissolved (mg/L as K)	Chloride, Dissolved (mg/L as Cl)	Sulfate Dissolved (mg/L as SO^4)	Fluoride, Dissolved (mg/L as F)	Silica, Dissolved (mg/L as SiO^2)	Boron, Dissolved (UG/L as B)	Solids, Residue at 105 Deg. C., Dissolved (mg/L)
H-1	3300	890	270	5700	70	8000	3900	2.8	1.3	2200	18900
H-2A	2700	820	170	2700	81	4100	2400	–	6.0	220	12000
H-3	4900	1200	480	9300	250	15000	3400	1.8	6.4	13000	32000
H-4A	2100	210	410	7000	130	7500	7000	2.5	6.4	13000	22300
H-5A	1300	240	170	1500	53	880	3200	2.8	9.0	11000	–
H-6A	2000	520	160	1100	46	1200	2700	1.4	7.7	2500	–
H-8A	2200	870	17	2400	84	3500	2100	.7	.9	3100	9410
H-9A	2000	550	170	800	28	750	2700	1.8	3.3	2600	5460
H-10A	17000	2500	2600	93000	510	160000	2700	1.3	1.9	3900	270000
WIPP-25	3100	910	240	3100	.8	5600	1900	1.5	25	1900	18700
WIPP-27	11000	1100	1900	34000	1800	61000	9400	.0	1.7	26000	106000
	17000	3600	2000	43000	10000	85000	2900	.4	13	230	173000
WIPP-30	2400	690	170	5500	190	8700	3200	1.9	.7	12000	19000

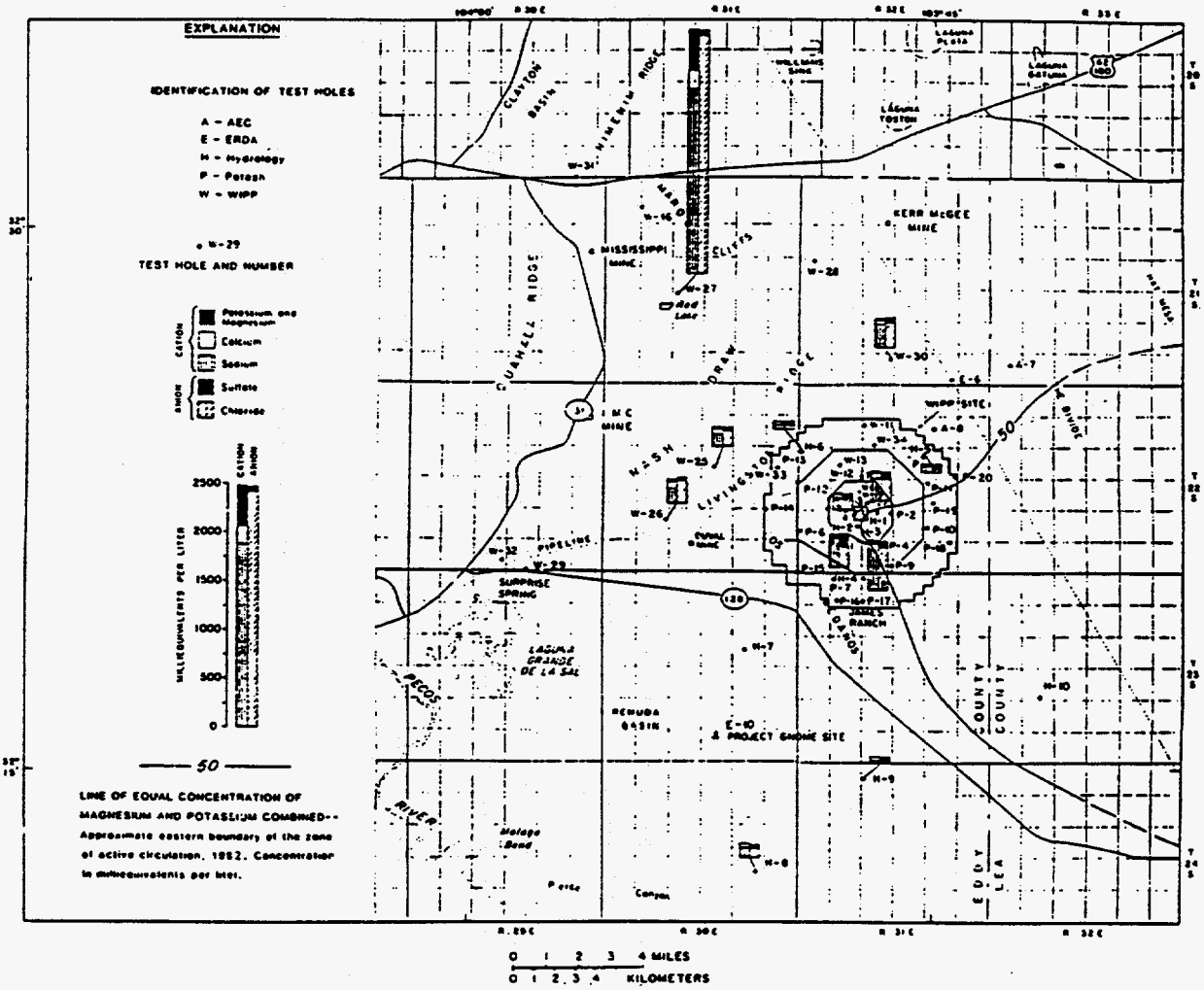

1 Figure 4-8. Concentrations (meq/L) of major chemical constituents in the Magenta.

Table 4-9. Summary of Transmissivity Data for the Forty-Niner Claystone.

WELL	FORTY-NINER CLAYSTONE DEPTH INTERVAL (ft)	TRANSMISSIVITY (ft^2/day)	REFERENCE
DOE-2	670-681	2.5×10^{-3} to 1.1×10^{-2}	Beauheim (1986)
H-3d	536-546	3.5×10^{-3} to 4.5×10^{-3}	Beauheim et al. (1991)
H-14	390-405	3.0×10^{-2} to 7.1×10^{-2}	Beauheim (1987a)
H-16	563-574	5.0×10^{-3} to 5.6×10^{-3}	Beauheim (1987a)

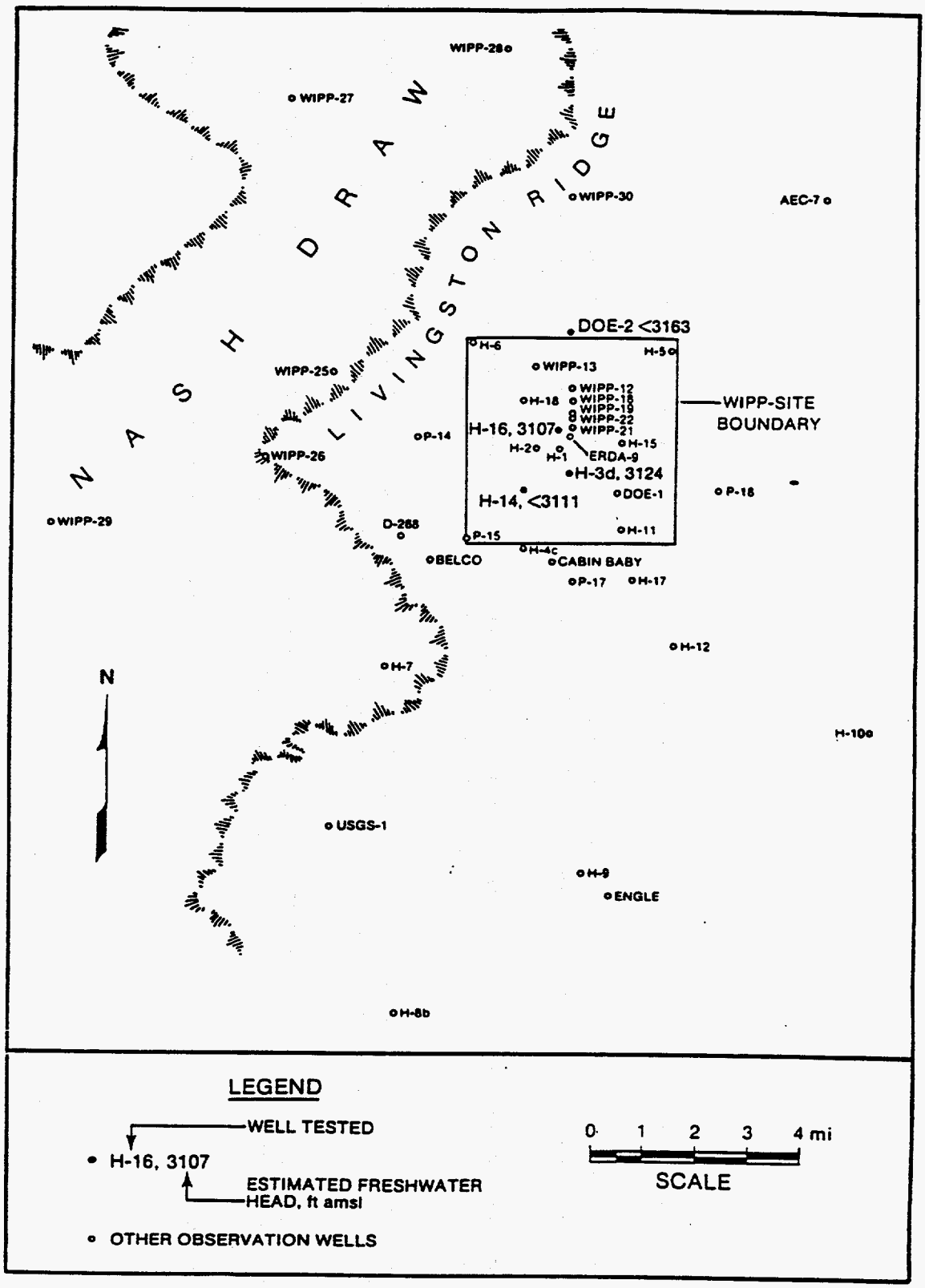

Figure 4-9. Estimated freshwater heads of the Forty-Niner claystone.

1 Table 4-10. Hydraulic-Head Information for the Forty-Niner Claystone.

WELL	GROUND-SURFACE ELEVATION (ft amsl)[a]	DEPTH TO MIDDLE OF FORTY-NINER CLAYSTONE (ft)[b]	FLUID PRESSURE AT MIDDLE OF CLAYSTONE (psig)[b]	FRESHWATER-HEAD ELEVATION (ft amsl)
DOE-2	3418	675	<182[c]	<3163
H-3d	3389	541	120	3124
H-14	3345	398	<71	<3111
H-16	3410	568	115	3107

[a] Data from Gonzales (1989)
[b] Data from Beauheim (1987a) except as noted
[c] Data recalculated from Beauheim (1986)

Figure 4-10 shows the static fluid-pressure estimates for the Forty-niner claystone at H-3d, H-14, H-16, and DOE-2 converted to freshwater heads. Firm conclusions cannot be drawn from so few data, but the data are not inconsistent with an assumption of southwesterly to westerly flow towards Nash Draw. The relatively low head at H-16 may, as suggested by Beauheim (1987a), be related more to localized drainage into the WIPP shafts than to the undisturbed regional head distribution.

4.2.6 Discussion of Rustler Hydraulic Heads

Comparisons of hydraulic heads between different water-producing units within the Rustler are useful, as they allow evaluation of the potential directions of vertical fluid flow between the water-producing units and the effectiveness of intervening confining beds, and illustrate areal variations in the hydraulic properties of the different Rustler members. A rigorous quantitative evaluation of hydraulic-head differences between units generally requires that the heads share a common elevation datum. No meaningful elevation datum can be defined, however, when the specific gravities (densities) of the fluids in the units to be compared are different.

A qualitative evaluation of the potential directions of fluid flow can be performed, however, using a procedure here described as the "equilibrium- fluid-density" approach. Static pressures at the mid-formation depth are calculated for the units of interest. By subtracting the pressure in the unit at the higher elevation from the pressure in the unit at the lower elevation, and dividing by the vertical distance separating the two units, a pressure-depth gradient can be calculated. In a system at equilibrium (i.e., no vertical hydraulic gradient), this pressure-depth gradient corresponds to the density of the fluid in the system. Thus, the calculated pressure-depth gradient can be converted to the equivalent density of the fluid that would be required to be present for the heads in the two units to be at equilibrium. If the density of this hypothetical fluid is lower than the densities of both actual fluids, the head in the upper unit is higher than the equilibrium condition and the potential flow direction is downward. If the hypothetical density is greater than that of both actual fluids, the head in the upper unit is lower than the equilibrium condition and the potential flow direction is upward. If the hypothetical density is equal to or intermediate between the densities of the actual fluids, then the hydraulic heads in the two units are very nearly at equilibrium and no qualitative conclusions about potential flow directions can be drawn. The greater the difference between the hypothetical equilibrium fluid density and the actual fluid densities, the greater the hydraulic gradient between units.

4.2.6.1 HYDRAULIC-HEAD DIFFERENTIALS BETWEEN THE UNNAMED LOWER MEMBER/UPPER SALADO AND THE CULEBRA

Adequate data for comparisons of the hydraulic heads in the unnamed lower member and/or Rustler-Salado contact residuum water-producing unit with those in the Culebra are available for 12 well locations. Table 4-11 presents calculations of potential flow directions between the unnamed member/upper Salado and the Culebra using the method outlined above. Regions around the WIPP site having different potential flow directions are shown areally in Figure 4-10. At wells H-2, H-16, and P-17, the hydraulic gradient between the unnamed lower member and the Culebra is upward.

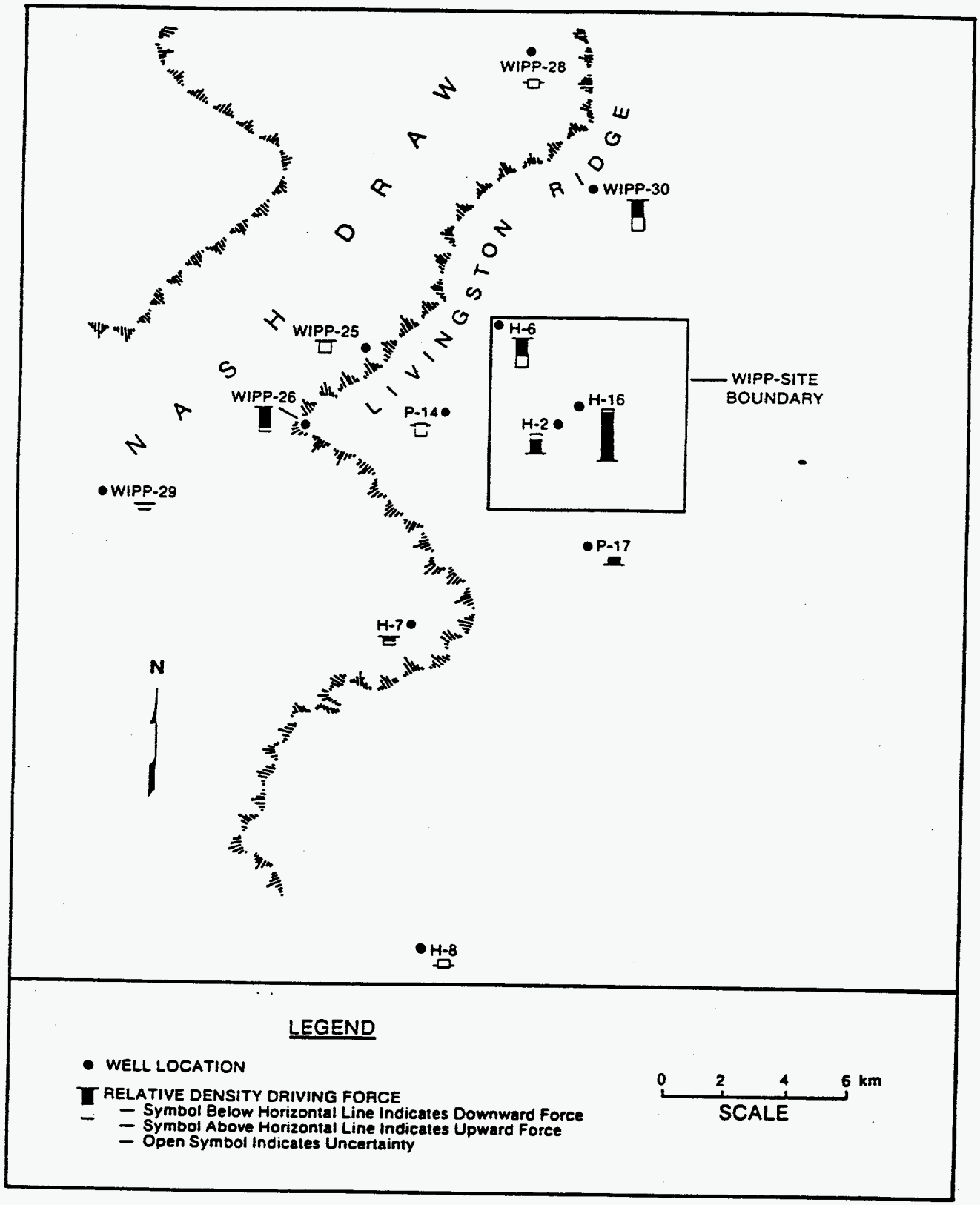

TRI-6344-55-0

Figure 4-10. Flow potentials between the Culebra dolomite and the unnamed member/upper Salado.

Table 4-11. Potential Flow Directions between the Culebra and Unnamed Member/Upper Salado.

WELL	DIFFERENCE IN DEPTH (R/S-CUL) (ft)	DIFFERENCE IN FORMATION PRESSURE (R/S-CUL) (psi)	PRESSURE-DEPTH GRADIENT (psi/ft)	EQUILIBRIUM FLUID DENSITY (g/cm^3)	RUSTLER/ SALADO FLUID DENSITY (g/cm^3)[a]	CULEBRA FLUID DENSITY (g/cm^3)[b]	POTENTIAL FLOW DIRECTION
H-2	135	>102.6+3.7 -6.3	>0.760+0.027 -0.047	>1.754+0.063 -0.108	1.225	1.006	upward
H-6	104	19.9±4.0	0.191±0.038	0.442±0.089	1.21	1.038	downward
H-7	128	46.8±2.5	0.366±0.020	0.844±0.045	1.048	0.999	downward
H-8	170	83.4+2.7 -3.6	0.491+0.016 -0.021	1.132+0.037 -0.049	1.13[c]	1.000	indeterminate
H-16	82	89.3±1.6	1.089±0.020	2.513±0.045	?	1.037[d]	upward
P-14	104	43.5±3.9	0.418±0.038	0.965±0.087	1.21[e]	1.018	indeterminate
P-17	143	>74.6[f]+? -0.9	>0.522[f]+? -0.006	>1.204[f]+? -0.015	?	1.061	upward
WIPP-25	133	>52.6±4.4	>0.395±0.033	>0.913±0.076	1.173	1.009	downward?
WIPP-26	80	>10.8+2.3 -0.4	>0.135+0.029 -0.005	>0.312+0.066 -0.012	1.04[g]	1.009	downward
WIPP-28	136	>61.6+4.0 -3.6	>0.453+0.029 -0.026	>1.045+0.068 -0.061	1.140	1.032	indeterminate
WIPP-29	206	91.2±2.3	0.443±0.011	1.022±0.026	1.072[g]	1.187[h]	indeterminate
WIPP-30	100	17.0+5.3 -4.9	0.170+0.053 -0.049	0.392+0.122 -0.113	1.202[g]	1.018	downward

[a] Data from Mercer (1983) except as noted
[b] Data from Cauffman et al. (1990) except as noted
[c] Data from Richey (1986)
[d] Specific-gravity value from Culebra in Air-Intake Shaft (Lyon, 1989)
[e] Calculated from water analysis presented in Mercer (1983) and Figure E.1 of Haug et al. (1987)
[f] Based on assumed R/S fluid density of 1.000 g/cm^3; values would increase if density were higher
[g] Data from Richey (1987a)
[h] Specific-gravity value from Randall et al. (1988)

At H-6, H-7, WIPP-26, and WIPP-30, the hydraulic gradient is downward from the Culebra to the unnamed member.

This pattern of vertical hydraulic gradients is generally explainable by the presence or absence of upper Salado dissolution. The three locations mentioned above where vertical gradients are upward, H-2, H-16, and P-17, are also locations where dissolution of the upper Salado has not occurred.

4.2.6.2 HYDRAULIC-HEAD DIFFERENTIALS BETWEEN THE CULEBRA AND THE MAGENTA

Because no hydraulic-head data are available for the Tamarisk, potential directions of vertical fluid flow through the central members of the Rustler can only be inferred by comparing hydraulic heads in the Culebra and Magenta. Table 4-12 shows the results of calculations of potential flow directions between the Culebra and the Magenta using the equilibrium-fluid-density approach outlined in Section 4.2.6. The areal distribution of vertical flow potentials is shown in Figure 4-11. The potential direction of fluid flow between the Magenta and Culebra appears to be downward at all 16 well locations for which hydraulic-head comparisons are possible except at H-6. At H-1, H-2, H-3, H-4, H-9, H-10, H-14, and H-16, the pressure/depth gradients between the Culebra and Magenta are negative, reflecting the fact that higher pressures are observed at the middle of the Magenta than are observed at the middle of the Culebra even though the Magenta overlies the Culebra. Strong potentials for downward flow also exist at DOE-2 and H-5, and lesser downward potentials exist at H-8, WIPP-28, and WIPP-30. Slight potentials for downward flow from the Magenta to the Culebra also appear to exist at WIPP-25 and WIPP-27, although differences between Magenta and Culebra fluid densities and the hypothetical equilibrium fluid density are small. Within the resolution of the calculations, Magenta and Culebra heads at H-6 appear to be in equilibrium. Where the Magenta is unsaturated at H-7 and WIPP-26, the Culebra head is below the base of the Magenta.

4.2.6.3 HYDRAULIC-HEAD DIFFERENTIALS BETWEEN THE MAGENTA AND THE FORTY-NINER

Magenta and Forty-niner claystone hydraulic heads can be compared at only four locations: DOE-2, H-3, H-14, and H-16. Table 4-13 shows calculations of potential flow directions performed using the equilibrium-fluid-density approach presented in Section 4.2.6. Despite uncertainties in actual fluid densities, the potential flow direction can be concluded to be upward from the Magenta to the Forty-niner claystone at all four locations considered. Hypothetical equilibrium fluid densities are 1.25 g/cm^3 or greater at all four wells.

4.3 Castile Formation

Pressurized brine reservoirs have been encountered in the Castile Formation. For the purposes of non-Salado flow and transport, parameterization of both the intact Castile and a representative Castile brine reservoir is necessary. Data for these Castile parameters are discussed in detail in Reeves et al. (1991, p. 2-1 to 2-16), Popielak et al. (1983), and Mercer (1987).

1 Table 4-12. Potential Flow Directions Between the Magenta and Culebra.

WELL	DIFFERENCE IN DEPTH (CUL-MAG) (ft)	DIFFERENCE IN FORMATION PRESSURE (CUL-MAG) (psi)	PRESSURE-DEPTH GRADIENT (psi/ft)	EQUILIBRIUM FLUID DENSITY (g/cm^3)	CULEBRA FLUID DENSITY (g/cm^3)[a]	MAGENTA FLUID DENSITY (g/cm^3)[b]	POTENTIAL FLOW DIRECTION
DOE-2	124	>5.6±5.7	>0.045±0.046	>0.104±0.113	1.041	1.005[c]	downward
H-1	112	-7.4±4.4	-0.066±0.039	--[d]	1.022	1.021	downward
H-2	105	-8.1+3.9 -1.3	-0.077+0.037 -0.012	--[d]	1.006	1.012	downward
H-3	111	-14.0+4.0 -1.4	-0.126+0.036 -0.013	--[d]	1.035	1.006[e]	downward
H-4	122	-13.2±2.6	-0.108±0.021	--[d]	1.014	1.020[f]	downward
H-5	112	4.9±4.2	0.044±0.038	0.101±0.087	1.102	1.008[f]	downward
H-6	114	50.0±2.2	0.439±0.019	1.012±0.045	1.038	1.003[f]	indeterminate
H-8	124	37.5+1.2 -0.3	0.302+0.010 -0.002	0.698+0.022 -0.006	1.000	1.008[g]	downward
H-9	123	-10.6+2.8 -1.1	-0.086+0.023 -0.009	--[d]	1.000	1.006[g]	downward
H-10	108	-37.1±8.9	-0.344±0.082	--[d]	1.047	1.171[g]	downward
H-14	122	-18.2+2.8 -1.9	-0.149+0.023 -0.016	--[d]	1.010	?	downward
H-16	110	-0.5±1.2	-0.005±0.011	--[d]	1.037[h]	?	downward
WIPP-25	145	59.1±2.0	0.408±0.014	0.941±0.032	1.009	1.004[i]	downward?
WIPP-27	120	50.4±1.6	0.420±0.013	0.969±0.031	1.093	1.09[i]	downward?
WIPP-28	135	26.2+2.1 -2.5	0.194+0.016 -0.019	0.448+0.036 -0.043	1.032	1.048	downward
WIPP-30	117	25.9+3.6 -4.0	0.221+0.031 -0.034	0.511+0.071 -0.079	1.018	1.01[i]	downward

[a] Data from Cauffman et al. (1990) except as noted
[b] Data from Mercer (1983) except as noted
[c] Average of Magenta fluid specific gravities at H-5c and H-6c (Lyon, 1989)
[d] Negative densities not possible; flow potential is clearly downward
[e] Specific-gravity data from Randall et al. (1988)
[f] Specific-gravity data from Lyon (1989)
[g] Data from Richey (1986)
[h] Specific-gravity value from Culebra in Air-Intake Shaft (Lyon, 1989)
[i] Data from Lambert and Robinson (1984)

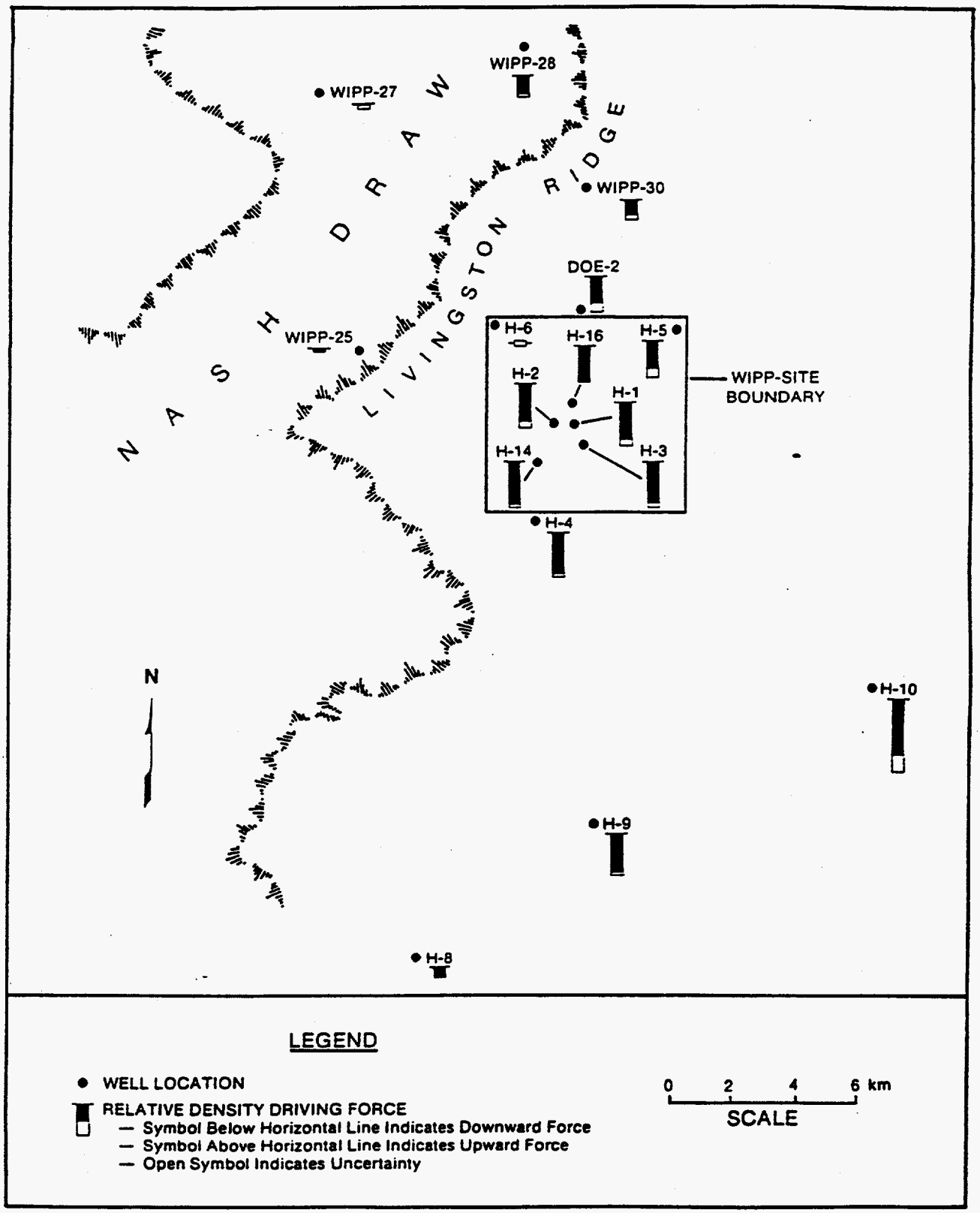

TRI-6344-56-0

Figure 4-11. Flow potentials between the Magenta dolomite and the Culebra dolomite.

1 Table 4-13. Potential Flow Directions between the Forty-Niner Claystone and Magenta.

WELL	DIFFERENCE IN DEPTH (MAG-49) (ft)	DIFFERENCE IN FORMATION PRESSURE (MAG-49) (psi)	PRESSURE-DEPTH GRADIENT (psi/ft)	EQUILIBRIUM FLUID DENSITY (g/cm^3)	MAGENTA FLUID DENSITY (g/cm^3)[a]	FORTY-NINER FLUID DENSITY (g/cm^3)	POTENTIAL FLOW DIRECTION
DOE-2	36	23	0.64	1.47	?	?	upward
H-3	31	25	0.81	1.86	1.006[b]	?	upward
H-14	38	41	1.08	2.49	?	?	upward
H-16	35	19	0.54	1.25	?	?	upward

[a] Specific gravities of Magenta fluids from H-3, H-4, H-5, and H-6 range from only 1.003 to 1.018 (Randall et al., 1988)

[b] Specific-gravity value from Randall et al. (1988)

4.4 Bell Canyon Formation

Data on the Bell Canyon Formation are available from five WIPP test holes as well as from studies reported in the petroleum literature. Drillstem tests (DSTs) of the Bell Canyon were performed in boreholes AEC-7 (Mercer, 1983), AEC-8 (SNL and D'Appolonia, 1983a), ERDA-10 (SNL and D'Appolonia, 1983b), DOE-2 (Mercer et al., 1987), and Cabin Baby-1 (Beauheim et al., 1983). The interpreted results of the DSTs are summarized in Table 4-14. Hiss (1976) and McNeal (1965) constructed potentiometric surface maps for the upper Bell Canyon, and their data were combined with the WIPP data by Mercer (1983) to produce the potentiometric surface map shown in Figure 4-12. Mercer (1983, p. 29) reports that the Bell Canyon channel sandstones typically have porosities ranging from 20 to 28 percent and permeabilities (citing Berg, 1979) ranging from 14 to 90 mD (~1 x 10^{-7} to ~9 x 10^{-7} m/s). The siltstones separating the sandstone channels have porosities ranging from 10 to 20 percent and permeabilities less than 0.1 mD (~1 x 10^{-9} m/s).

4.5 Formations Below the Bell Canyon Formation

Data on units below the Bell Canyon Formation in the vicinity of the WIPP site are sparse. The data available come from drilling and DST records compiled in the late 1970s and early 1980s. Figure 4-13 shows a stratigraphic column for the WIPP site starting at the Precambrian basement and extending to the Castile. A number of the formations shown are targets for petroleum exploration, including the Ellenburger, Silurian, Morrow, Atoka, Strawn, Bone Spring, Brushy Canyon, and Bell Canyon. According to Lambert (in Lambert and Mercer, 1978, p. III-2), these zones, with the possible exception of the Bone Spring, "have sufficient pressure to stand fluid above the storage horizon plus porosity and permeability sufficiently large enough to allow flow rates of several hundred barrels per day." The Atoka and Strawn Formations appear to have the highest hydraulic heads and water productions of these units. Heads in the Atoka are reported between 3375 and 6552 ft above sea level (for a fluid density of 1.08 g/cm^3), and water production rates of 0.6 to 6 gpm at ground surface have been sustained for several years. Heads in the Strawn are reported between 3350 and 6203 ft above sea level, with sustained productions of 3 to 8 gpm of water. Measured permeabilities in the Pennsylvanian formations range from 0.1 mD (~1 x 10^{-9} m/s) to about 50 mD (~5 x 10^{-7} m/s) and porosities range from 6 to 20 percent (Roswell Geological Society, 1977). With regard to the Bone Spring, Lambert (in Lambert and Mercer, 1978, p. III-3) states that "bottom-hole pressure data indicate the majority of the seven wells tested had insufficient heads to prevent downward movement of shallower water and, therefore, contamination of this zone with radionuclides could possibly occur." Thus, in the event of a borehole breach of the WIPP repository, deep units could serve either as pressure sources to drive fluids upward to strata such as the Culebra or as sinks receiving fluids from higher units.

4.6 Documentation of Experimental Data and Interpretive Techniques

Experimental data were collected from field hydraulic tests and field tracer tests. These test results are documented in a series of Hydrologic Data Reports (#1 through #8) (Hydro Geo Chem, 1985; Intera and Hydro Geo Chem, 1985; Intera, 1986; Saulnier et al., 1987; Stensrud et al., 1987, 1988a, 1988b, 1990), Basic Data Reports (e.g., Mercer et al., 1987), and USGS reports (e.g., Richey,

Table 4-14. Summary of Bell Canyon DST Results.

Summary of Bell Canyon DST Results

Hole	Tested Interval (ft. below ground surface)	Unit Name	Hydraulic Conductivity (ft/day)	Reference
AEC-7	4481-4702 4597-4702	Ramsey, Trap, and Olds Lower 37 ft. of Castile Anhydrite I down through Olds	$4x10^{-2}$ $4x10^{-2}$	Mercer (1983)
AEC-8	4292-4393 4809-4815 4832-4848	Lamar and upper Ramsey Lower Hays? Lower Hays?	$2x10^{-6}$ $7x10^{-3}$ $2x10^{-2}$	Mercer (1983)
ERDA-10	3847-3913 4114-4417	Lamar and Ramsey Lower Hays	$4x10^{-4}$ $5x10^{-2}$	Mercer (1983)
Cabin Baby-1	4036-4089 4093-4125 4131-4163 4170-4291	Lamar Ramsey Olds Hays	$1x10^{-6}$ $5x10^{-5}$ to $2x10^{-4}$ $5x10^{-5}$ to $2x10^{-4}$ $1x10^{-3}$ to $4x10^{-3}$	Beauheim et al. (1983)
DOE-2	4138-4180[1] 4177-4218[2] 4220-4325[3]	Ramsey Olds Hays	$2x10^{-4}$ $2x10^{-4}$ $5x10^{-3}$	Beauheim (1986)

[1] Effective thickness 4144-4172
[2] Effective thickness 4187-4217
[3] Effective thickness 4255-4325

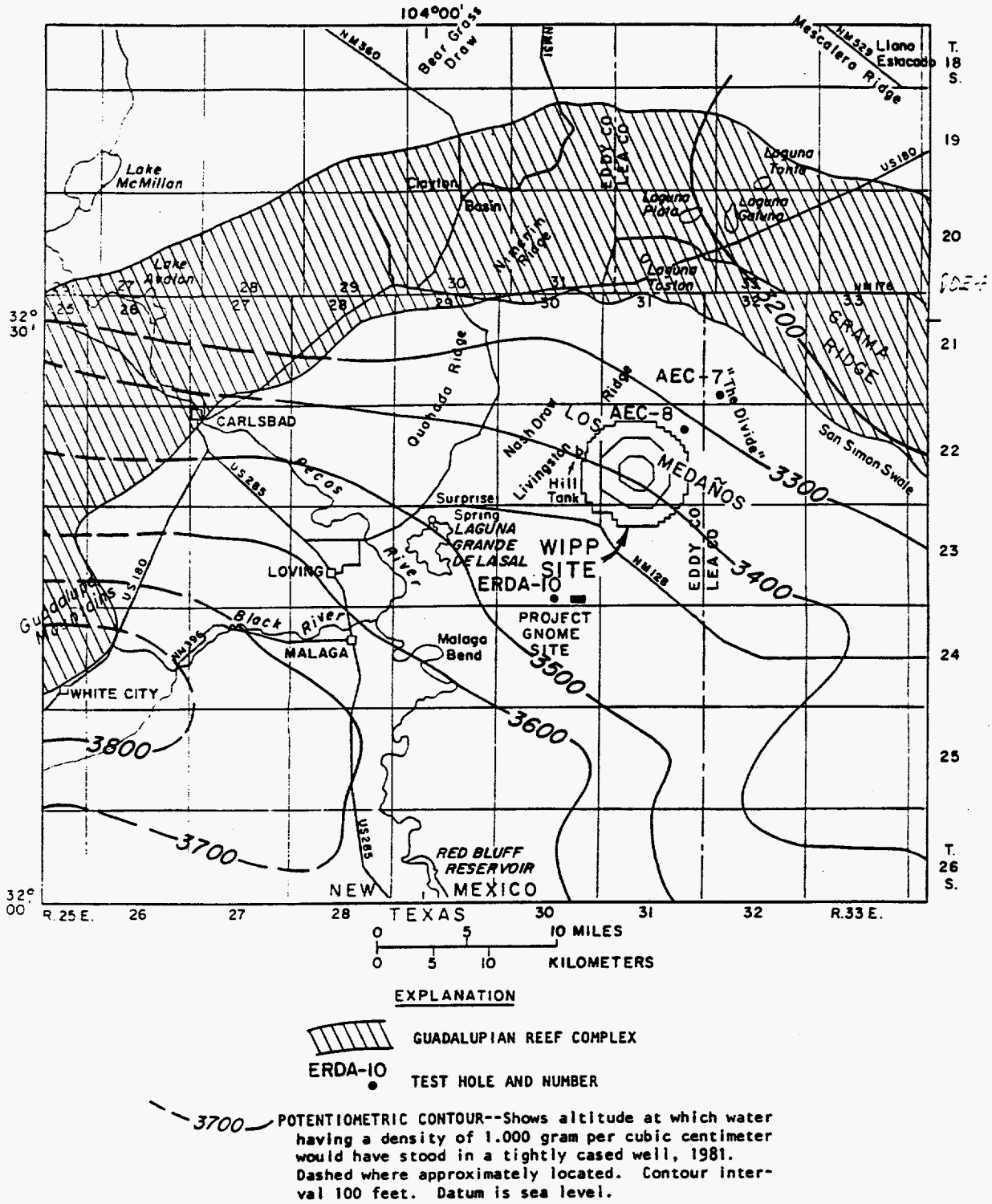

Figure 4-12. Potentiometric surface of the hydrologic unit in the upper part of the Bell Canyon Formation (Delaware Mountain Group) at and near the proposed Waste Isolation Pilot Plant (WIPP) site.

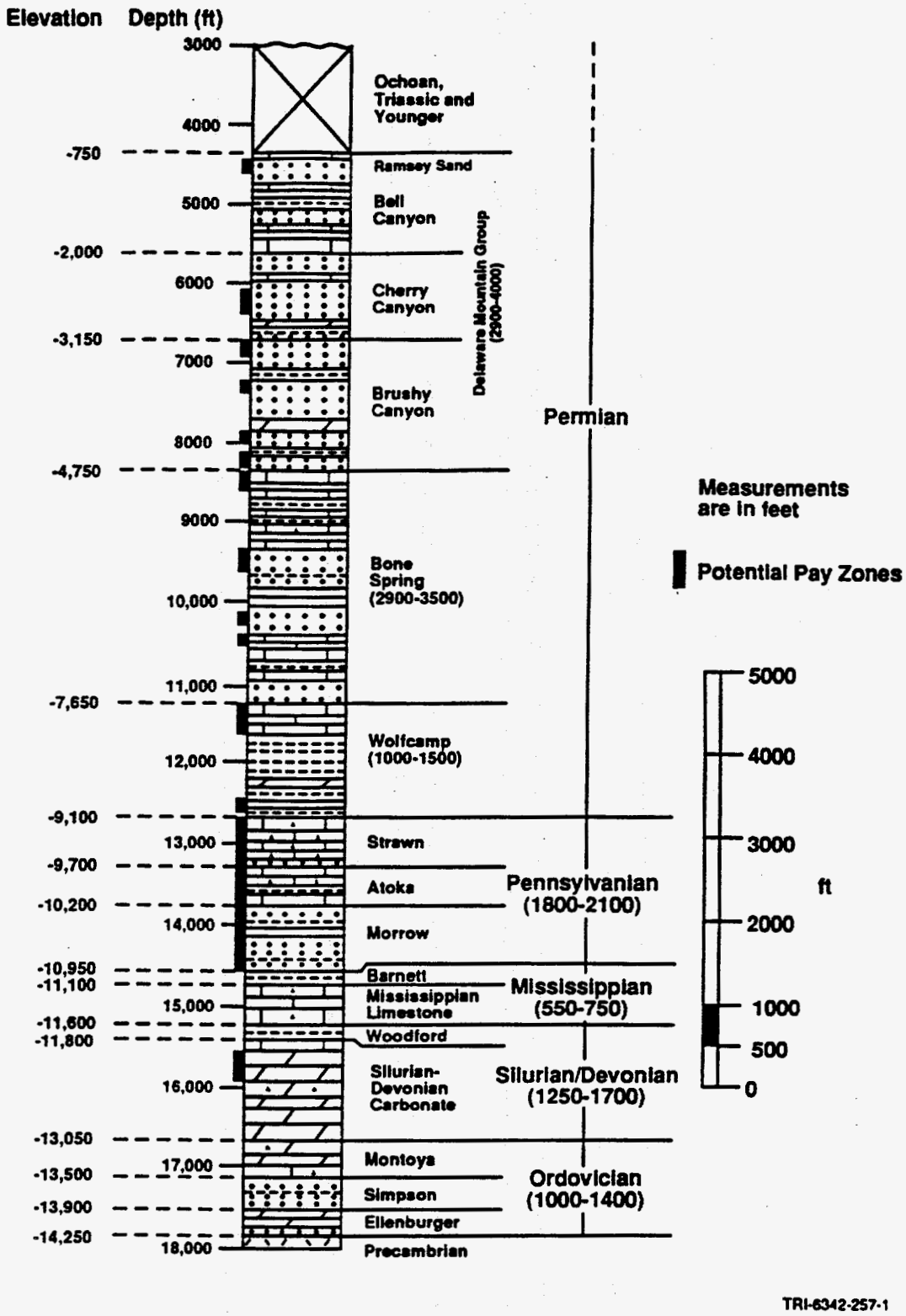

Figure 4-13. Stratigraphic Column of Units Below the Castile Formation (from Powers et al., 1978; after Foster, 1974).

1986). Interpretation of the raw data is described in interpretive reports referenced throughout this section.

5.0 REFERENCES

Adams, J.E. 1944. "Upper Permian Ochoa Series of the Delware Basin, West Texas and Southeastern New Mexico," *American Association of Petroleum Geologists Bulletin.* Vol. 28, 1596-1625.

Anderson, R.Y. 1981. "Deep-Seated Salt Dissolution in the Delaware Basin, Texas and New Mexico," in *Environmental Geology and Hydrology in New Mexico*, S.G. Wells and W. Lambert, eds., New Mexico Geological Society Special Publication no. 10, 133-145.

Anderson, R.Y. 1982. "Deformation-Dissolution Potential of Bedded Salt, Waste Isolation Pilot Plant Site, Delaware Basin, New Mexico," in *Scientific Basis for Nuclear Waste Management, Materials Research Society Proceedings*, V. Lutze, ed., Vol. 11, 449-458. New York: Elsevier Science Publishing Co.

Anderson, R.Y., Dean, W.E., Kirkland Jr., D.W., and Snider, H.I., 1972. "Permian Castile Varved Evaporite Sequence, West Texas and New Mexico," *Geological Society of America Bulletin*, Vol. 83,p. 59-86.

Anderson, R.Y., Kietzke, K.K., and Rhodes, D.J., 1978. Development of Dissolution Breccias, Norther Delaware Basin, New Mexico and Texas, in *Geology and Mineral Deposits of Ochoan Rocks in Delaware Basin and Adjacent Areas*, G.S. Austin, ed., Circular 159, New Mexico Bureau of Mines and Mineral Resources, Socorro, NM, p. 46-52.

Avis, J.D., and G.J. Saulnier, Jr. 1990. *Analysis of the Fluid-Pressure Responses of the Rustler Formation at H-16 to the Construction of the Air-Intake Shaft at the Waste Isolation Pilot Plant (WIPP) Site.* SAND89-7067. Albuquerque, NM: Sandia National Laboratories.

Avogadro, A., and G.de Marsily. 1983. "The Role of Colloids in Nuclear Waste Disposal." *Materials Research Society Symposium Proceedings.* Vol. 26, 495-505.

Bachman, G.O. 1987. *Karst in Evaporites in Southeastern New Mexico.* SAND86-7078. Albuquerque, NM: Sandia National Laboratories.

Bachman, G.O. 1973. *Surficial Features and Late Cenozoic History in Southeastern New Mexico*, Open-file Report 4339-8, U.S. Geological Survey.

Bachman, G.O., 1974. *Geologic Processes and Cenozoic History Related to Salt Dissolution in Southeastern New Mexico,* Open-file Report 74-194, U.S. Geological Survey.

Bachman, G.L., 1976. *Cenozoic Deposits of Southeastern New Mexico and an Outline of the History of Evaporite Dissolution*, J. of Research, Vol. 4, U.S. Geological Survey, P. 135-149.

Bachman, G.O., 1980. *Regional Geology and Senozoic History of Pecos Region, Southeastern New Mexico*, Open-file Report 80-1099, U.S. Geological Survey.

Bachman, G.O., 1981. *Geology of Nash Draw, Eddy County, New Mexico*, Open-file Report 81-31, U.S. Geological Survey.

Bachman, G.O., 1984. *Regional Geology of Ochoan Evaporites, Northern Part of Delaware Basin,* Circular 184, New Mexico Bureau of Mines and Mineral Resources, Socorro, NM.

Bachman, G.O., 1985. *Assessment of Near-surface Dissolution at and near the Waste Isolation Pilot Plant* (WIPP), Southeastern New Mexico," *SAND84-7178*, Sandia National Laboratories, Albuquerque, N.M.

Baes, C. F., and R.E. Mesmer. 1976. *The Hydrolysis of Cations.* Wiley Interscience.

Bear, J., and A. Verruijt. 1987. *Modeling Groundwater Flow and Pollution.* Boston, MA: D. Reidel Publishing Company.

Beauheim, R.L., and Holt, R.M., 1990. "Hydrology of the WIPP Site," *Geological and Hydrological Studies of Evaporites in the Northern Basin for the Waste Isolation Pilot Plant (WIPP), New Mexico*, Geologic Society of America 1990 Annutal Meeting Field Trip #14 Guidebook, Dallas, TX, Dallas Geologic Society pp. 131-179.

Beauheim, R.L. 1986. *Hydraulic-Test Interpretations for Well DOE-2 at the Waste Isolation Pilot Plant (WIPP) Site*. SAND86-1364. Albuquerque, NM: Sandia National Laboratories.

Beauheim, R.L. 1987a. *Interpretations of Single-Well Hydraulic Tests Conducted At and Near the Waste Isolation Pilot Plant (WIPP) Site, 1983-1987*. SAND87-0039. Albuquerque, NM: Sandia National Laboratories.

Beauheim, R.L. 1987b. *Interpretation of the WIPP-13 Multipad Pumping Test of the Culebra Dolomite at the Waste Isolation Pilot Plant (WIPP) Site*. SAND87-2456. Albuquerque,

NM: Sandia National Laboratories.

Beauheim, R.L. 1987c. *Analysis of Pumping Tests of the Culebra Dolomite Conducted at the H-3 Hydropad at the Waste Isolation Pilot Plant (WIPP) Site*. SAND86-2311. Albuquerque, NM: Sandia National Laboratories.

Beauheim, R.L. 1989. *Interpretation of H-11b4 Hydraulic Tests and the H-11 Multipad Pumping Test of the Culebra Dolomite at the Waste Isolation Pilot Plant (WIPP) Site*. SAND89-0536. Albuquerque, NM: Sandia National Laboratories.

Beauheim, R.L., and R.M. Holt. 1990. "Hydrogeology of the WIPP Site," *Geological and Hydrological Studies of Evaporites in the Northern Delaware Basin for the Waste Isolation Pilot Plant (WIPP), New Mexico, Field Trip #14 Guidebook, Geological Society of America 1990 Annual Meeting, Dallas, TX, October 29-November 1, 1990*. Leaders: D.W. Powers, R.M. Holt, R.L. Beauheim, and N. Rempe. SAND90-2035J. Dallas, TX: Dallas Geological Society. 131-179.

Beauheim, R.L., T.F. Dale, and J.F. Pickens. 1991. *Interpretations of Single-Well Hydraulic Tests of the Rustler Formation Conducted in the Vicinity of the Waste Isolation Pilot Plant Site, 1988-1989*. SAND89-0869. Albuquerque, NM: Sandia National Laboratories.

Beauheim, R.L., B.W. Hassinger, and J.A. Klaiber. 1983. *Basic Data Report for Borehole Cabin Baby-1 Deepening and Hydrologic Testing*. WTSD-TME-020. Albuquerque, NM: US DOE.

Bell, J.T., C.F. Coleman, D.A. Costanzo, and R.E. Biggers. 1973a. "Plutonium polymerization—III. The nitrate precipitation of Pu(IV) polymer." *Journal of Inorganic and Nuclear Chemistry*. vol. 35: 629-632.

Bell, J.T., D.A. Costanzo, and R.E. Biggers. 1973b. "Plutonium polymerization—II. Kinetics of the plutonium polymerization." *Journal of Inorganic and Nuclear Chemistry*. vol. 35: 623-628.

Bellin, A., P. Salandin, and A. Rinaldo. 1992. "Simulation of Dispersion in Heterogeneous Porous Formations: Statistics, First-Order Theories, Convergence of Computations," *Water Resources Research*. Vol. 28, no. 9, 2211-2228.

Bennett, D.G., S.K. Liew, L. Nanu, D. Read, and J.B. Thomas. 1993. "Modelling colloidal transport of

radionuclides through porous media." In *High Level Radioactive Waste Management, Proceedings of the Fourth Annual International Conference*; Las Vegas, Nevada, 638-645.

Berg, R.R. 1979. "Reservoir Sandstones of the Delaware Mountain Group, Southeast New Mexico," *Guadalupian Delaware Mountain Group of West Texas and Southeast New Mexico*. Ed. N.M. Sullivan. Permian Basin Publication 79/18. Midland, TX: Permian Basin Section, Society of Economic Paleontologists and Mineralogists. 75-95.

Bertram-Howery, S.G., M.G. Marietta, R.P. Rechard, P.N. Swift, D.R. Anderson, B.L. Baker, J.E. Bean, Jr., W. Beyeler, K.F. Brinster, R.V. Guzowski, J.C. Helton, R.D. McCurley, D.K. Rudeen, J.D. Schreiber, and P. Vaughn. 1990. *Preliminary Comparison with 40 CFR Part 191, Subpart B for the Waste Isolation Pilot Plant, December 1990*. SAND90-2347. Albuquerque, NM: Sandia National Laboratories.

Bird, R.B., W.E. Stewart, and E.N. Lightfoot. 1960. *Transport Phenomena*. Wiley & Sons, New York.

Bodine, M.W., Jr., and B.F. Jones. 1986. *The Salt Norm: A Quantitative Chemical-Mineralogical Characterization of Natural Waters*. United States Geological Survey Water Resources Report 86-4086. Reston, VA: United States Geological Survey.

Bodine, M.W., Jr., B.F. Jones, and S.J. Lambert. 1991. "Chapter 4: Normative Analysis of Groundwaters from the Rustler Formation Associated with the Waste Isolation Pilot Plant, Southeastern New Mexico," *Hydrogeochemical Studies of the Rustler Formation and Related Rocks in the Waste Isolation Pilot Plant Area, Southeastern New Mexico*. Eds. M.D. Siegel, S.J. Lambert, and K.L. Robinson. SAND88-0196. Albuquerque, NM: Sandia National Laboratories. 4-1 through 4-140.

Borns, D.J., and Shaffer, S-E., 1985. *Regional Well-Log Correlation in the New Mexico Portion of the Delaware Basin*, SAND83-1798, Sandia National Laboratories, Albuquerque, NM.

Brookins, D.G., Lambert, S.J., and Ward, D.B., 1990, *Authigenic Clay Minerals in the Rustler Formation*, WIPP Site Area, New Mexico, SAND89-1405, Sandia National Laboratories, Albuquerque, NM.

Brinster, K.F. 1991. *Preliminary Geohydrologic Conceptual Model of the Los Medaños Region*

Near the Waste Isolation Pilot Plant for the Purpose of Performance Assessment. SAND89-7147. Albuquerque, NM: Sandia National Laboratories.

Brush, L.H. 1990. *Test Plan for Laboratory and Modeling Studies of Repository and Radionuclide Chemistry for the Waste Isolation Pilot Plant.* SAND90-0266. Albuquerque, New Mexico: Sandia National Laboratories.

Brusseau, M.L., R.E. Jessup, and P.S.C. Rao. 1989. "Modeling the Transport of Solutes Influenced by Multiprocess Nonequilibrium," *Water Resources Research.* Vol. 25, no. 9, 1971-1988.

Buddemeier, R. W., and J.R. Hunt. 1988. "Transport of Colloidal Contaminants in Groundwater: Radionuclide Migration at the Nevada Test Site." *Applied Geochemistry* 3, 535-548.

Cauffman, T.L., A.M. LaVenue, and J.P. McCord. 1990. *Ground-Water Flow Modeling of the Culebra Dolomite. Volume II: Data Base*. SAND89-7068/2. Albuquerque, NM: Sandia National Laboratories.

Chapman, J.B. 1986. *Stable Isotopes in Southeastern New Mexico Groundwater: Implications for Dating Recharge in the WIPP Area.* EEG-35. Santa Fe, NM: Environmental Evaluation Group.

Choppin, G.R. 1983. "Solution chemistry of the actinides." *Radiochimica Acta.* vol. 32: 43-53.

Choppin, G.R. 1988. "Humics and radionuclide migration." *Radiochimica Acta.* vol. 44/45: 23-28.

Chugg, J.C., Anderson, G.W., Kink, D.L., and Jones, L.H., 1952. *Soil Survey of Eddy Area, New Mexico*, U.S. Department of Agriculture, P. 82, plus figures.

Cleveland, J.M. 1979. "Critical review of plutonium equilibria of environmental concern." In *Chemical Modeling in Aqueous Systems*; E.A. Jenne, Ed.; American Chemical Society Symposium Series: 321-338.

COHMAP (Cooperative Holocene Mapping Project) Members. 1988. "Climatic Changes of the

Last 18,000 Years: Observations and Model Simulations," *Science*. Vol. 241, 1043-1052.

Cooper, J.B., and Glanzman, V.M. 1971. *Geohydrology of Project Gnome Site, Eddy County, New Mexico*. United States Geological Survey Professional Paper 712-A. Washington, D.C.: United States Geological Survey.

Corbet, T.F., and M.G. Wallace. 1993. "Post-Pleistocene Patterns of Shallow Groundwater Flow in the Delaware Basin, Southeastern New Mexico and West Texas," *New Mexico Geological Society Guidebook, 44th Annual Field Conference, Carlsbad Region, New Mexico and West Texas*. Eds. D.W. Love, J.W. Hawley, B.S. Kues, J.W. Adams, G.W. Austin, and J.M. Barker. SAND93-1318J. Roswell, NM: New Mexico Geological Society. 321-325.

Costanzo, D.A., R.E. Biggers, and J.T. Bell. 1973. "Plutonium polymerization—I. A spectrophotometric study of the polymerization of plutonium(IV)." *Journal of Inorganic and Nuclear Chemistry*. vol. 35: 609-622.

Crawford, J. E., and Wallace, C.S., 1993. *Geology and Mineralization of the Culberson Sulfur Deposit: in Carlsbad Region, New Mexico and West Texas*, D.W. Love et al., eds., Forty-fourth Annual Field Conference Guidebook, New Mexico Geological Society, Socorro, NM, p. 301-316.

Cvetkovic, V.D., and A.M. Shapiro. 1990. "Mass Arrival of Sorptive Solute in Heterogeneous Porous Media," *Water Resources Research*. Vol. 26, no. 9, 2057-2067.

Dagan, G. 1989. *Theory of Flow and Transport in Porous Formations*. New York, NY: Springer-Verlag.

Dagan, G., and V. Cvetkovic. 1993. "Spatial Moments of a Kinetically Sorbing Solute Plume in a Heterogeneous Aquifer," *Water Resources Research*. Vol. 29, no. 12, 4053-4061.

D'Appolonia. 1982. *Data File Report, ERDA-6 & WIPP-12 Testing, Volume I - Text*. Report to Westinghouse Electric Corporation and US DOE WIPP Office.

D'Appolonia. 1983. *Data File Report, ERDA-6 & WIPP-12 Testing, Part B, Revisions, Addenda, and Errata, Volumes IVA through V, Revised September, 1983*. Report to Westinghouse Electric Corporation and US DOE WIPP Office.

Davies, P.B. 1987. "Modeling Areal, Variable-Density, Ground-Water Flow Using Equivalent Freshwater Head -- Analysis of Potentially Significant Errors," *Proceedings of the Solving Ground Water Problems with Models Conference and Exposition, Denver, CO, February 10-12, 1987.* Dublin, OH: National Water Well Association. Vol. 2, 888-903.

Davies, P.B. 1989. *Variable-Density Ground-Water Flow and Paleohydrology in the Waste Isolation Pilot Plant (WIPP) Region, Southeastern New Mexico.* Open-File Report 88-490. Albuquerque, NM: U.S. Geological Survey.

Dearlove, J.P.L., G. Longworth, M. Ivanovich, J.I. Kim, B. Delakowitz, and P. Zeh. 1990. "Organic colloid transport of radionuclides at Gorleben, West Germany." In *Waste Management '90*; Tucson, Arizona, 565-569.

Dennehy, K. F. 1982. *Results of Hydrologic Tests and Water-Chemistry Analyses, Wells H-6A, H-6B, and H-6C, at the Proposed Waste Isolation Pilot Plant Site, Southeastern New Mexico.* United States Geological Survey Water-Resources Investigations 82-8. Albuquerque, NM: United States Geological Survey.

Dennehy, K. F., and Mercer, J. W. 1982. *Results of Hydrologic Tests and Water- Chemistry Analyses, Wells H-5A, H-5B, and H-5C, at the Proposed Waste Isolation Pilot Plant Site, Southeastern New Mexico.* United States Geological Survey Water-Resources Investigations 82-19. Albuquerque, NM: United States Geological Survey.

Derjaguin, B.V., and L. Landau. 1941. "A theory of the stability of strongly charged lyophobic sols and the coalescence of strongly charge particles in electrolytic solutions." *Acta Phys.-Chim. USSR.* vol. 14: 633.

Destouni, G., and V.D. Cvetkovic. 1991. "Field Scale Mass Arrival of Sorptive Solute into the Groundwater," *Water Resources Research.* Vol. 27, no. 6, 1315-1325.

Dosch, R.G. 1980. *Assessment of Potential Radionuclide Transport in Site-Specific Geologic Formations.* SAND79-2468. Albuquerque, NM: Sandia National Laboratories.

Dosch, R.G. 1981. *Solubility and Sorption Characteristics of Uranium (VI) Associated with Rock Samples and Brines/Groundwaters from WIPP and NTS.* SAND80-1595. Albuquerque, NM: Sandia National Laboratories.

Dosch, R.G., and A.W. Lynch. 1978. *Interaction of Radionuclides with Geomedia Associated with the Waste Isolation Pilot Plant (WIPP) Site in New Mexico*. SAND78-0297. Albuquerque, NM: Sandia National Laboratories.

Dunham, R.J., 1972. *Capitan Reef, New Mexico and Texas: Facts and Questions to Aid Interpretation and Group Discussion*, Publ. 72-14, Permian Basin Section SEPM, p. 297.

Dykhuizen, R.C. 1992. "Diffusive Matrix Fracture Coupling Including the Effects of Flow Channeling," *Water Resources Research*. Vol. 28, no. 9, 2447-2450.

Eager, G.P., 1983. *Core from the Lower Dewey Lake, Rustler, and Upper Salado Formation, Culberson County, Texas*, Permian Basin Section Society of Economic Paleontologists and Mineralogists Core Workshop No. 2, p. 273-283.

Earth Technology Corporation. 1988. *Final Report for Time Domain Electromagnetic (TDEM) Surveys at the WIPP Site*. SAND87-7144. Albuquerque, NM: Sandia National Laboratories.

Enfield, C.G., and G. Bengtsson. 1988. "Macromolecular Transport of Hydrophobic Contaminants in Aqueous Environments," *Ground Water*. Vol. 26, no. 1, 64-70.

Ferrall, C.C., and Gibbond, J.F., 1980. *Core Study of Rustler Formation over the WIPP Site*, SAND79-7110, Sandia National Laboratories, Albuquerque, NM.

Fetter, C.W. 1993. *Contaminant Hydrogeology*. New York, NY: Macmillan Publishing Company.

Foster, R.W., 1974. *Oil and Gas Potential of a Proposed Site for the Disposal of High-Level Radioactive Waste*, Open-File Report, Contract No. AF(40-1)-4423, Oak Ridge National Laboratory, Oak Ridge, TN.

Francis, A.J., and J.B. Gillow. 1994. *Effects of microbial processes on gas generation under expected Waste Isolation Pilot Plant repository conditions. Progress report through 1992*. Sandia National Laboratories, SAND93-7036, Albuquerque, New Mexico.

Freeze, R.A., and J.A. Cherry. 1979. *Groundwater*. Englewood Cliffs, NJ: Prentice-Hall.

Freeze, R.A., and P.A. Witherspoon. 1967. "Theoretical Analyses of Regional Ground Water Flow: 2. Effect of Water Table Configuration and Subsurface Permeability Variation," *Water Resources Research.* Vol. 3, 623-634.

Garber, R.A. Grover, G.A., and Harris, P.M., 1989. *Geology of the Capitan Shelf Margin-Subsurface Data from the Northern Delaware Basin*, in Subsurface and Outcrop Examination of the Capitan Shelf Margin, Northern Delaware Basin, Harris, P.M., and Grove, G.A., eds.,: SEPM Core Workshop No. 13, p. 3-269.

Gelhar, L.W. 1993. *Stochastic Subsurface Hydrology*. Englewood Cliffs, NJ: Prentice-Hall.

Gelhar, L.W., and C.L. Axness. 1983. "Three-Dimensional Stochastic Analysis of Macrodispersion in Aquifers," *Water Resources Research.* Vol. 19, no. 1, 161-180.

Gonzalez, D.D. 1983. *Hydrogeochemical Parameters of Fluid-Bearing Zones in the Rustler and Bell Canyon Formations: Waste Isolation Pilot Plant (WIPP), Southeast New Mexico (SENM)*. SAND83-0210. Albuquerque, NM: Sandia National Laboratories.

Gregory, J. 1978. Flocculation by inorganic salts. In *The Scientific Basis of Flocculation* (ed. K. J. Ives), 89-99, Sijthoff and Noordhoff.

Guilinger, J.R., 1993. *The Geology and Development of the Phillips Ranch Sulfur Deposit: In Geology of the Carlsbad Region, New Mexico and West Texas*, D.W. et al., eds., Forty-fourth Annual Field Conference Guidebook, New Mexico Geological Society, Socorro, NM, pp. 21-23.

Hardy, W.B. 1900. "A preliminary investigation of the conditions which determine the stability of irreversible hydrosols." *Proceedings of the Royal Society of London.* vol. 66: 110-125.

Harms, J.C., and Williamson, C.R., 1988. "Deep-water density current deposits of Delaware Mountain Group (Permian), Delaware Basin, Texas and New Mexico, *American Association of Petroleum Geologists Bulletin*, Vol. 72, p. 299-317.

Haug, A., V.A. Kelley, A.M. LaVenue, and J.F. Pickens. 1987. *Modeling of Ground-Water Flow in the Culebra Dolomite at the Waste Isolation Pilot Plant (WIPP) Site: Interim Report.* SAND86-7167. Albuquerque, NM: Sandia National Laboratories.

Hawley, J.W., 1993. *The Ogallala and Gatuna Formations in the Southeastern New Mexico Region, a Progress Report, in Carlsbad Region, New Mexico and West Texas*, D.W. Love et al., eds., New Mexico Geological Society, Forty-fourth Annual Field Conference Guidebook, p. 261-269.

Hays, J.D., J. Imbrie, and N.J. Shackleton. 1976. "Variations in the Earth's Orbit: Pacemaker of the Ice Ages," *Science*. Vol. 194, 1121-1132.

Heftmann, E., ed. 1961. *Chromatography: Adsorption, Partition, Ion Exchange, Electrochromatography, Column, Slab, Paper, Gas*. New York, NY: Reinhold Pub. Corp.

Helton, J.C., J.W. Garner, R.D. McCurley, and D.K. Rudeen. 1991. *Sensitivity Analysis Techniques and Results for Performance Assessment at the Waste Isolation Pilot Plant*. SAND90-7103. Albuquerque, NM: Sandia National Laboratories.

Helton, J.C., J.W. Garner, R.P. Rechard, D.K. Rudeen, and P.N. Swift. 1992. *Preliminary Comparison with 40 CFR Part 191, Subpart B for the Waste Isolation Pilot Plant, December 1991. Volume 4: Uncertainty and Sensitivity Analysis Results*. SAND91-0893/4. Albuquerque, NM: Sandia National Laboratories.

Hiemenz, P.C. 1986. *Principles of Colloid and Surface Chemistry*. New York, N.Y.: Marcel Dekker, Inc.

Hills, J.M., and Kottlowski, F.E., 1983. *Southwest/Southwest Mid-Continent Region: American Association of Petroleum Geologists*, Correlation Chart Series.

Hiss, W.L. 1976. "Stratigraphy and Ground-Water Hydrology of the Capitan Aquifer, Southeastern New Mexico and Western Texas." PhD dissertation. Boulder, CO: University of Colorado at Boulder.

Holt, R.M., and D.W. Powers. 1990. *Geologic Mapping of the Air Intake Shaft at the Waste Isolation Pilot Plant*. DOE-WIPP 90-051. Carlsbad, NM: Westinghouse Electric Corporation.

Holt, R.M., and Powers, D.W., 1984. *Geotechnical Activities in the Waste Handling Shaft Waste Isolation Pilot Plant (WIPP) Project Southeastern New Mexico*, WTSD-TME-038, U.S. Department of Energy, Carlsbad, NM.

Holt, R.M., and Powers, D.W., 1986. *Geotechnical Activities in the Exhaust Shaft*, DOE-WIPP-86-008, U.S. Department of Energy, Carlsbad, NM.

Honeyman, B.D. 1991. "Surface chemistry, colloids and trace-element scavenging." In *Marine Particles: Analysis and Characterization*; D. C. Hurd and D.W. Spencer, Ed.; American Geophysical Union: Washington, D.C., Geophysics Monograph 63: 437-451.

Honeyman, B.D., and P.H. Santschi. 1992. "The role of particles and colloids in the transport of radionuclides and trace metals in the oceans." In *Environmental Particles*; J. Buffle and H.P. van Leeuwen, Ed.; Lewis Publishers, Inc.: Chelsea, Michigan; vol. 1: 379-423.

Houghton, J.T., G.J. Jenkins, and J.J. Ephraums. 1990. *Climate Change: The IPCC Scientific Assessment.* New York, NY: Cambridge University Press.

Hubbert, M.K. 1940. "The Theory of Ground-Water Motion," *The Journal of Geology*. Vol. 48, no. 8, pt. 1, 785-944.

Hwang, Y., P.L. Chambré, W.W.-L. Lee, and T.H. Pigford. 1990. "Analytic studies of colloid transport in fractured porous media." *Materials Research Society Symposium Proceedings.* vol. 176, 599-605.

Hydro Geo Chem, Inc. 1985. *WIPP Hydrology Program, Waste Isolation Pilot Plant, SENM Hydrologic Data Report #1*. SAND85-7206. Albuquerque, NM: Sandia National Laboratories.

Imbrie, J. 1985. "A Theoretical Framework for the Pleistocene Ice Ages," *Journal of the Geological Society.* Vol. 142, 417-432.

Imbrie, J., and J.Z. Imbrie. 1980. "Modeling the Climatic Response to Orbital Variations," *Science.* Vol. 207, 943-953.

Imbrie, J., J.D. Hays, D.G. Martinson, A. McIntyre, A.C. Mix, J.J. Morley, N.G. Pisias, W.L. Prell, and J.J. Shackleton. 1984. "The Orbital Theory of Pleistocene Climate: Support from a Revised Chronology of the Marine ^{18}O Record," in A.L. Berger, J. Imbrie, J. Hays, G. Kukla, and B. Saltzman, eds., *Milankovitch and Climate, Proceedings of the NATO Advanced Research Workshop on Milankovitch, Palisades, NY, November 30-December 4, 1982.* Boston, MA: D. Reidel Publishing Co., 269-305, Part 1.

Intera Technologies, Inc. 1986. *WIPP Hydrology Program, Waste Isolation Pilot Plant, Southeastern New Mexico, Hydrologic Data Report #3*. SAND86-7109. Albuquerque, NM: Sandia National Laboratories.

Intera Technologies, Inc., and Hydro Geo Chem, Inc. 1985. *WIPP Hydrology Program, Waste Isolation Pilot Plant, Southeastern New Mexico, Hydrologic Data Report #2*. SAND85-7263. Albuquerque, NM: Sandia National Laboratories.

Izett, G.A., and Wilcox, R.E., 1982. *Map Showing Localities and Inferred Distribution of the Huckleberry Ridge, Mesa Falls, and Lava Creek Ash Beds in the Western United States and Southern Canada*, U.S. Geological Survey, Misc. Investigations Map I-1325, Scale 1:400,000.

Johnson, J.S., 1978. *Stratigraphy and Mineral Resources of Guadalupian and Ochoan Rocks in the Texas Panhandle and Western Oklahoma, in Geology and Mineral Deposits of Ochoan Rocks in Delaware Basin and Adjacent Areas*, G.S. Austin. ed., Circular 159, New Mexico Bureau of Mines and Mineral Resources, Socoroo, NM, p. 57-62

Jones, C.L. 1978. *Test Drilling for Potash Resources: Waste Isolation Pilot Plant Site, Eddy County, New Mexico*. Open-File Report 78-592. Denver, CO: U.S. Geological Survey. Vols. 1-2.

Jones, D.L. 1978. *Test Drilling for Potash Resources: Waste Isolation Pilot Plant Site, Eddy County, New Mexico*, Open-file Report 78-592, U.S. Geological Survey, Denver, CO. Vol. 1 & 2.

Jones, C.L., Bowles, C.G., and Bell, K.G., 1960. *Experimental Drillhole Logging in Potash Deposits of the Carlsbad District*, New Mexico, Open-file Report, U.S. Geological Survey, p. 25.

Jones, T.L., V.A. Kelley, J.F. Pickens, D.T. Upton, R.L. Beauheim, and P.B. Davies. 1992. *Integration of Interpretation Results of Tracer Tests Performed in the Culebra Dolomite at the Waste Isolation Pilot Plant Site*. SAND92-1579. Albuquerque, NM: Sandia National Laboratories.

Kelley, V.A., and G.J. Saulnier, Jr. 1990. *Core Analyses for Selected Samples from the Culebra Dolomite at the Waste Isolation Pilot Plant Site*. SAND90-7011. Albuquerque, NM:

Sandia National Laboratories.

Kim, J. I. 1991. "Actinide Colloid Generation in Groundwater." *Radiochimica Acta* vol. 52/53: 71-81.

King, P.B., 1948. *Geology of the Southern Guadalupe Mountains, Texas*, Professional Paper 215, U.S. Geological Survey, Washington, D.C.

King, R.E., 1947. *Sedimentation in Permian Castile Sea*, American Association of Petroleum Geologists Bulletin, Vol, 31 p. 470-477.

Klemmick, G.F., 1993. *Geology of the Pokorny Sulfur Deposit, Culberson County, Texas, : in Geology of the Carlsbad Region, New Mexico and West Texas*, D.W. Love et al., eds., Forty-fourth Annual Field Conference Guidebook, New Mexico Geological Society Socorro, NM, p. 18-19.

Kraus, K.A. 1956. "Hydrolytic behavior of the heavy elements." In *Proceedings of the First United Nations International Conference on the Peaceful Uses of Atomic Energy*, Geneva. 245-257.

Lambert, S.J. 1987. *Feasibility Study: Applicability of Geochronologic Methods Involving Radiocarbon and Other Nuclides to the Groundwater Hydrology of the Rustler Formation, Southeastern New Mexico.* SAND86-1054. Albuquerque, NM: Sandia National Laboratories.

Lambert, S.J. 1991. Chapter 5: "Isotopic Constraints on the Rustler and Dewey Lake Groundwater Systems," *Hydrogeochemical Studies of the Rustler Formation and Related Rocks in the Waste Isolation Pilot Plant Area, Southeastern New Mexico.* Eds. M.D. Siegel, S.J. Lambert, and K.L. Robinson. SAND88-0196. Albuquerque, NM: Sandia National Laboratories. 5-1 through 5-79.

Lambert, S.J. 1992. "Geochemistry of the Waste Isolation Pilot Plant (WIPP) Site, Southeastern New Mexico, U.S.A.," *Applied Geochemistry*. SAND91-0612. Vol. 7, no. 6, 513-531.

Lambert, S.J., and J.A. Carter. 1987. *Uranium-Isotope Systematics in Groundwaters of the Rustler Formation, Northern Delaware Basin, Southeastern New Mexico. I. Principles and Preliminary Results.* SAND87-0388. Albuquerque, NM: Sandia National Laboratories.

Lambert, S.J., and D.M. Harvey. 1987. *Stable-Isotope Geochemistry of Groundwaters in the Delaware Basin of Southeastern New Mexico*. SAND87-0138. Albuquerque, NM: Sandia National Laboratories.

Lambert, S.J., and J.W. Mercer. 1978. *Hydrologic Investigations of the Los Medaños Area, Southeastern New Mexico, 1977*. SAND77-1401. Albuquerque, NM: Sandia National Laboratories.

Lambert, S.J., and Robinson, K.L. 1984. *Field Geochemical Studies of Groundwaters in Nash Draw, Southeastern New Mexico*. SAND83-1122. Albuquerque, NM: Sandia National Laboratories.

Lambert, S.J., 1991. *Isotopic Constraints on the Rustler and Dewey Lake Groundwater Systems, Chapter 5, in Hydrogeochemical Studies of the Rustler Formation and Related Rocks in the Waste Isolation Pilot Plant Area*, Southeastern New Mexico, Siegel, M.D., Lambert, S.J., and Robinson, K.L., eds., SAND88-0196, Sandia Naitonal Laboratories, Albuquerque, NM.

Lang, W.B., 1935. *Upper Permian Formation of Delaware Basin of Texas and New Mexico*, American Association of Petroleum Geologists Bulletin, Vol. 19 p. 262-276.

Lang, W.B., 1939. *Salado Formation of the Permian Basin*, American Association of Petroleum Geologists Bulletin, Vol. 23, p. 1569-1572.

Lang, W.B., 1942. *Basal Beds of Salado Formation in Fletcher Potash Core Test Near Carlsbad, New Mexico*, American Association of Petroleum Geologists Bulletin, Vol. 26, p. 63-79.

Lappin, A.R. 1988. *Summary of Site-Characterization Studies Conducted From 1983 Through 1987 at the Waste Isolation Pilot Plant (WIPP) Site, Southeastern New Mexico*. SAND88-0157. Albuquerque, NM: Sandia National Laboratories.

Lappin, A.R., R.L. Hunter, D.P. Garber, P.B. Davies, R.L. Beauheim, D.J. Borns, L.H. Brush, B.M. Butcher, T. Cauffman, M.S.Y. Chu, L.S. Gomez, R.V. Guzowski, H.J. Iuzzolino, V. Kelley, S.J. Lambert, M.G. Marietta, J.W. Mercer, E.J. Nowak, J. Pickens, R.P. Rechard, M. Reeves, K.L. Robinson, and M.D. Siegel. 1989. *Systems Analysis, Long-Term Radionuclide Transport, and Dose Assessments, Waste Isolation Pilot Plant (WIPP), Southeastern New Mexico; March 1989*. SAND89-0462. Albuquerque, NM: Sandia National Laboratories.

Laul, J.C., and M.R. Smith. 1988. "Disequilibrium Study of Natural Radionuclides of Uranium and Thorium Series in Cores and Briny Groundwaters from Palo Duro Basin, Texas," *Radioactive Waste Management and the Nuclear Fuel Cycle*. Vol. II, no. 2, 169-225.

LaVenue, A.M., and B.S. RamaRao. 1992. *A Modeling Approach To Address Spatial Variability within the Culebra Dolomite Transmissivity Field.* SAND92-7306. Albuquerque, NM: Sandia National Laboratories.

LaVenue, A.M., A. Haug, and V.A. Kelley. 1988. *Numerical Simulation of Ground-Water Flow in the Culebra Dolomite at the Waste Isolation Pilot Plant (WIPP) Site: Second Interim Report.* SAND88-7002. Albuquerque, NM: Sandia National Laboratories.

LaVenue, A.M., T.L. Cauffman, and J.F. Pickens. 1990. *Ground-Water Flow Modeling of the Culebra Dolomite. Volume I: Model Calibration.* SAND89-7068/1. Albuquerque, NM: Sandia National Laboratories.

LaVenue, A.M., Haug, A., and Kelley, V.A., 1988. *Numerical Simulation of Ground-Water Flow in the Culebra Dolomite at the Waste Isolation Pilot Plant (WIPP Site: Second Interim Report,* SAND99-7002, Sandia National Laboratories, Albuquerque, NM.

Leslie, A., Kendall, A., and Harwood, G., 1993. *The Castile Formation: A Continuing Paradox: in Geology of the Carlsbad Region, New Mexico and West Texas*, D.W. Love et al., eds., Forty fourth Annual, Field Conference Guidebook, New Mexico Geological Society, P. 13-14.

Lieser, K. H., A. Ament, R. Hill, R.N. Singh, U. Stingl, and B. Thybusch. 1990. "Colloids in groundwater and their influence on migration of trace elements and radionuclides." *Radiochimica Acta* 49, 83-100.

Lieser, K. H., B. Gleitsmann, S. Peschke, and T. Steinkopff. 1986a. "Colloid Formation and Sorption of Radionuclides in Natural Systems." *Radiochimica Acta* vol. 40: 39-47.

Lieser, K.H., B. Gleitsmann, and T. Steinkopff. 1986b. "Sorption of trace elements or radionuclides in natural systems containing groundwater and sediments." *Radiochimica Acta.* vol. 40: 33-37.

Lloyd, M.H., and R.G. Haire. 1978. "The chemistry of plutonium in sol-gel processes." *Radiochimica Acta.* vol. 25: 139-148.

Lowenstein, T.K., 1988. *Origin of Depositional Cycles in a Permian "Saline Gian": The Salado (McNutt Zone) Evaporites of New Mexico and Texas*, Geological Society of America Bulletin. Vol. 100, p. 592-608.

Lucas, S.G., and Anderson, O.J., 1993a. *Stratigraphy of the Permian-Triassic Boundary* in

Southeastern New Mexico and West Texas, in Carlsbad Region, New Mexico and West Texas, D.W. Love et al., eds., New Mexico Geological Society, Forty-fourth Annual Field Conference Guidebook, p. 219-230.

Lucas, S.G., and Anderson, O.J., 1993b. *Triassic Stratigraphy in Southeastern New Mexico and Southwestern Texas, in Carlsbad Region, New Mexico and West Texas*, D.W. Love et al., eds., New Mexico Geological Society, Forty-Fourth Annual Field Conference Guidebook, p. 231-235.

Lyklema, J. 1978. "Surface chemistry of colloids in connection with stability." In *The Scientific Basis of Flocculation*; K.J. Ives, Ed.; Sijthoff and Noordhoff: Dordrecht, The Netherlands: 3-36.

Lynch, A.W., and R.G. Dosch. 1980. *Sorption Coefficients for Radionuclides on Samples from the Water-Bearing Magenta and Culebra Members of the Rustler Formation*. SAND80-1064. Albuquerque, NM: Sandia National Laboratories.

Machette, M.N., 1985. *Calcic Soils of the Southwestern United States, in Soils and Quaternary Geology of the Soughwestern United States*. Weide, D.L., ed., Special Paper 203, Geological Society of America. p. 1-21.

Mackay, D.M., D.L. Freyberg, P.V. Roberts, and J.A. Cherry. 1986. "A Natural Gradient Experiment on Solute Transport in a Sand Aquifer. 1: Approach and Overview of Plume Movement," *Water Resources Research*. Vol. 22, no. 13, 2017-2029.

Maiti, T.C., M.R. Smith, and J.C. Laul. 1989. "Colloid Formation Study of U, Th, Ra, Pb, Po, Sr, Rb, and Cs in Briny (High Ionic Strength) Groundwaters: Analog Study for Waste Disposal," *Nuclear Technology*. Vol. 84, no. 1, 82-87.

Matijevi , E. 1973. "Colloid Stability and Complex Chemistry." *Journal of Colloid and Interface Science* vol. 43: 217-245.

McCarthy, J.F., and C. Degueldre. 1993. *Sampling and characterization of colloids and particles in ground water for studying their role in contaminant transport.* In *Environmental Particles*. J. Buffle and H.P. van Leeuwen, Ed. *IUPAC Environmental Analytical and Physical Science Series* Vol. 2, Lewis Publishers, Inc., 247-315.

McDonald, M.G., and A.W. Harbaugh. 1988. *A Modular Three-Dimensional Finite-Difference Ground-Water Flow Model.* United States Geological Survey Open File Report 83-875. Reston, VA:

United States Geological Survey.

McDonald, M.G., A.W. Harbaugh, B.R. Orr, and D.J. Ackerman. 1991. *A Method of Connecting No-Flow Cells to Variable-Head Cells for the U.S .Geological Survey Modular Finite-Difference Ground-Water Flow Model.* United States Geological Survey Open File Report 91-536. Reston, VA: United States Geological Survey.

McDowell-Boyer, L.M., J.R. Hunt, N. and Sitar. 1986. "Particle transport through porous media." *Water Resources Research* vol. 22, 1901-1921.

McNeal, R.P. 1965. "Hydrodynamics of the Permian Basin," *Fluids in Subsurface Environments*, AAPG Memoir 4, 308-326.

Mercer, J.W. 1983. *Geohydrology of the Proposed Waste Isolation Pilot Plant Site, Los Medaños Area, Southeastern New Mexico*. Water-Resources Investigations Report 83-4016. Albuquerque, NM: U.S. Geological Survey.

Mercer, J.W., R.L. Beauheim, R.P. Snyder, and G.M. Fairer. 1987. *Basic Data Report for Drilling and Hydrologic Testing of Drillhole DOE-2 at the Waste Isolation Pilot Plant (WIPP) Site*. SAND86-0611. Albuquerque, NM: Sandia National Laboratories.

Mercer, J.W., and B.R. Orr. 1979. *Interim Data Report on the Geohydrology of the Proposed Waste Isolation Pilot Plant Site Southeast New Mexico*. Water-Resources Investigations 79-98. Albuquerque, NM: U.S. Geological Survey.

Mercer, J.W., 1983. *Geohydrology of the Proposed Waste Isolation Pilot Plant Site, Los Medanos Area,* Southeastern New Mexico, Water Resources Investigation Report 83-4016, U.S. Geological Survey, Albuquerque, NM.

Mercer, J.W., Beauheim, R.L., Snyder, R.P., and Fairere, G.M., 1987. *Basic Data Report for Drilling and Hydrologic Testing of Drillhole DOE-2 at the Waste Isolation Pilot Plant (WIPP) Site*, SAND86-0611, Sandia National Laboratories, Albuquerque, NM.

Miller, D.N., 1955. *Petrology of the Pierce Canyon Formation, Delaware Basin, Texas and New Mexico Ph. D. Thesis :* Austin, University of Texas.

Miller, D. N., 1966. *Petrology of Pierce Canyon Redbeds, Delaware Basin, Texas and New Mexico,* American Association of Petroleum Geologists Bulletin, Vol. 80, p. 283-307.

Mitchell, J.F.B. 1989. "The "Greenhouse Effect" and Climate Change," *Reviews of Geophysics*. Vol. 27,

115-139.

Molecke, M.A. 1983. *A Comparison of Brines Relevant to Nuclear Waste Experimentation.* SAND83-0516. Albuquerque, New Mexico: Sandia National Laboratories.

Myers, J., P. Drez, and P. James. 1991. *Chapter 6: The redox state and the occurrence and influence of organics in the Culebra.* In *Hydrogeochemical studies of the Rustler Formation and related rocks in the Waste Isolation Pilot Plant area, southeastern New Mexico* (ed. M.D. Siegel, S.J. Lambert, and K.L. Robinson). Sandia National Laboratories, SAND88-0196, Albuquerque, New Mexico.

Neuman, S.P., and P.A. Witherspoon. 1969a. "Theory of Flow in a Confined Two-Aquifer System," *Water Resources Research.* Vol.5, 803-816.

Neuman, S.P., and P.A. Witherspoon. 1969b. "Applicability of Current Theories of Flow in Leaky Aquifers," *Water Resources Research.* Vol. 5, 817-829.

Newell, N. D., et al., 1953. *The Permian Reef Complex of the Guadalupe Mountains Region, Texas and New Mexico-A Study in Paleoecology,* San Francisco, W.H. Freemand and Co., p. 236.

Nitsche, H., K. Roberts, R.C. Gatti, T. Prussin, K. Becraft, S.C. Leung, S.A. Carpenter, and C.F. Novak. 1992. *Plutonium solubility and speciation studies in a simulant of air intake shaft water from the Culebra Dolomite at the Waste Isolation Pilot Plant.* SAND92-0659. Albuquerque, New Mexico: Sandia National Laboratories.

Novak, C.F. 1992. *An Evaluation of Radionuclide Batch Sorption Data on Culebra Dolomite for Aqueous Compositions Relevant to the Human Intrusion Scenario for the Waste Isolation Pilot Plant.* SAND91-1299. Albuquerque, NM: Sandia National Laboratories.

Nowak, E.J. 1980. *Radionuclide Sorption and Migration Studies of Getters for Backfill Barriers.* SAND79-1110. Albuquerque, NM: Sandia National Laboratories.

Nuttall, H.E., R. Jain, and Y. Fertelli. 1991. "Radiocolloid transport in saturated and unsaturated fractures," High Level Radioactive Waste Management, Proceedings of the Second Annual International Conference, Las Vegas, Nevada, April 28-May 3, 1991, 189-196.

Overbeek, J.T.G. 1982. "Colloids, a fascinating subject: Introductory lecture." *R. Soc. Chem.*

vol. 43: 1-21.

Popielak, R.S., R.L. Beauheim, S.R. Black, W.E. Coons, C.T. Ellingson, and R.L. Olsen. 1983. *Brine Reservoirs in the Castile Formation, Waste Isolation Pilot Plant (WIPP) Project, Southeastern New Mexico*. WTSD-TME-3153. Albuquerque, NM: D'Appolonia Consulting Engineers, Inc.

Powers, D.W., and R.M. Holt. 1990. "Sedimentology of the Rustler Formation near the Waste Isolation Pilot Plant (WIPP) Site," *Geological and Hydrological Studies of Evaporites in the Northern Delaware Basin for the Waste Isolation Pilot Plant (WIPP), New Mexico, Field Trip #14 Guidebook, Geological Society of America 1990 Annual Meeting, Dallas, TX, October 29-November 1, 1990*. Leaders: D.W. Powers, R.M. Holt, R.L. Beauheim, and N. Rempe. Dallas, TX: Dallas Geological Society. 79-106.

Powers, D., R. Holt, R.L. Beauheim, and N. Rempe. 1990. "Geological and Hydrological Studies of Evaporites in the Northern Delaware Basin for the Waste Isolation Pilot Plant (WIPP), New Mexico," *Geological and Hydrological Studies of Evaporites in the Northern Delaware Basin for the Waste Isolation Pilot Plant (WIPP), New Mexico, Field Trip #14 Guidebook, Geological Society of America 1990 Annual Meeting, Dallas, TX, October 29-November 1, 1990*. Leaders: D.W. Powers, R.M. Holt, R.L. Beauheim, and N. Rempe. Dallas, TX: Dallas Geological Society. 1-5.

Powers, D.W. and Holt, R.M., 1993. *The Upper Cenozic Gatuna Formation of Southeastern New Mexico: in Carlsbad Region, New Mexico and West Texas*, D.W. Love et al., eds., Forty-fourth Annual Field Conference Guidebook, New Mexico Geological Society, Socorro, NM, p. 271-282.

Powers, D.W., and LeMone, D. V., 1987. *A Summary of Ochoan Stratigraphy, Western Delaware Basin*, Guidebook 18, El Paso Geological Society, p. 63-68

Powers, D.W., Lambert, S.J., Shaffer, S-E., Hill, L.R., and Weart, W.D., eds., 1978. *Geological Characterization Report for the Waste Isolation Pilot Plant (WIPP) Site, Southeastern New Mexico*. SAND78-1596, Sandia National Laboratories, Albuquerque, NM.

Powers, D. W., and Holt, R. M., 1990a, *Geologic mapping of the Air Intake shaft at the Waste Isolation Pilot Plant*, DOE/WIPP 90-051, U.S. Department of Energy, Carlsbad, NM.

Rai, D., and J.L. Swanson. 1981. "Properties of plutonium (IV) polymer of environmental importance." *Nuclear Technology*. vol. 54: 107-112.

Rasmuson, A., and I. Neretnieks. 1986. "Radionuclide Transport in Fast Channels in Crystalline Rock," *Water Resources Research*. Vol. 22, no. 8, 1247-1256.

Reeves, M., G.A. Freeze, V.A. Kelley, J.F. Pickens, D.T. Upton, and P.B. Davies. 1991. *Regional Double-Porosity Solute Transport in the Culebra Dolomite Under Brine-Reservoir-Breach Release Conditions: An Analysis of Parameter Sensitivity and Importance*. SAND89-7069. Albuquerque, NM: Sandia National Laboratories.

Richardson, G.B., 1904. *Report of a Reconnaissance of Trans-Pecos Texas North of the Texas and Pacific Railway,* Texas University Bulletin 23, p. 119.

Richey, S.F. 1986. *Hydrologic-Test Data from Wells at Hydrologic-Test Pads H-7, H-8, H-9, and H-10 Near the Proposed Waste Isolation Pilot Plant Site, Southeastern New Mexico*. United States Geological Survey Open-File Report 86-413. Albuquerque, NM: United States Geological Survey.

Richey, S.F. 1987a. *Preliminary Hydrologic Data for Wells Tested in Nash Draw, Near the Proposed Waste Isolation Pilot Plant Site, Southeastern New Mexico*. United States Geological Survey Open-File Report 87-3. Albuquerque, NM: United States Geological Survey.

Richey, S.F. 1987b. *Water-Level Data from Wells in the Vicinity of the Waste Isolation Pilot Plant, Southeastern New Mexico*. United States Geological Survey Open-File Report 87-120. Albuquerque, NM: United States Geological Survey.

Robinson, T.W., and Lang, W. B 1938. *Geology and Ground-water Conditions of the Pecos River Valley in the Vicinity of Laguna Grande de la Sal, New Mexico, with Special Reference to the Salt Content of the River Water,* Twelfth and Thirteenth Biennial Reports of the State Engineer of New Mexico, p. 77-118.

Robinson, J.Q., and Powers, D.W., 1987. *A Clastic Deposit Within the Lower Castile Formation, Western Delaware Basin, New Mexico*, El Paso Geological Society Guidebook 18, p. 69-79.

Rosholt, J.N., and McKinney, C.R., 1980. *Uranium Series Disequilibrium Investigations Related to the WIPP Site, New Mexico, Part II Uranium Trend Dating of Surficial Deposits and Gypsum Spring Deposit Near WIPP Site, New Mexico*, Open-file report 80-870, U.S. Geological Survey, Denver, CO.

Roswell Geological Society. 1977. *The Oil and Gas Fields of Southeastern New Mexico*. Roswell, NM: Roswell Geological Society.

Rundberg, R.S., A.J. Mitchell, I.R. Triay, and N.B. Torstenfelt. 1988. "Size and density of a ^{242}Pu colloid." *Scientific Basis for Nuclear Waste Management XI*. vol. 112: 243-248.

Sandia National Laboratories and US Geological Survey 1981. *Basic Data Report for Drillhole WIPP 33 (Waste Isolation Pilot Plant - WIPP).* SAND80-2011. Albuquerque, NM: Sandia National Laboratories.

Sandia WIPP Project. 1992. *Preliminary Performance Assessment for the Waste Isolation Pilot Plant, December 1992. Volume 3: Model Parameters.* SAND92-0700/3. Albuquerque, NM: Sandia National Laboratories.

Sato, T., and R. Ruch. 1980. *Stabilization of Colloidal Dispersions by Polymer Adsorption.* Marcel Dekker, Inc.

Saulnier, G.J., Jr. 1987. *Analysis of Pumping Tests of the Culebra Dolomite Conducted at the H-11 Hydropad at the Waste Isolation Pilot Plant (WIPP) Site.* SAND87-7124. Albuquerque, NM: Sandia National Laboratories.

Saulnier, G.J., Jr., and J.D. Avis. 1988. *Interpretation of Hydraulic Tests Conducted in the Waste-Handling Shaft at the Waste Isolation Pilot Plant (WIPP) Site.* SAND88-7001. Albuquerque, NM: Sandia National Laboratories.

Saulnier, G.J., Jr., G.A. Freeze, and W.A. Stensrud. 1987. *WIPP Hydrology Program, Waste Isolation Pilot Plant, Southeastern New Mexico, Hydrologic Data Report #4.* SAND86-7166. Albuquerque, NM: Sandia National Laboratories.

Schiel, K. A., 1988. *The Dewey Lake Formation; End Stage Deposit of a Peripheral Foreland Basin; M.S. Thesis*, University of Texas at EL Paso, El Paso, TX, p. 181.

Schiel, K. A., 1994. *A New Look at the Age, Depositional Enbironment and Paleougeographic Setting of the Dewey Lake Formation (Late Permian),* West Texas Geological Society Bulletin, Vol. 33, No. 9, p. 5-13.

Schlesinger, M.E., and J.F.B. Mitchell. 1987. "Climate Model Simulations of the Equilibrium Climatic Response to Increased Carbon Dioxide," *Reviews of Geophysics.* Vol. 25, 760-798.

Sewards, T., Glenn, R., and Keil, K., 1991. *Mineralogy of the Rustler Formation in the WIPP-19 Core,* SAND97-7036, Sandia National Laboratories, Albuquerque, NM.

Serne, R.J., D. Rai, M.J. Mason, and M.A. Molecke. 1977. *Batch Kd Measurements of Nuclides to Estimate Migration Potential at the Proposed Waste Isolation Pilot Plant in New Mexico.* PNL-2448. Richland, WA: Battelle Pacific Northwest Laboratories.

Sewards, T. 1991. *Characterization of Fracture Surfaces in Dolomite Rock, Culebra Dolomite Member,*

Rustler Formation. SAND90-7019. Albuquerque, NM: Sandia National Laboratories.

Siegel, M.D., and S. Anderholm. 1994. "Geochemical Evolution of Groundwater in the Culebra Dolomite near the Waste Isolation Pilot Plant, Southeastern New Mexico, USA." *Geochimica et Cosmochimica Acta* vol. 58, 2299-2323.

Siegel, M.D., and S.J. Lambert. 1991. Chapter 1: "Summary of Hydrogeochemical Constraints on Groundwater Flow and Evolution in the Rustler Formation," *Hydrogeochemical Studies of the Rustler Formation and Related Rocks in the Waste Isolation Pilot Plant Area, Southeastern New Mexico*. Eds. M.D. Siegel, S.J. Lambert, and K.L. Robinson. SAND88-0196. Albuquerque, NM: Sandia National Laboratories. 1-1 through 1-109.

Siegel, M.D., S.J. Lambert, and K.L. Robinson, eds. 1991a. *Hydrogeochemical Studies of the Rustler Formation and Related Rocks in the Waste Isolation Pilot Plant Area, Southeastern New Mexico*. SAND88-0196. Albuquerque, NM: Sandia National Laboratories.

Siegel, M.D., K.L. Robinson, and J. Myers. 1991b. *Chapter 2: Solute relationships in groundwater from the Culebra dolomite and related rocks in the Waste Isolation Pilot Plant area, southeastern New Mexico*. In *Hydrogeochemical studies of the Rustler Formation and related rocks in the Waste Isolation Pilot Plant area, southeastern New Mexico*. M.D. Siegel, S.J. Lambert, and K.L. Robinson. Ed.; SAND88-0196. Albuquerque, New Mexico: Sandia National Laboratories.

Siegel, M.D., S.L. Robinson, and J. Myers. 1991b. "Solute Relationships in Groundwaters from the Culebra Dolomite and Related Rocks in the Waste Isolation Pilot Plant Area, Southeastern New Mexico," *Hydrogeochemical Studies of the Rustler Formation and Related Rocks in the Waste Isolation Pilot Plant Area, Southeastern New Mexico*. Eds. M.D. Siegel, S.J. Lambert, and K.L. Robinson. SAND88-0196. Albuquerque, NM: Sandia National Laboratories. 2-1 through 2-164.

Sipes, Williamson & Aycock, Inc., 1976. Hydrocarbon Evaluation, Proposed southeastern New Mexico Radioactive Material Storage Site, Eddy Country, New Mexioc, SAND77-7033, Vols. I and II, Sandia National Laboratories, Albuquerque, NM.

Snyder, R.P. 1985. *Dissolution of Halite and Gypsum, and Hydration of Anhydrite to Gypsum, Rustler Formation, in the Vicinity of the Waste Isolation Pilot Plant, Southeastern New Mexico*. USGS-OFR-85-229. Denver, CO: U.S. Geological Survey.

Snyder, R.P., 1985. *Dissolution of Halite and Gypsum, and Hydration of Anhydrite to Gypsum, Rustler Formation, in the Vicinity of the Waste Isolation Pilot Plant, Southeastern New Mexico*, Open-file Report 85-229, U.S. Geological Survey, Denver, CO.

Stensrud, W.A., M.A. Bame, K.D. Lantz, A.M. LaVenue, J.B. Palmer, and G.J. Saulnier, Jr. 1987. *WIPP Hydrology Program, Waste Isolation Pilot Plant, Southeastern New Mexico, Hydrologic Data Report #5*. SAND87-7125. Albuquerque, NM: Sandia National Laboratories.

Stensrud, W.A., M.A. Bame, K.D. Lantz, T.L. Cauffman, J.B. Palmer, and G.J. Saulnier, Jr. 1988a. *WIPP Hydrology Program, Waste Isolation Pilot Plant, Southeastern New Mexico, Hydrologic Data Report #6*. SAND87-7166. Albuquerque, NM: Sandia National Laboratories.

Stensrud, W.A., M.A. Bame, K.D. Lantz, J.B. Palmer, and G.J. Saulnier, Jr. 1988b. *WIPP Hydrology Program, Waste Isolation Pilot Plant, Southeastern New Mexico, Hydrologic Data Report #7*. SAND88-7014. Albuquerque, NM: Sandia National Laboratories.

Stensrud, W.A., M.A. Bame, K.D. Lantz, J.B. Palmer, and G.J. Saulnier, Jr. 1990. *WIPP Hydrology Program, Waste Isolation Pilot Plant, Southeastern New Mexico, Hydrologic Data Report #8*. SAND89-7056. Albuquerque, NM: Sandia National Laboratories.

Stout, D.L., and S.A. Carroll. 1992. *A literature review of actinide-carbonate mineral interactions*. SAND92-7328, Albuquerque, NM: Sandia National Laboratories.

Swift, P.N. 1993. "Long-Term Climate Variability at the Waste Isolation Pilot Plant, Southeastern New Mexico, USA," *Environmental Management*. SAND91-7055. Vol. 17, no. 1, 83-97.

Theng, B.K.G. 1979. *Formation and Properties of Clay-Polymer Complexes. Developments in Soil Science*. Vol. 9, Elsevier Scientific Publishing Co.

Tien, P-L., F.B. Nimick, A.B. Muller, P.A. Davis, R.V. Guzowski, L.E. Duda, and R.L. Hunter. 1983. *Repository Site Data and Information in Bedded Salt: Palo Duro Basin, Texas*. NUREG/CR-3129, SAND82-2223. Albuquerque, NM: Sandia National Laboratories.

Tiller, C.L., and C.R. O'Melia. 1993. Natural organic matter and colloidal stability: Models and measurements. In *Colloids in the Aquatic Environment. Colloids and Surfaces A: Physicochemical and Engineering Aspects,* T.F. Tadros and J. Gregory, Ed.; Elsevier Applied Science: London, 73: 89-102.

Tipping, E. 1993. "Modelling ion binding by humic acids." In *Colloids in the Aquatic Environment. Colloids and Surfaces A: Physicochemical and Engineering Aspects,* T.F. Tadros and J. Gregory, Ed.; Elsevier Applied Science: London, 73: 117-131.

Tóth, J. 1963. "A Theoretical Analysis of Groundwater Flow in Small Drainage Basins," *Journal of Geophysical Research*. Vol. 68, no. 16, 4795-4812.

Toth, L.M., H.A. Friedman, and M.M. Osborne. 1981. "Polymerization of Pu(IV) in aqueous nitric acid solutions." *Journal of Inorganic and Nuclear Chemistry*. vol. 43: 2929-2934.

Triay, I. R., D.E. Hobart, A.J. Mitchell, T.W. Newton, M.A. Ott, P.D. Palmer, R.S. Rundberg, and J.L. Thompson. 1991. "Size Determinations of Plutonium Colloids using Autocorrelation Photon Spectroscopy." *Radiochimica Acta* 52/53: 127-131.

U.S. Department of Energy. 1994. *Draft Compliance Status Report for the Waste Isolation Pilot Plant. March 1994, Revision 0, Draft.* DOE/WIPP 94-019, Carlsbad, New Mexico.

U.S. Department of Energy. 1994b. *Waste Isolation Pilot Plant Transuranic Waste Baseline Inventory Report.* CAO-94-1005. Revision 0, May 1994.

van der Lee, J., G. de Marsily, and E. Ledoux. 1993. "Are colloids important for transport rate assessment of radionuclides?" In *High Level Radioactive Waste Management, Proceedings of the Fourth Annual International Conference*; Las Vegas, Nevada, 646-652.

van Olphen, H. 1977. *Introduction to Clay Colloid Chemistry.* 2nd ed., Wiley.

Verwey, E.J.W., and J.T.G. Overbeek. 1948. *Theory of the Stability of Lyophobic Colloids. The Interaction of Sol Particles having an Electric Double Layer.* New York, N.Y.: Elsevier Publishing Company, Inc.

Vilks, P. 1994. *The role of colloids and suspended particles in radionuclide transport in the Canadian concept for nuclear fuel waste disposal.* AECL-10280, Whiteshell Laboratories, Atomic Energy of Canada, Ltd., Pinawa, Manitoba.

Vince, J.D., 1963, *Surface Geology of the Nash Draw Quadrangle, Eddy County, New Mexico,* U.S. Geological Survey Bulletin 1141-B, 46 p.

Vlassopoulos, D., S.A. Wood, and A. Mucci. 1990. "Gold speciation in natural waters: II. The importance of organic complexing—Experiments with some simple model ligands." *Geochimica et Cosmochimica Acta.* vol. 54: 1575-1586.

Washington, W.M., and G.A. Meehl. 1984. "Seasonal Cycle Experiment on the Climate Sensitivity due to Doubling of CO_2 with an Atmospheric General Circulation Model

Coupled to a Simple Mixed-Layer Ocean Model," *Journal of Geophysical Research.* Vol. 89. 9475-9503.

Weber, W.J., Jr., P.M. McGinley, and L.E. Katz. 1991. "Sorption Phenomena in Subsurface Systems: Concepts, Models and Effects on Contaminant Fate and Transport," *Water Research.* Vol. 25, no. 5, 499-528.

Wilson, C.A., and J.F.B. Mitchell. 1987. "A Doubled CO_2 Climate Sensitivity Experiment with a Global Climate Model Including a Simple Ocean," *Journal of Geophysical Research.* Vol. 92, 13,315-13,343.

WIPP PA (Performance Assessment) Department. 1992. *Preliminary Performance Assessment for the Waste Isolation Pilot Plant, December 1992. Volumes 1,2,4,5.* SAND92-0700/1,2,4,5. Albuquerque, NM: Sandia National Laboratories.

WIPP PA (Performance Assessment) Division. 1991. *Preliminary Comparison with 40 CFR Part 191, Subpart B for the Waste Isolation Pilot Plant, December 1991. Volume 3: Reference Data.* Eds. R.P. Rechard, A.C. Peterson, J.D. Schreiber, H.J. Iuzzolino, M.S. Tierney, and J.S. Sandha. SAND91-0893/3. Albuquerque, NM: Sandia National Laboratories.

Conf paper cycled separately. TCl